



UNIVERSITÀ DEGLI STUDI  
DI GENOVA



ISTITUTO  
ITALIANO DI  
TECNOLOGIA

**Università degli Studi di Genova**  
**Fondazione Istituto Italiano di Tecnologia**  
**Corso di Dottorato in “Neuroscienze” XXXII Ciclo**

Coordinatore Prof. Angelo Schenone

Curriculum “Neuroscienze e Neurotecnologie” (CODE-6198)

Academic Year 2019-2020

***The encoding of cognitive flexibility by the prefrontal cortex and its modulation by dopamine- and clinically-relevant genetic variants***

Supervisor: Dr Francesco Papaleo

(NBT-IIT, Genova, Italy)

**Francesca Scarsi**



*To my boyfriend and my family, in particular to my two grandfathers whom are not here with me anymore, and whom sustained me and believed in me everytime.*



# Contents

Summary.....	10
Introduction.....	11
Schizophrenia .....	11
Cognitive flexibility and implication for schizophrenia .....	12
Attentional set-shifting tasks.....	13
Automated two-chamber “Operon” ID/ED task for mice .....	16
The prefrontal cortex (PFC) in executive functions.....	18
Neural correlates of set-shifting in the PFC.....	19
Dopamine system, PFC, and cognitive flexibility .....	20
Dopamine D2 long (D2L) and short isoform (D2S) .....	21
The dystrobrevin binding protein 1 (DTNBP1) gene, encoding dysbindin-1.....	22
Aims of the thesis .....	25
<i>Specific aim 1.</i> How do the PFC neurons encode different phases of cognitive flexibility in a WT mice model?.....	25
<i>Specific aim 2.</i> How do clinically-relevant and dopamine-related functional genetic variants affect cognitive flexibility and/or PFC-neuronal activity? .....	25
Materials and Methods .....	27
Results .....	33
1) Selective increase of oxygen consumption in mice mPFC during the extradimensional set shift stage of the Operon ID/ED .....	33
2) The behavior of wt mice with silicon probes .....	35
3) Electrophysiology of wt implanted with silicon probes .....	44
1. SIMPLE DISCRIMINATION (SD).....	48
2. COMPOUND DISCRIMINATION (CD).....	51
3.COMPOUND DISCRIMINATION REVERSAL (CDRe).....	54
4. INTRA-DIMENSIONAL SHIFT (IDS).....	57
5. INTRA-DIMENSIONAL SHIFT REVERSAL (IDSRe).....	60
6. INTRA-DIMENSIONAL SHIFT 2 (IDS2).....	63
7. INTRA-DIMENSIONAL SHIFT 2 REVERSAL (IDS2Re).....	66
8. EXTRA-DIMENSIONAL SHIFT (EDS).....	69
9. EXTRA-DIMENSIONAL SHIFT REVERSAL (EDSRe).....	73
4) D2L +/- mice show cognitive deficits in serial reversal learning compared to wt mice.....	76
5) Electrophysiology of D2L +/- mice.....	81
6) Dys +/- mice show deficits in the EDS, compared to wt mice.....	84
7) Electrophysiology of dys +/- mice .....	89
8) Dys +/--D2L +/- mice show a restored behavioral performance.....	92

9) Electrophysiology of dys+/-D2L+/- mice .....	98
Conclusion .....	104
Future perspective.....	109
Bibliography.....	110
Acknowledgment.....	123

## Figure Index:

Figure 1. Human tasks used for studying cognitive dysfunctions. ....	14
Figure 2. Automatized attentional set-shifting task.....	17
Figure 3. WT mice vs Sandy (dys-/-) mice. ....	23
Figure 4. Timeline of experiments. ....	29
Figure 5. Stereotaxic positioning of the oxytometry carbon paste electrodes implanted in the mPFC of WT mice. ....	34
Figure 6. Consumption of oxygen in mPFC during the different stages of the task of WT mice. ....	35
Figure 7. Stereotaxic positioning of the silicon probes electrodes implanted in the mPFC of WT mice.....	36
Figure 8. The number of trials to reach the criterion of WT mice.....	37
Figure 9. The time spent to reach the criterion of WT mice.....	37
Figure 10. The number of trials and time to reach the criterion of two different groups of WT mice. ....	39
Figure 11. The number of trials to reach the criterion of WT mice.....	41
Figure 12. The time spent to reach the criterion of WT mice.....	41
Figure 13. Latency to respond of WT mice.....	42
Figure 14. Latency to correct and incorrect responses of WT mice.....	43
Figure 15. Latency to reward of WT mice. ....	44
Figure 16. Behavioral events considered for electrophysiological analysis.....	45
Figure 17. Type of single-unit recorded in WT mice. ....	47
Figure 18. Firing rate of mPFC cells, recorded in WT mice, during SD stage. ....	49
Figure 19. Instantaneous Firing Rate (IFR) of mPFC cells, recorded in WT mice, for the correct choice of SD stage. ....	50
Figure 20. Instantaneous Firing Rate (IFR) of mPFC cells, recorded in WT mice, for the incorrect choice of SD stage. ....	51
Figure 21. Firing rate of mPFC cells, recorded in WT mice, during CD stage. ....	52
Figure 22. Instantaneous Firing Rate (IFR) of mPFC cells, recorded in WT mice, for the correct choice of CD stage. ....	53
Figure 23. Instantaneous Firing Rate (IFR) of mPFC cells, recorded in WT mice, for the incorrect choice of CD stage. ....	54
Figure 24. Firing rate of mPFC cells, recorded in WT mice, during CDRe stage.....	55
Figure 25. Instantaneous Firing Rate (IFR) of mPFC cells, recorded in WT mice, for the correct choice of CDRe stage.....	56
Figure 26. Instantaneous Firing Rate (IFR) of mPFC cells, recorded in WT mice, for the incorrect choice of CDRe stage.....	57
Figure 27. Firing rate of mPFC cells, recorded in WT mice, during IDS stage. ....	58
Figure 28. Instantaneous Firing Rate (IFR) of mPFC cells, recorded in WT mice, for the correct choice of IDS stage. ....	59
Figure 29. Instantaneous Firing Rate (IFR) of mPFC cells, recorded in WT mice, for the incorrect choice of IDS stage. ....	60
Figure 30. Firing rate of mPFC cells, recorded in WT mice, during IDSRe stage.....	61

Figure 31. Instantaneous Firing Rate (IFR) of mPFC cells, recorded in WT mice, for the correct choice of IDSRe stage. ....	62
Figure 32. Instantaneous Firing Rate (IFR) of mPFC cells, recorded in WT mice, for the incorrect choice of IDSRe stage. ....	63
Figure 33. Firing rate of mPFC cells, recorded in WT mice, during IDS2 stage. ....	64
Figure 34. Instantaneous Firing Rate (IFR) of mPFC cells, recorded in WT mice, for the correct choice of IDS2 stage. ....	65
Figure 35. Instantaneous Firing Rate (IFR) of mPFC cells, recorded in WT mice, for the incorrect choice of IDS2 stage. ....	66
Figure 36. Firing rate of mPFC cells, recorded in WT mice, during IDS2Re stage. ....	67
Figure 37. Instantaneous Firing Rate (IFR) of mPFC cells, recorded in WT mice, for the correct choice of IDS2Re stage. ....	68
Figure 38. Instantaneous Firing Rate (IFR) of mPFC cells, recorded in WT mice, for the incorrect choice of IDS2Re stage. ....	69
Figure 39. Firing rate of mPFC cells, recorded in WT mice, during EDS stage. ....	70
Figure 40. Instantaneous Firing Rate (IFR) of mPFC cells, recorded in WT mice, for the correct choice of EDS stage. ....	71
Figure 41. Instantaneous Firing Rate (IFR) of mPFC cells, recorded in WT mice, for the incorrect choice of EDS stage. ....	72
Figure 42. Instantaneous Firing Rate (IFR) of mPFC cells, recorded in WT mice, for the correct choice of EDS stage. ....	73
Figure 43. Firing rate of mPFC cells, recorded in WT mice, during EDSRe stage. ....	74
Figure 44. Instantaneous Firing Rate (IFR) of mPFC cells, recorded in WT mice, for the correct choice of EDSRe stage. ....	75
Figure 45. Instantaneous Firing Rate (IFR) of mPFC cells, recorded in WT mice, for the incorrect choice of EDSRe stage. ....	76
Figure 46. Stereotaxic positioning of the silicon probes electrodes implanted in the mPFC of D2L+/- mice .....	77
Figure 48. Time spent to reach the criterion in the reversal stages of the task, obtained from WT and D2L+/- mice. ....	78
Figure 49. Latency to respond of D2L+/- mice. ....	79
Figure 50. Latency to correct and incorrect responses of D2L+/- mice. ....	80
Figure 51. Latency to reward of D2L+/- mice. ....	81
Figure 52. Type of single-unit recorded in D2L+/- mice. ....	82
Figure 53. Firing rate of mPFC cells, recorded in WT and D2L+/- mice, during IDS2Re stage. ....	83
Figure 54. Instantaneous Firing Rate (IFR) of mPFC cells, recorded in WT and D2L+/- mice, for the correct and incorrect choices of IDS2Re stage. ....	84
Figure 55. Stereotaxic positioning of the silicon probes electrodes implanted in the mPFC of dys+/- mice. ....	85
Figure 56. The number of trials to reach the criterion in all the stages of the task, obtained from WT and dys+/- mice. ....	86
Figure 57. Time spent to reach the criterion in all the stages of the task, obtained from WT and dys+/- mice. .....	86
Figure 58. Latency to respond of dys+/- mice. ....	87
Figure 59. Latency to correct and incorrect responses of dys+/- mice. ....	88
Figure 60. Latency to reward of dys+/- mice. ....	89
Figure 61. Type of single-unit recorded in dys+/- mice. ....	90
Figure 62. Firing rate of mPFC cells, recorded in WT and dys+/- mice, during EDS stage. ....	91
Figure 63. Instantaneous Firing Rate (IFR) of mPFC cells, recorded in WT and dys+/- mice, for the correct and incorrect choices of EDS stage. ....	92

Figure 64. Stereotaxic positioning of the silicon probes electrodes implanted in the mPFC of <i>dys</i> <sup>+/-</sup> <i>D2L</i> <sup>+/-</sup> mice. ....	93
Figure 65. The number of trials to reach the criterion in IDS2Re and EDS, obtained from WT, <i>dys</i> <sup>+/-</sup> , <i>D2L</i> <sup>+/-</sup> and <i>dys</i> <sup>+/-</sup> <i>D2L</i> <sup>+/-</sup> mice . ....	94
Figure 66. Time spent to reach the criterion in IDS2Re and EDS stages of the task, obtained from WT, <i>dys</i> <sup>+/-</sup> , <i>D2L</i> <sup>+/-</sup> and <i>dys</i> <sup>+/-</sup> <i>D2L</i> <sup>+/-</sup> mice. ....	95
Figure 67. Latency to respond of <i>dys</i> <sup>+/-</sup> <i>D2L</i> <sup>+/-</sup> mice. ....	96
Figure 68. Latency to correct and incorrect responses of <i>dys</i> <sup>+/-</sup> <i>D2L</i> <sup>+/-</sup> mice. ....	97
Figure 69. Latency to reward of <i>dys</i> <sup>+/-</sup> <i>D2L</i> <sup>+/-</sup> mice. ....	98
Figure 70. Type of single-unit recorded in <i>dys</i> <sup>+/-</sup> <i>D2L</i> <sup>+/-</sup> mice. ....	99
Figure 71. Firing rate of mPFC cells, recorded in WT, <i>dys</i> <sup>+/-</sup> , and <i>dys</i> <sup>+/-</sup> <i>D2L</i> <sup>+/-</sup> mice, during EDS stage. ....	100
Figure 72. Instantaneous Firing Rate (IFR) of mPFC cells, recorded in WT, <i>dys</i> <sup>+/-</sup> , and <i>dys</i> <sup>+/-</sup> <i>D2L</i> <sup>+/-</sup> mice, for the correct and incorrect choices of EDS stage. ....	101
Figure 73. Firing rate of mPFC cells, recorded in WT, <i>D2L</i> <sup>+/-</sup> , and <i>dys</i> <sup>+/-</sup> <i>D2L</i> <sup>+/-</sup> mice, during IDS2Re stage. ....	102
Figure 74. Instantaneous Firing Rate (IFR) of mPFC cells, recorded in WT, <i>D2L</i> <sup>+/-</sup> , and <i>dys</i> <sup>+/-</sup> <i>D2L</i> <sup>+/-</sup> mice, for the correct and incorrect choices of IDS2Re stage. ....	103

## Table index:

Table 1. An example of the ID/ED ‘stuck in set’ paradigm adapted and modified from previous studies (Garner et al., 2006; Papaleo et al., 2008). ....	28
Table 2. mPFC activity changing of WT mice before and after responses, in the different stages of the task. ....	106
Table 3. mPFC activity changing of WT (top), <i>dys</i> <sup>+/-</sup> (middle), and <i>dys</i> <sup>+/-</sup> <i>D2L</i> <sup>+/-</sup> (bottom) mice before and after responses, in EDS. ....	107
Table 4. mPFC activity changing of WT (top), <i>D2L</i> <sup>+/-</sup> (middle), and <i>dys</i> <sup>+/-</sup> <i>D2L</i> <sup>+/-</sup> (bottom) mice before and after responses, in IDS2Re. ....	108





## Summary

Cognitive flexibility, defined as the ability to switch a specific response in a quick manner depending on changes in the environment, is an executive function critically altered in psychiatric disorders such as schizophrenia (Nęcka and Orzechowski, 2004; Collins and Koechlin, 2012; Lunt *et al.*, 2012). The prefrontal cortex (PFC) is a major hub involved in the mediation of cognitive flexibility. This brain area receives consistent dopaminergic inputs (Carr *et al.*, 1999; Björklund and Dunnett, 2007; Puig, Antzoulatos and Miller, 2014), indeed, dopamine signaling within the PFC is suggested to be implicated in the causes and treatment responses of cognitive deficits evident in schizophrenia. However, how the PFC might code different components of cognitive flexibility at the single-cell level and how this might be modulated by dopamine- and clinically-relevant functional genetic variants is still not clear. Here, I addressed this by using *in vivo* electrophysiology recordings in the PFC of wild-type and clinically-relevant mouse mutants with genetic variants altering D2 receptors while performing a cognitive flexibility task with high clinical translational relevance.

In particular, while mice were performing a recently validated automated Intra-/Extra-Dimensional Attentional Set-Shifting task for mice (Scheggia *et al.*, 2014, 2018), I recorded PFC activity with *in vivo* oximetry and then single-unit extracellular electrophysiology. I used wild-type mice and three different genetically modified mice with the alteration of the dopamine/D2 signaling: Dysbindin +/- mice, with overexpression of cortical D2 receptors, D2L +/- mice, with an unbalance of D2 isoforms and the combination of these genetic variants (dys+/-D2L+/-).

The main finding I found was that, while WT animals show an increase in both oxygen consumption and neuronal activity, particularly during the extra-dimensional shift (EDS) following correct response, the same effect was altered in dys+/- mice. Unbalancing the ratio of the two D2 isoforms, there was an alteration of the neural activity during serial reversal learning. The concurrent alteration of both genes differentially impacted mice's behavior together with their respective cortical activity across the different stages.

These findings provide specific associations between schizophrenia-relevant genetic variants related to dopamine/D2 signaling and PFC neuronal activity related to cognitive flexibility. This has implications in the understanding of cognitive flexibility alterations present in psychiatric disorders and in the possible development of genetic-based personalized approaches for these deficits.

# Introduction

Within the central nervous system, the fine modulation of dopamine release appears to be one of the most critical aspects that are often affected in genetic or neurodegenerative disorders (Rangel-Barajas, Coronel and Florán, 2015; Robinson and Gradinaru, 2018). Such impairment of the dopaminergic system can be associated with a variation of the number of neurons (i.e. Parkinson's disease) (Giguère, Nanni and Trudeau, 2018; Mamelak, 2018), modification of the release (i.e. drug addiction) (Volkow *et al.*, 2007; Wanat *et al.*, 2009), or at the level of the dopaminergic receptors (i.e. schizophrenia) (Abi-Dargham *et al.*, 2000; Seeman, 2010, 2013). While, the dopaminergic system, is one of the most studied, its exact function in multiple structures of the brain is making it one of the most complex. One structure, receiving significant input from dopaminergic neurons, is the prefrontal cortex (PFC) (Carr *et al.*, 1999; Björklund and Dunnett, 2007; Puig, Antzoulatos and Miller, 2014), which is also one of the brain structures most involved in cognitive flexibility (Yoon *et al.*, 2008; Keeler and Robbins, 2011; Orellana and Slachevsky, 2013; Granseth, Andersson and Lindström, 2015; Zhang *et al.*, 2015). In schizophrenic disorders, cognitive flexibility's impairments are considered as being associated with a dysfunction of dopamine in the PFC (Gaspar, Bloch and Moine, 1995; Santana, Mengod and Artigas, 2009). Here, following a short description of Schizophrenia and the related symptoms, I will focus on the tasks use for their diagnoses. Finally, using our novel described behavioral task, I will show, in mice, how cognitive flexibility is encoded in the PFC by dopaminergic receptors in normal and clinically relevant conditions. Here, in rodent models of schizophrenia together with our task in mice, adapted from the human tasks, I uncover the participation of the PFC and dopaminergic receptors in behavioral flexibility.

## Schizophrenia

Schizophrenia spectrum disorders and other psychotic disorders show a prevalence of about 0.7-1% of the world population, affecting both males and females, even if in males it might appear earlier than females and might present slightly qualitatively different symptoms. While not yet specifically defined, it is accepted that the etiology of schizophrenia implicates multiple contributing factors, including genetic and environmental (Hultman *et al.*, 1999; Dean and Murray, 2005; Gejman, Sanders and Duan, 2010). As an example of genetic factors, first-degree relatives of a patient with schizophrenia have a 10% increased risk to develop the disorder. The risk while reduced is maintained at 3% with second-degree relatives, for a risk of less than 1% in the general population (McDonald and Murphy, 2003; Chou *et al.*, 2017). Moreover, the two major genetic risk factors to develop schizophrenia are considered to be 1) having a monozygotic twin affected or 2) two affected parents (Gejman, Sanders and Duan, 2010; Henriksen, Nordgaard and Jansson, 2017). Some epigenetic and environmental risks have also been associated with schizophrenia, these risks include exposure to cannabis or malnutrition in critical developmental periods, childhood trauma, stress-related minority ethnicity, residence in an urban area, and possibly social isolation (Brown, 2011; Walder *et al.*, 2014). While the exact etiology is

unknown, currently the diagnosis of schizophrenia is based on the assessment of different behavioral alterations, that can be grouped into two major types (Jablensky, 2010; Patel *et al.*, 2014):

- 1) Positive symptoms: These symptoms include enhanced or repetitive functions considered as an abnormal exaggeration of ideas, perception or idea including delusions, hallucinations, grossly disorganized or abnormal motor behavior.
- 2) Negative symptoms: These symptoms include the loss or impairment of functions including diminished emotional expression, avolition, alogia, anhedonia, and anti-social behavior.

Despite not yet defining the pathology such as positive and negative symptoms, it is commonly accepted that at the core of the schizophrenia neuropathology there are cognitive deficits. These cognitive deficits most commonly reported include impairment of attention and working memory, together with reduced executive functions and cognitive flexibility. Notably, these cognitive (and concomitant social) dysfunctions precede the manifestation of psychosis (Cornblatt *et al.*, 1997, 1998; Erlenmeyer-Kimling, 2000), and they persevere or worsen over time (Albus *et al.*, 2002). Moreover, cognitive dysfunctions continues to be present after remission of psychosis, and are less effectively affected by currently available treatments (Cuesta, Peralta and Zarzuela, 2001; Harvey and Keefe, 2001; Snitz *et al.*, 2005; Keefe *et al.*, 2011; MacKenzie *et al.*, 2018; Scheggia *et al.*, 2018). Thus, to date, cognitive alterations in schizophrenia are considered the most incapacitating long-term features, having the most critical impact on public health due to combined economic and social costs (National Institute of Health and Clinical Excellence, 2014).

## Cognitive flexibility and implication for schizophrenia

Cognitive processes, most commonly reported to be impaired in schizophrenia, refer to “Executive functions”, which include all cognitive abilities necessary to carry out a behavior, and/or that serve to optimize performance by coordinating the various components of complex cognitive domains (Miyake *et al.*, 2000; Miller and Cohen, 2001; Lehto and Elorinne, 2003; Espy *et al.*, 2004; Nęcka and Orzechowski, 2004; Burgess and Simons, 2005; Collins and Koechlin, 2012; Lunt *et al.*, 2012).

These executive functions are hierarchically organized into three main categories:

- 1) inhibitory control: the ability to suppress one response in favor of another
- 2) working memory: the ability to maintain and manipulate multiple pieces of information at the same time while performing complex tasks and is coordinated by related executive processing (e.g. attention, inhibition, and planning behavior)
- 3) cognitive flexibility: the ability to adjust a specific response or attention in a quick manner, while facing change in environmental circumstances (attentional set-shifting and reversal learning) (Miyake *et al.*, 2000; Lehto and Elorinne, 2003).

These executive functions change throughout body and mind development and are considered to reach maturation during or after adolescence (Best and Miller, 2010; Arain *et al.*, 2013).

Most psychiatric disorders, including schizophrenia, present disruptions of executive functions (Morice and Delahunty, 1996; Moritz *et al.*, 2002; Hill, 2004; Brown, Reichel and Quinlan, 2009; Kleinmans *et al.*, 2011). Some evidence suggests that these cognitive deficits can be considered as predisposing factors to developing a psychiatric disorder, or as a potential early marker of subsequent illness (Trivedi, 2006; Etkin, Gyurak and O'Hara, 2013). Additionally, cognitive deficits can be considered as predictors of recovery, even if controversial findings are still present (González-Blanch *et al.*, 2010).

One of the first work describing impairment of executive function in schizophrenia is by Kraepelin in 1913, in which he reported that patients with schizophrenia present mental deficiency, distraction, inattentive behavior, and they could not keep the thought in mind (Kraepelin, 1913). In the following years, neuropsychological studies have shown that the most prominent cognitive impairments exhibited by patients with schizophrenia include deficits in abstract and conceptual thinking, distractibility, loose associations, disorganized or socially inappropriate behavior (Braver, Barch and Cohen, 1999). In these studies, impairment of executive functions is considered to be a feature of schizophrenia and is directly related to poor functional outcomes in patients (Blanchard *et al.*, 2011; Fett *et al.*, 2011). Cognitive disorders, in schizophrenia, are heterogeneous and sometimes they are selective and specific. These disorders are manifested by different patterns of associated and dissociated performance on different cognitive tasks (Kuperberg and Heckers, 2000). In schizophrenia, neuropsychological deficits are associated with psychosocial dysfunction and are dissociated from psychiatric symptoms, global cognitive efficiency, and intelligence (Addington and Addington, 1999; Dickerson *et al.*, 1999; Goldberg and Green, 2002, Badcock, Michie and Rock, 2005; Kopald *et al.*, 2012; Green, Lee and Ochsner, 2013). Below I will briefly describe how executive functions, and in particular cognitive flexibility, is commonly assessed in patients with schizophrenia.

## Attentional set-shifting tasks

On a clinical level, executive functions can be assessed by specific parameters, such as action generation and action selection in the so-called “attention set-shifting tasks”(ASST). In humans, these tasks provide an adequate measurement of cognitive-attentional set formation and the ability to switch between different task rules. In psychology study, a widely used and well-validated task for studying this function is the Wisconsin Card Sorting Task (WCST) (*Figure 1A*) (Berg, 1948; Milner, 1982; Everett *et al.*, 2001; Eling, Derckx and Maes, 2008; Nyhus and Barceló, 2009).

The WCST consists of four cards used as a stimulus and 128 possible combinations that represent figures with different forms (stars, circles, crosses, and triangles), colors (yellow, green, red, and blue), and the number of objects (one, two, three, and four). Among trials, the subject receives a card from which he is asked to follow a specific “rule” that is unknown to the subject. Classically, the test is based on the succession of 10 trials, with direct delivery of the response, either “correct” or “incorrect”. Following the 10 consecutive correct trials

with the same rule, the experimenter switches the rule for the next 10 consecutive correct trials. The 3 classic rules to follow are the shape, the number or the color. The interpretation of data is based on a within-trial response (“did the subject followed the rules?”), a between trial response (did the subject followed the rule of the previous trials?), a perseverative answer (“did the subject repeated multiple time the same answer, despite the “correct/incorrect” answer to previous trial?). Based on the outcome decisions, the experimenter will be able to define the number of trials necessary to switch from one rule to another (behavioral flexibility), non-perseverative answer or perseverative answer (can be correct or error). The test is considered to be finished when all 6 categories have been covered or the 128 combinations have been tested (see Figure 1A).

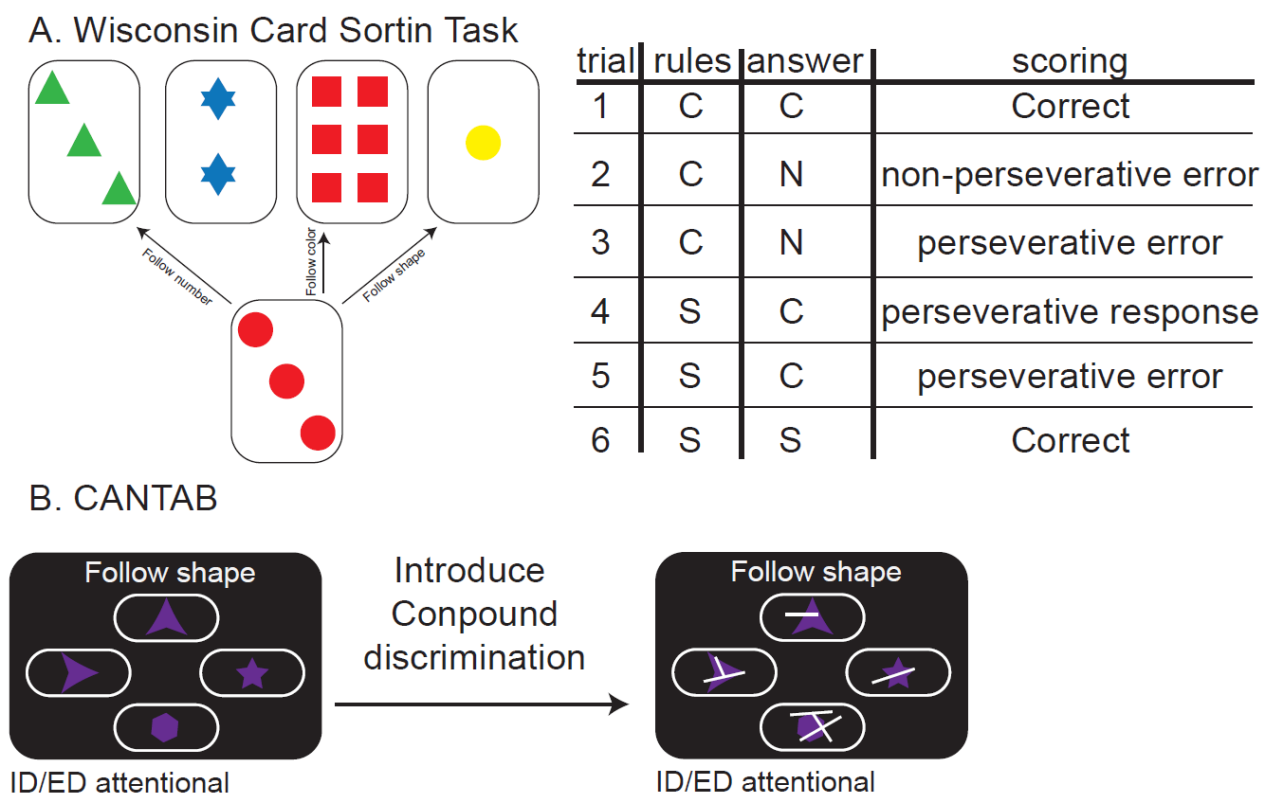


Figure 1. Human tasks used for studying cognitive dysfunctions. A) Wisconsin Card Sorting Task. On the left, there is an example of the performance of the task: a card is given to the subject and he has to understand whether to follow number, color, or shape. On the right, the table is an example of a possible performance of 6 consecutive trials done by the subject. B) the Intra- and Extra-dimensional set-shifting task (IE/ED) CANTAB. On the left is reported the SD stage in which only one dimension is present (shape). Once the SD and its reversal SDR<sub>e</sub> is completed, a new dimension (line) is introduced and used as a confounder.

While the WCST is commonly used in clinical and psychological studies, a more modern and refined task has been developed, the Intra- and Extra-dimensional set-shifting task (IE/ED). This task is one of the 3 main tests of the Cambridge Neuropsychological Test Automated Battery (CANTAB), together with the tower of London (testing planning functions) and the working memory task. For clarity purposes, I will only describe the IE/ED

tasks, but more details explanations can be found elsewhere (Roberts, Robbins and Everitt, 1988; Barnett *et al.*, 2010).

In the ID/ED, the performance of the testing subjects is evaluated through 9 different and sequential stages with different stimuli and/or rules.

The test starts with a simple discrimination stage (SD) in which only one dimension is presented and the subject has to choose between the two stimuli. After six correct consecutive responses, the reversal stage (SDRE) is introduced, in which the correct choice is inverted. Following several trials of SD and SDRe, the test will introduce compound discrimination, in which a second dimension is aligned (CD1), and then superimposed to the start dimension (CD2). Commonly, the first dimension is the shape of a symbol (see Figure 1B), while the second is the line, and CD2 is followed by the corresponding reversal stage. Then, an intra-dimensional shift is introduced, in which the shapes and lines change, and the first dimension is always the relevant (IDS). This stage is followed by its reversal (IDSR). Finally, once the attentional set is established meaning that the subject is able to follow the adequate dimension, an attentional shifting is introduced in the extradimensional shift stage (EDS). In that EDS stage, the dimension that was previously considered as irrelevant is now considered relevant, while the dimension previously relevant became irrelevant. (Jazbec *et al.*, 2007). Also this stage is followed by its reversal (EDSRE).

Compared to the WCST, the ID/ED task incorporates several metrics to compare cognitive set-formation and shifting abilities, challenging three main forms of cognitive flexibility:

- 1) the intra-dimensional shift: reinforce the cognitive attentional-set towards the specific relevant dimension, improving the task performance
- 2) the reversal learning: allow determining whether the subject can shift from a previously rewarded cue to the previously not-rewarded choice
- 3) the extra-dimensional shift: measure the ability to apply a new strategy that involves disengage and shift from a previously formed cognitive set

Finally, while the psychological test is often based on two-dimensions, ID/ED task allows the same assessment with 3 dimensions, which allows for the differentiation of two distinct cognitive mechanisms during the EDS stage (Owen *et al.*, 1993). That is, using three distinct dimensions allows testing the inability to release attention from a relevant perception dimension during EDS (i.e. perseveration or also called ‘stuck-in-set’). While using only two dimensions, allow testing the inability to re-engage attention to a previously irrelevant dimension during EDS (i.e. ‘learned irrelevance’). Neuropsychological studies in patients diagnosed with schizophrenia have consistently found a deficit in the performance of attentional set-shifting paradigms with both the WCST and the CANTAB ID/ED. Interestingly, the development of these tests allows the acquisition of imaging data, in normal and disease-related patients. For example, dysfunction of the frontal lobe is found in patients with psychologic dysfunction (Weinberger, Berman and Zec, 1986; Owen *et al.*, 1991) or patients diagnosed with schizophrenia that present impairment in the EDS stage (Elliott *et al.*, 1995; Pantelis *et al.*, 1999; Turner *et al.*, 2004; Ceaser *et al.*, 2008). The development of these tests has been of great interest to the understanding of behavioral flexibility in psychiatric disorders and of possible underlying mechanisms mostly

using functional MRI assessments (Kramer *et al.*, 2007; Tyrer *et al.*, 2010; Heisler *et al.*, 2015). However, the neuronal mechanisms underlying the different components of cognitive flexibility using these tasks are still limited by the resolution of currently available techniques. In this context, research in animal studies is proving to be effective, still, an appropriate choice of the correct test must be addressed as briefly explained in the following paragraph.

## Automated two-chamber “Operon” ID/ED task for mice

Recently, the various components of the WCST and ID/ED tasks have been successfully modified and adapted for animal models research (Bissonette and Powell, 2012; Scheggia *et al.*, 2014; Tait, Chase and Brown, 2014). In general, the inter-species conservation of the central nervous system, and the data reported so far suggest that executive function and the brain. Indeed, in humans, non-human primates and rodents, the performance on attentional set-shifting tasks are similar, with a first challenging stage during the first reversal followed by the next challenging stage with the extra-dimensional shift (Roberts, Robbins and Everitt, 1988; Birrell and Brown, 2000; Trobalon *et al.*, 2003; Scheggia *et al.*, 2014).

In 2014 (Scheggia *et al.*, 2014) my group developed a mouse-adapted equivalent and fully automated version of the ID/ED CANTAB. This Operon is characterized by two opposed chambers separated by a transparent Plexiglas door, which is automatically dropped in each trial and allows the mouse to switch to the second chamber (*Figure 2A*). The apparatus has been optimized in order to be testing 2 or 3 different stimuli that could vary in three different perceptual dimensions: visual (*Figure 2B-1*), olfactory (*Figure 2B-3*) and tactile (*Figure 2B-4*) with as the outcome to the relevant dimension a classical sugar pellet (*Figure 2B-2*).

Similarly to the IE/ED CANTAB, the operon is based on the succession of nine stages briefly described below:

- Simple Discrimination (SD) introduces mice to a dimension (odor or light or texture) that is relevant in all the tasks until the EDS. Mice follow one of the two stimuli to receive the reward (*Figure 2C*)
- Compound Discrimination (CD) introduces the second dimension, (light or texture or odor), which is the irrelevant one. The correct and incorrect stimuli are the same as in SD. (*Figure 2D*)
- Reversal of the Compound Discrimination (CDRe) leaves the stimuli and the relevant dimension unchanged, but here the mice learn that the previously correct stimulus is now incorrect. These same conditions will be found for the other reversal phases (i.e., IDSRe, IDS2Re, and EDSRe) (*Figure 2E*).
- Intra-dimensional shift (IDS) introduce new stimuli for both the relevant and irrelevant dimensions (a total change design). However, ensure that the testing subjects keep following the same relevant dimension in order to find the correct response (*Figure 2F*)
- Reversal of the Intra-dimensional shift (IDSRe) uses the same conditions as in CDRe (*Figure 2G*).
- Intra-dimensional shift 2 (IDS2) uses the same conditions as in IDS.
- Reversal of the Intra-dimensional shift 2 (IDSRe2) uses the same conditions as in CDRe.
- Extra-dimensional shift (EDS) changes the role of the dimensions, that is the previously relevant dimension now becomes irrelevant (*Figure 2H*)
- Reversal of the Extra-dimensional shift (EDSRe) uses the same conditions as in CDRe.



At the level of the EDS, two possibilities are based on the 2-dimensions or 3-dimensions design:

- 1) If the paradigm used is of two dimensions, the previously irrelevant now becomes relevant dimension and vice versa;
- 2) if the paradigm used is of three dimensions, the previously irrelevant dimension is discarded, the previous relevant become irrelevant, and the new dimension is introduced and used as relevant. The conditions are the same as the other non-reversal stages;

At the difference of the CANTAB, in the automated version for mice, the IDS/IDSRe stages are repeated under the IDS2 and IDS2Re. This slight difference has been introduced to allow the mice to develop a strong attentional set and to provide with “stronger” conclusion in the EDS.

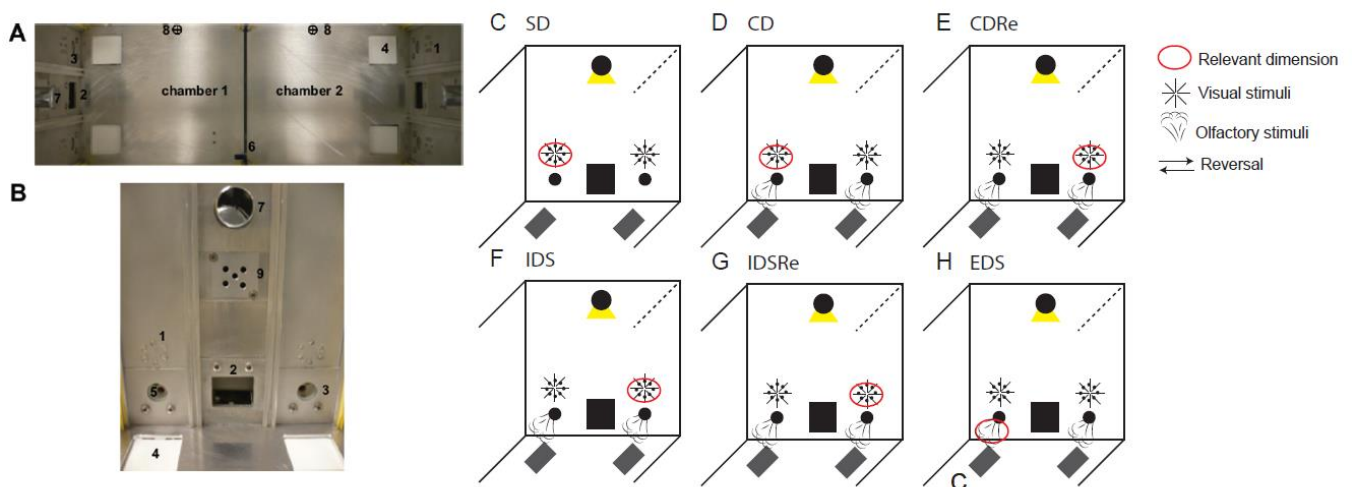


Figure 2. Automatized attentional set-shifting task. A) The two identical chambers of the operon, separated by a door. B) The characterization of each chamber. 1: disposition of the LEDs; 2: food magazine where the sugar pellets will be released in case of correct choice; 3,5: nose pokes, where mice have to poke and where odors come out; 4: texture; 6: plexiglas door; 7: house light; 8: photobeam.

The design of the Operon, based on the CANTAB, has been optimized to allow the mice tested to develop a robust set acquisition towards the correct, in opposition to the incorrect stimulus. This novel operant-based task presents several advantages over previously used ID/ED task for rodents: (1) it has less labor-intensive procedures than the manual versions; (2) it eliminates any source of subjectivity in the measured parameters; (3) it eliminates potential experimental bias due to reinforcement-related cues; (4) it avoids arbitrary environmental conditions; (5) and it allows manipulation of multiple dimensions with a large range of different stimuli, in accordance with the equivalent human tasks used in the clinical setting. Overall, these advantages will enable us to test executive functions in mice, together with the introduction of genetic mutation relevant in schizophrenia and to provide a tool for possible therapeutic approaches, such as drug-screening. Finally, one advantage to apply the CANTAB in mice is the possibility to use a more invasive and robust approach to characterize the participation of structure in a specific behavior. In particular, during my thesis, I took advantage of this novel task to dissect electrophysiological readouts of executive function performance and

the impact of different clinically relevant genetic variants, using a mice model for a classic mutation in schizophrenia. As the symptomatology of schizophrenia together with imaging studies suggest that executive function impairment is associated with dysfunction of the prefrontal cortex (Miller, 2000; Orellana and Slachevsky, 2013; Gruber, Santucci and Aach, 2014), I decided to focus on the mice equivalent, the medial prefrontal cortex.

## The prefrontal cortex (PFC) in executive functions

In human, non-human primate and rodent, executive functions have been associated with prefrontal cortex (PFC) functionality (Yoon *et al.*, 2008; Keeler and Robbins, 2011; Orellana and Slachevsky, 2013; Granseth, Andersson and Lindström, 2015; Zhang *et al.*, 2015). Indeed, the PFC has long been considered to be the main area controlling high-order cognitive functions, including planning, organization and decision making (Ingvar and Franzén, 1974; Weinberger and Berman, 1996; Goldman-rakic, 1998; Karlsgodt *et al.*, 2009). Lesions studies suggest that, while the PFC is typically not necessary for learning and performing simple tasks, the shift of the task requires the change of PFC activity, and affecting such change will significantly slow proper adjustment in behavior. Accordingly, humans with accidental damages to frontal areas often show behavioral impairments that include inflexibility, perseveration, isolation, and apathy (Barrash, Tranel and Anderson, 2000) or antisocial behavior (Anderson *et al.*, 1999). When these patients were tested using the CANTAB, studies report deficits in performance during the EDS, while a low effect on IDS (Owen *et al.*, 1993). Studies using the WCST on patients presenting lesions of the frontal cortex conclude to an increase in “perseverative” compare to “non-perseverative” error (i.e. they frequently continued to sort cards according to a previously acquired rule, even when the rule has been explicitly changed) (Milner, 1963). These conclusions suggest that not only patients with frontal lobe lesions were presenting impairment of cognitive flexibility, but also they were showing “perseverative” behavior. Functional MRI (fMRI) measurements during the ID/ED task and measurements of regional cerebral blood flow (rCBF) during the WCST further confirmed that dorsal PFC is crucially implicated in attentional set-shifting abilities (Hampshire and Owen, 2006). In conclusion, the WCST and the ID/ED of the CANTAB are considered sensitive tasks for revealing PFC dysfunctions, but the limitation of the imaging studies in humans together with the lesions studies cannot provide a clear understanding of the exact role of the frontal cortex in executive functions. Furthermore, it is important to note that the PFC doesn't act on its own but it functions in connections also with other brain regions such the striatum (Chudasama and Robbins, 2006) and the parietal cortex (Fox, Barense and Baxter, 2003; Crowe *et al.*, 2013), making the conclusion based exclusively on PFC activity relatively challenging.

The PFC is often referred to as a single brain region, but many subdivisions into distinct areas have been made, each defined by specific cytoarchitecture, cytochemistry, connectivity, and functional properties. While the cortical anatomy and functions seem to be highly conserved, defining and comparing the functional properties of these areas across species is complex: a large interspecies difference in the layering per area has been described, raising the debate on whether or not rodents possess a region equivalent to the human dorsolateral

PFC. In General, the rodent equivalent to the dorsolateral PFC in humans is the medial PFC (mPFC), as both structures lack a granular zone in this area (Ongur and Price, 2000; Elston, 2003). However, it has been noted that the formation of the general laminar pattern in the PFC shows a relation with phylogenesis. Indeed, in “higher” mammalian species, such as humans and non-human primates, PFC regions possess a granular layer IV, as well as an agranular layer while in rodents, the granular PFC regions are reduced (Ongur and Price, 2000; Elston, 2003). In rodents, the mPFC is classified into three distinct neuroanatomical subregions based on connectivity and cytoarchitecture: the anterior cingulate (ACC), prelimbic (plPFC), and infralimbic (ilPFC) cortices (Vertes, 2004). These three regions have strong homology at the level of their functional and connectivity to the human Brodmann areas 24b, 32, and 25, respectively (Gabbott *et al.*, 2005). The mPFC is mainly composed of glutamatergic pyramidal neurons (~80–90%) and an array of local interneuron populations (~10–20%).

The excitatory pyramidal neurons mediate output projections to other cortical areas such as sensory and association cortices, as well as to subcortical areas of the cognitive circuitry including the striatum, the amygdala, and the postero-parietal cortex.

Neuroimaging studies (rCBF and fMRI) have associated stuck-in-set perseverative scores in attentional set-shifting tasks with reduced activity within the PFC, while other types of perseveration, such as recurrent or continuous, fail to correlate with PFC activity. Moreover, consistent with frontal lobe patients (Owen *et al.*, 1993), lesion studies in non-human primates and in rodents have demonstrated that parts of the PFC have a functional homology to human lateral PFC in attentional set-shifting tasks (Berg, 1948; Milner, 1982; Roberts, Robbins and Everitt, 1988; Dias, Robbins and Roberts, 1996; Birrell and Brown, 2000; Everett *et al.*, 2001; Bissonette *et al.*, 2008; Eling, Derckx and Maes, 2008; Nyhus and Barceló, 2009; Barnett *et al.*, 2010; Keeler and Robbins, 2011; Zhang *et al.*, 2015; Granseth, Andersson and Lindström, 2015).

In particular, damage of the lateral (in primates) or medial (in rodents) PFC impairs set-shifting abilities while sparing reversal learning.

Clinical study of human patients with lesions of the OFC (Rahman *et al.*, 1999), or study lesions in non-primates and rodents (Dias, Robbins and Roberts, 1996; McAlonan and Brown, 2003; Bissonette *et al.*, 2008) have found an impairment of the reversal learning stages, but not the EDS stage. This data suggests a double dissociation or functional specialization between PFC and OFC (Dias, Robbins and Roberts, 1996; Brown and Bowman, 2002; Robbins, 2007; Bissonette *et al.*, 2008). *Similarly, in rodents, lesions of the dorsomedial striatum* revealed a deficit in serial reversal learning (Castañé, Theobald and Robbins, 2010; Clarke *et al.*, 2011). Thus, the neural substrates that control the cognitive functions assessed by attentional set-shifting tasks seem to be well conserved between humans, primates, rats, and mice (Robbins, 2007; Goyal *et al.*, 2008).

## Neural correlates of set-shifting in the PFC

The activity of PFC has been linked in rodents to set-shifting abilities (Rich and Shapiro, 2009; Totah *et al.*, 2009; Cho *et al.*, 2015; Kim *et al.*, 2016). Specifically, two research papers are of great interest for further study. The first one, Kim *et al.*, 2016 (Kim *et al.*, 2016) studied the pre-limbic/intra-limbic (PL/IL) neuronal

activity during a plus-maze task in rats. In that study, two main conclusions emerge: 1) these two regions help the initiation and the establishment of a new strategy (as PL dynamics anticipated learning performance while IL lagged); 2) their activity changed as the rats switch memory strategies while performing identical behaviors, underling the PFC contribution to the coordination of memory strategies.

The second work of interest, (Cho *et al.*, 2015) is based on the fact that a subpopulation of PFC interneurons, co-expressing the calcium-binding protein Parvalbumin (PV), also considers as fast-spiking interneurons (FSI), fire normally at  $\gamma$  frequencies. Using the classically described digging version of the ASST, they found a decrease of the  $\gamma$  rhythms of FSI during specific stages, in particular when the “rule” associated with the reward is shifted. The conclusions of the study underlie that the rule-shifting task measures a specific aspect of cognitive flexibility, that is dependent on the normal functioning of PFC interneurons.

However, in both studies, the exact role of the PFC in the flexibility of cognitive functions, the adaptation to rules, and the processes required for problem-solving are not considered. Additionally, while dopamine activity in the PFC is often associated with behavioral flexibility, both research focuses on the intrinsic properties of the PFC neurons, while ignoring the possible role of dopamine in such functions.

## Dopamine system, PFC, and cognitive flexibility

In schizophrenia, several hypotheses on the emergence of symptoms and the etiology have been proposed, with one of the most robust based on dopamine deficiency (Abi-Dargham *et al.*, 2000; Seeman, 2010, 2013). This dopamine hypothesis has direct implications in therapeutic strategies with the use of antipsychotic drugs targeting D2-receptors for the treatment of schizophrenia symptomatology (Seeman, 2010; Li, L. Snyder and E. Vanover, 2016; Scheggia *et al.*, 2018). This neurochemical view of schizophrenia yielded medications that transformed the treatment of psychosis, and in some cases, result in remission of the positive symptoms of the illness (Amminger *et al.*, 1997; Puri and Steiner, 1998). However, how alterations of D2 signaling might be linked to cognitive flexibility deficits and related treatments is still not clear.

The PFC receives remarkably dense input from dopamine neurons (Carr *et al.*, 1999; Björklund and Dunnett, 2007; Puig, Antzoulatos and Miller, 2014), and, in agreement, dopamine exerts powerful influences on PFC and related executive functions (Gaspar, Bloch and Moine, 1995; Santana, Mengod and Artigas, 2009). Dopamine signaling is processed throughout two distinct classes of receptors based on the associated G-coupled protein: D1-like family, associated with the Gs (excitatory) protein (include subunit D1 and D5) and the D2-like family, associated to the Gi-(inhibitory) protein (include subunit D2, D3 and D4). Interestingly, the D1-like receptors show a lower affinity to dopamine than the D2-like, suggesting a response mostly during the phasic stage of dopamine activity (Girault and Greengard, 2004; Burkett and Young, 2012).

Dopamine D1- and D2-like family receptors often appear to yield the opposite effects in terms of behavioral outcomes and they operate via different intracellular signaling pathways (Vallone, Picetti and Borrelli, 2000; Jenni, Larkin and Floresco, 2017). Furthermore, in several brain structures and specific neurons, but not all, these two classes of receptors are expressed on separate cells (Gaspar, Bloch and Moine, 1995; Hasbi, O’Dowd and George, 2011), but despite these functional and anatomical differences in their expression, animal study

has shown that both D1-like receptors and D2-like receptors were involved in the regulation of cognitive functions (Ragozzino, 2002; Floresco and Magyar, 2006).

Extensive work on the role of D1-signalisation in the PFC has been done using cognitive functions tasks (Vijayraghavan *et al.*, 2007; Takahashi, Yamada and Suhara, 2012; Spencer, Devilbiss and Berridge, 2015), ignoring the possible participation of D2 receptor (DRD2). Indeed, there are evidences suggesting an implication of D2-like family receptors in the modulation of PFC-dependent executive functions. In particular, several studies have found that potentiation of D2 pathways in the PFC of humans, non-human primates, and rodents facilitate executive functions (Glickstein, Hof and Schmauss, 2002; Wang, Vijayraghavan and Goldman-Rakic, 2004; Puig, Antzoulatos and Miller, 2014; Amato, Vernon and Papaleo, 2018; Scheggia *et al.*, 2018). Based on these evidences linking DRD2 to PFC-dependent executive functions, the fact that schizophrenia therapeutic mostly targets DRD2, and the impairment of PFC activity in schizophrenia patients that undergo the CANTAB or the WCST, I focus my work on the role of DRD2 in encoding executive functions.

## Dopamine D2 long (D2L) and short isoform (D2S)

In the central nervous system, DRD2 has two distinct isoforms: the short isoform, D2S, and the long isoform, D2L. These two isoforms are co-expressed in a positive D2L/D2S ratio (Usiello *et al.*, 2000; Kaalund *et al.*, 2014). D2L differs from D2S by the presence of the 29 amino acids in the third intracellular loop, a region involved in the interaction between receptors and G-proteins. D2L and D2S have also different functions. Treatments with the D2-specific agonist, quinpirole, suppress locomotor activity throughout the reduction of dopamine release (Eilam, Golani and Szechtman, 1989; Starke, Gothert and Kilbinger, 1989), while similar treatments with D2 antagonist, haloperidol, increase dopamine release (Boulay *et al.*, 2000). Interestingly, such effects of D2-antagonist have been observed in D2R<sup>-/-</sup> mice, in which both D2L and D2S receptors are suppressed, and not in D2L<sup>-/-</sup> mice, where D2S isoform is conserved. Such results suggest that the preservation of D2R presynaptic responses is ascribed to D2S receptors.

The effect of D1 agonist treatments that increase locomotor activity (Protais, Dubuc and Costentin, 1983) are reduced or abolished in D2L<sup>-/-</sup> mice, suggesting an inhibitory control of the D1-response by D2S. Altogether, these evidences suggest that D2S can be considered to be of crucial interest for presynaptic DRD2 and negatively modulates DRD1-dependent responses (Usiello *et al.*, 2000).

Therapeutic responses to antipsychotic drugs are highly dependent on a strict range of D2 occupancy, with the lower or higher binding being potentially detrimental to neurocognitive functions. It has been suggested that commonly used antipsychotic drugs preferentially bind D2L receptors (Usiello *et al.*, 2000; De Mei *et al.*, 2009). Thus, chronic treatments based on the specific antagonist of D2L-receptors might shift the D2L/D2S balance toward the D2S isoform.

At the difference of D2S, which is considered as a presynaptic form, D2L is often defined as a post-synaptic receptor, which mediates the responses of D2-receptors and their cooperative activities with D1-receptors (Usiello *et al.*, 2000).

In schizophrenia, several studies have found a variation of D2-receptors (Abi-Dargham *et al.*, 2000; Bertolino *et al.*, 2009; Zhang, Lencz and Malhotra, 2010; Kaalund *et al.*, 2014). For example, in a post mortem study, researchers have found an increase of the D2S/D2L ratio, specifically in the dorsolateral PFC of patients diagnosed with schizophrenia. Such perturbations of dopamine signaling in the PFC can thus contribute to cognitive deficits, as unbalance of D2S/D2L ratio is often associated with poor plasticity of the network involved in working memory. Functional genetic variants in the D2 gene might be of high interest to the participation of the D2S/D2L ratio in schizophrenia-related phenotypes (Bertolino *et al.*, 2009). However, the mechanistic that combine D2 genetic variations influencing PFC activity and schizophrenic related executive functions remains unclear.

## The dystrobrevin binding protein 1 (DTNBP1) gene, encoding dysbindin-1

Dysbindin-1, a gene implicated in the regulation of vesicle formation, synaptic release (Chen *et al.*, 2008) and also a key component of the biogenesis of lysosome-related organelles complex (BLOC-1) (Li *et al.*, 2003) is encoded by the dystrobrevin-binding protein 1 gene (DTNBP1). This DTNBP1 gene is widely expressed in human and mouse central nervous system (Benson *et al.*, 2001). Recent studies in mice show that dysbindin-1 is more highly expressed during embryonic and early postnatal development compared to adulthood and BLOC-1 is involved in neurite outgrowth (Ghiani *et al.*, 2010). Altogether, these findings highlight a potential role of dysbindin-1 in the normal development of brain structures and functions.

Together with abnormal neuronal development, mutation of dysbindin-1 has been associated with abnormal behavior in humans, as variation in the *DTNBP1* gene is been shown to play a role in the alterations of cognitive ability (Burdick *et al.*, 2006; Fallgatter *et al.*, 2006; Hashimoto, Noguchi, Hori, Nakabayashi, *et al.*, 2009; Hashimoto, Noguchi, Hori, Ohi, *et al.*, 2009; Luciano *et al.*, 2009; Markov *et al.*, 2009; Wolf *et al.*, 2011). Genetic variations reducing dysbindin-1 expression, impact cognitive abilities in humans as well as in mice (Scheggia *et al.*, 2018) and lead to the up-regulation of D2 receptors available at the neuronal surface (Iizuka *et al.*, 2007).

In the context of schizophrenia, genetic variations, and in particular the single nucleotide polymorphism rs1018381, are often found in patients presenting poor performance in executive control tasks (Straub *et al.*, 2002; Thimm *et al.*, 2010). Such interpretation of the mutation and the behavioral effect are considered to be related to a decrease of neuronal activity in the left superior frontal gyrus and the lateral PFC (Thimm *et al.*, 2010). However, while these two regions are key in the pathophysiology of schizophrenia, their exact correlation with the genetic mutation remains unknown. Additional evidences suggest that variability in the dysbindin gene, and in particular the polymorphism rs1047631, contribute to interindividual differences during cognitive performance, and in particular working memory capacity (Wolf *et al.*, 2011).

Several studies have found a correlation between genetic variation in DTNBP1 and psychiatric conditions. One of the first reports for schizophrenia, was provided by the Irish Study of High-Density Schizophrenia

Families that include 1770 individuals (Straub *et al.*, 2002). Subsequent studies have confirmed the link between DTNBP1 and schizophrenia in multiple, independent populations (Schwab *et al.*, 2003; Van Den Bogaert *et al.*, 2003) and it remains among the leading candidate genes in meta-analyses (Allen *et al.*, 2008). Relatively common SNPs and/or combinations of them (haplotypes) in DTNBP1 have been associated with schizophrenia. Most of these variants were reported to confer an increased risk to develop schizophrenia, but five studies also reported haplotypes conferring protection against (i.e., reduced risk for) the disorder (Kirov *et al.*, 2004; Williams *et al.*, 2004; Vilella *et al.*, 2008; Hashimoto, Noguchi, Hori, Ohi, *et al.*, 2009).

Patients diagnosed with schizophrenia generally have lower expression levels of dysbindin-1 mRNA and protein in the cortex and hippocampus, regions commonly associated with dysfunction of executive control and working memory (Talbot *et al.*, 2004; Weickert *et al.*, 2004, 2008; Tang *et al.*, 2009). The cause of altered dysbindin-1 gene and protein expression found in schizophrenia is probably not limited to the DTNBP1 haplotypes reported to be associated with the disorder.

An animal model of dysbindin-1 functions is available in the sandy (dys) mouse (*Figure 3*), which has a naturally occurring deletion mutation of exons 6 and 7 in the gene (DTNBP1) encoding of the mouse protein. The mutation results in loss of dysbindin-1 in homozygous animals. Mice with disrupted dysbindin (*dys*<sup>-/-</sup>) show selective alterations in internal trafficking of specific components related to dopamine and glutamate signaling, including D2 receptors and NR2A receptor subunits (Karlsgodt *et al.*, 2011; Papaleo *et al.*, 2012).

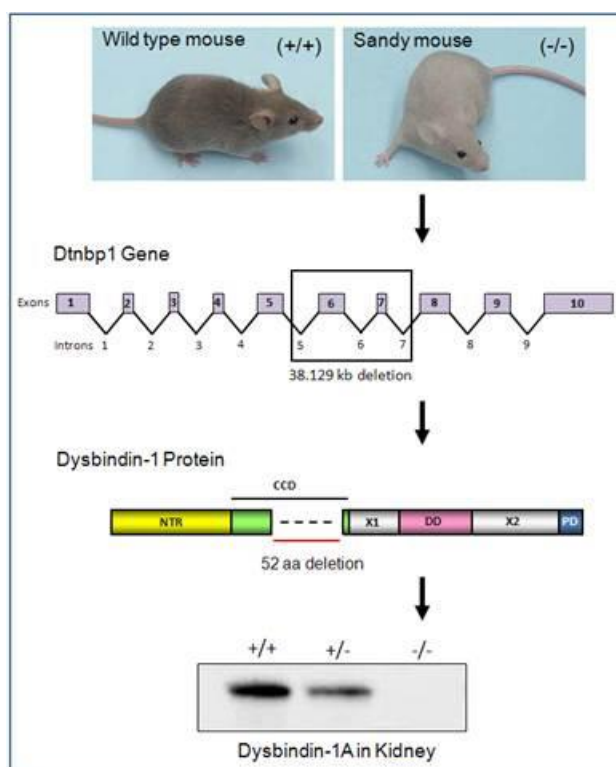


Figure 3. WT mice vs Sandy (*dys*<sup>-/-</sup>) mice. Here are reported: the DTNBP1 gene, with the square around the two exons (6 and 7) of the gene deleted in *dys*<sup>-/-</sup> mice, and the Dysbindin-1 protein with the part deleted in *dys*<sup>-/-</sup> mice.

Studies using cortical neuronal cultures taken from *dys*<sup>-/-</sup> mice have shown signaling alterations that may underlie the deficits in cognitive performance. In particular, dysbindin-1 has been associated with various aspects of synaptic function in both dopamine and glutamate neurons (Cox *et al.*, 2009; Dickman and Davis, 2009; Papaleo and Weinberger, 2011). *In vitro* experiments suggest that *dys*<sup>-/-</sup> mice have increased cell surface expression of the dopamine D2 receptor due to an increase in the rate of the membrane insertion (Ji *et al.*, 2009). In particular, pyramidal excitatory neurons of the PFC layer II/III recorded in *dys*<sup>-/-</sup> mice showed an increase in their activity together with a decrease of the D2-mediated response compare to WT mice (Ji *et al.*, 2009; Papaleo *et al.*, 2012). Not only the impairment of dysbindin-1 functions affect dopamine signaling, but evidence suggests an impairment of glutamatergic signaling (Numakawa *et al.*, 2004).



## Aims of the thesis

The overarching goal of my thesis work was to understand at the level of single-cell activity how the PFC encodes cognitive flexibility, adaptation to behavioral strategies switches, and problem-solving processed.

In particular, I wanted to focus on the exact role of the dopaminergic signaling found in the PFC in the context of executive functions, their possible implication in psychiatric disorders, and their related therapeutic approaches.

Because, intrinsic limitation of human studies and imaging do not allow temporal and spatial resolution required for the understanding of such aims, I used genetically modified mice together with single-unit *in vivo* recording in freely behaving mice that underwent the Operon ID/E.

These overall objectives were addressed through two aims, based on the normal and clinically relevant model:

### *Specific aim 1.* How do the PFC neurons encode different phases of cognitive flexibility in a WT mice model?

Using *in vivo* recordings in freely moving mice performing the Operon ID/ED, I first tested the involvement of the mPFC in different part of this cognitive task. In particular, using two different approaches, the first one based on oxygen level consumption and the second one based on single-cell recording, I tested the specific timestamp of the PFC participation. Oxygene level consumption has been selected to provide parallelism to human studies, while single-cell recording was chosen to provide the time resolution needed to understand the participation in different stages of the complex behavioral task used. In particular, the recorded signals were analyzed in relation with the presentation of different cognitive rules (i.e.. simple discrimination, simple and serial reversal, attentional control within and between different dimensions), different dimensions (i.e. olfactory or visual), and during the different phases of the cognitive challenge (i.e. when mice started to be presented with a new rule to follow or when they acquired that specific rule).

### *Specific aim 2.* How do clinically-relevant and dopamine-related functional genetic variants affect cognitive flexibility and/or PFC-neuronal activity?

Here, I wanted to focus on dopamine/D2-relevant functional genetic variants with clear clinical relevance for schizophrenia and its pharmacological treatments. As explained above, I used three different models of genetically modified mice. The first one with the hemideletion of the gene encoding dysbindin-1 (dys+/-), the second one with the depletion of the dopamine D2-receptor long isoform (D2L +/-). Finally, due to the evidence of the molecular interactions between Dys1 and D2L, we used a mouse model with the hemideletion of both (dys+/- x D2L+/-), further characterized as double-mutant. Similarly to what has been done in specific

aim 1, I tested the effect of each individual mutation in the cognitive flexibility using the OperonID/ED. Finally, I used single-cell recording in vivo, to first characterize the effect of the genetic variations on PFC neuronal activity, but also the effect on the way PFC neurons encode behavioral flexibility.

## Materials and Methods

**Animals.** All procedures were approved by the Italian Ministry of Health (Animal license n. 230/2009-B) and strictly adhere to the recommendations in the Guide for the Care and Use of Laboratory Animals of the National Institutes of Health. Dys-heterozygous (dys+/-), D2L +/- and wild-type (dys/D2L +/+) littermate mice were generated using controlled breeding between male heterozygous double mutant (dys +/- x D2L+/-, DM) with female WT mice (C57BL/6J, Charles River Laboratories (France)). For all offspring the genotype was confirmed at two stages points, weaning period and termination, using ear snips and tails DNA. All adult male mice used in this study were between 3 to 7 months of age. Animals were cage housed with 2 to 4 littermates. During the entire period of the experiments, mice's environmental conditions were controlled with a temperature (  $22^{\circ}\text{C} \pm 2^{\circ}\text{C}$ ) and a dark/light cycle maintained (lights ON 07.00-19.00). All animals were given ad libitum access to water and behavioral testing occurs during the light phase. Different cohorts of naïve mice were used for every single experiment. Experimenters were blind to the genotype during testing.

### **ID/ED Operon task.**

*Apparatus.* The experimental apparatus consisted of two identical chambers with Plexiglas walls and aluminum floor (16 x 16 x 16 cm for each chamber), connected to a PC equipped with MED-PC IV software (Med Associates, St. Albans, VT, USA). Chambers were separated by a transparent Plexiglas door. The door could be automatically dropped to allow the mouse to change the chamber. Each chamber presented two nose-poke holes with infrared photobeams (ENV-314M), and, between them, a food magazine with photo beams (ENV-303M) where a pellet dispenser delivered the food reinforcement (ENV-203-14P). A fan and a houselight (ENV-315M) were located above each of the two food magazines. Each nose-poke hole was equipped with a series of changeable stimuli that could vary in three different perceptual dimensions (odor, view, tact). For *olfactory stimuli*, liquid odorant was diluted in mineral oil (1:20; M5904, Sigma Aldrich) and presented on paper filter disc (15uL, 2 cm) enclosed in metal pods placed on a rotating wheel mounted beside each nose-poke hole outside the chambers. There were ten different odor stimulus exemplars that were possible to be presented to the testing subject. For *visual stimuli*, light-emitting diodes (LED) were placed on top of each nose-poke hole. Up to six different colors stimulus exemplars were possible to be presented to the testing subject. For *tactile stimuli*, changeable floor textures were mounted in front of each nose poke hole. There were up to ten different textures of stimulus exemplars when possible. Thus, the discriminative association between a correct response (which will result in food delivery) and a nose poke hole could be varied by their odor, visual cue or the floor texture.

*Testing.* To conduct the behavioral tests I used the two-dimension ID/ED paradigm, with odor and light as stimuli selected (Scheggia *et al.*, 2014). For habituation to the apparatus, in the first two days, mice were put for 60 minutes in the apparatus with only neutral stimuli (Habituation 1), trained to move from one chamber to the other (Habituation 2) and the third day, mice were trained to perform two randomly presented simple discriminations (e.g. lights on vs. lights off; apricot vs. lemon) so that they were familiar with the stimulus

dimensions (Habituation 3). A criterion of 8 correct choices out of 10 consecutive trials was set for the mice to complete each following testing stage. The time from the raising of the middle door divider to a nose-poke response and the time to finish each stage were also recorded. Each session was terminated after 40 minutes or if a mouse failed to make any response for five consecutive minutes, whichever came first. The test was then continued the next day. The order of the discriminations was always the same, but the dimensions and the pairs of exemplars were randomly changed and equally represented within groups and counterbalanced between groups (*Table 1*).

Stage	Dimension		Discrimination1		Discrimination2		Discrimination1		Discrimination2	
	Relevant	Irrelevant	LIGHT/ODOR		LIGHT/ODOR		ODOR/LIGHT		ODOR/LIGHT	
SD	Light	Odor	<b>L1</b>	L2	<b>L1</b>	L2	<b>O1</b>	O2	<b>O1</b>	O2
CD	Light	Odor	<b>L1/O1</b>	L2/O2	<b>L1/O2</b>	L2/O1	<b>O1/L1</b>	O2/L2	<b>O1/L2</b>	O2/L1
CDRe	Light	Odor	<b>L2/O1</b>	L1/O2	<b>L2/O2</b>	L1/O1	<b>O2/L1</b>	O1/L2	<b>O2/L2</b>	O1/L1
IDS	Light	Odor	<b>L3/O3</b>	L4/O4	<b>L3/O4</b>	L4/O3	<b>O3/L3</b>	O4/L4	<b>O3/L4</b>	O4/L3
IDSRe	Light	Odor	<b>L4/O3</b>	L3/O4	<b>L4/O4</b>	L3/O3	<b>O4/L3</b>	O3/L4	<b>O4/L4</b>	O3/L3
IDS2	Light	Odor	<b>L5/O5</b>	L6/O6	<b>L5/O6</b>	L6/O5	<b>O5/L7</b>	O6/L8	<b>O5/L8</b>	O6/L7
IDS2Re	Light	Odor	<b>L6/O5</b>	L5/O6	<b>L6/O6</b>	L5/O5	<b>O6/L7</b>	O5/L8	<b>O6/L8</b>	O5/L7
EDS	Odor	Light	<b>O7/L7</b>	O8/L8	<b>O7/L8</b>	O8/L7	<b>L5/O7</b>	L6/O8	<b>L5/O8</b>	L6/O7
EDSRe	Odor	Light	<b>O8/L7</b>	O7/L8	<b>O8/L8</b>	O7/L7	<b>L6/O7</b>	L5/O8	<b>L6/O8</b>	L5/O7

Table 1. An example of the ID/ED ‘stuck in set’ paradigm adapted and modified from previous studies (Garner et al., 2006; Papaleo et al., 2008). SD: Simple Discrimination; CD: Compound Discrimination; CDRe: Compound Discrimination Reversal; IDS: Intra-Dimensional Shift; IDSRe: Intra-Dimensional Shift Reversal; IDS2: Intra-Dimensional Shift 2; IDS2Re: Intra-Dimensional Shift 2 Reversal; EDS: Extra-Dimensional Shift; EDSRe: Extra-Dimensional Shift Reversal. Pairs of stimuli (either ‘Discrimination 1’ or ‘Discrimination 2’) are randomly presented in each stage, and the mouse must choose the correct stimulus in each pair. In the first stage (SD or simple discrimination), the stimuli presented in the two holes differed along one of three dimensions and the mouse is rewarded for choosing the correct exemplar. Mice were counterbalanced so that half received light as the initial relevant dimension, other half received odor. In the example table 1, the correct exemplar is reported in bold. Stimuli: L1: blue. L2: yellow. L3: white. L4: orange. L5: red. L6: green. L7: yellow+white. L8: blue+orange. O1: vanilla. O2: lavender. O3: strawberry. O4: cinnamon. O5: peach. O6: sage. O7: oregano. O8: grapefruit.

The performance was measured in all phases of all experiments using a number of trials to reach the criterion; time (in minutes) to reach the criterion; time (in seconds) to make a response (latency to respond). A session started when a mouse was placed in one of the two chambers where all the stimuli were neutral. Then the transparent door was dropped to give the mouse access to the other chamber where the stimuli cues were on.



Figure 4. Timeline of experiments. Mice had to perform 4 types of habituations (from hab1 to hab3 2) to become familiar with the apparatus. After successes all of them, they are stopped two days with all the food put back into the cage, they were undergoing surgery, and after one week of recovery (in which they were put back to food restriction in the last 3 days), they started again with the last habituation (hab3 2), and finally tested through the entire stages of the task.

**Surgery.** After successfully completing stages hab 1, hab 2, hab 3 odor/light and hab 3 light/odor of the ID/ED Operon task (*Figure 4*), mice were prepared for cranial implantations surgery. Mice were deeply anesthetized using vaporized isoflurane (2% in O<sub>2</sub>) before to be positioned on a mice stereotaxic mask (Kopf) using mice ear-bars and mice nose-mask. Following careful shaving of the mice head, a small cutaneous application of anesthetic cream and the administration i.p. of painkiller (Baytril) and antibiotic (Ketophrene) a large transversal cut was done on the mice head skin. Skull was prepared using peroxide hydrogen (H<sub>2</sub>O<sub>2</sub>), 2 to 4 anchor screws (FST, Heidelberg, Germany) and in skull scratches. Next, a small unilateral cranial window was performed above the PFC (side were randomized) and the tetrodes/electrodes were gently lowered to reach half their final distance. In order to protect the brain from infection and to avoid movement artifact, tetrodes/electrodes were surrounded by a fast-curing silicone (Kwik-Kast silicone elastomer, World Precision Instruments) and the entire apparatus affixed using dental cement acrylic. Two reference electrodes further used as ground and reference electrodes were prior positioned above the cerebellum and then connected to their appropriate channel on the recording implant.

In my experiment, two groups of animals were recorded using either a multielectrode arrays design or a custom-made movable tetrode design. The microelectrode array (Neuronexus, Michigan) is based on a 16 channels vertical configuration located on 4 equally distant shanks (A4x3mm-100-125-177-Z16). Individual channel impedance was set at 1M $\Omega$  and a contact surface of 177 $\mu$ m<sup>2</sup> was used to favorize single unit acquisition. The second design using tetrodes (Axona, Ltd.) was set as 4 twisted tetrodes (tungsten 12 $\mu$ m, #M408870, CFW) with their impedance adjust at 0.4M $\Omega$  using the goal-cyanided coating.

Both implants were positioned within (for the non-movable multielectrode design) or halfway (for the tetrodes configuration) to the PFC using the coordinates AP: +1.9 mm; ML: 0.30 mm; DV: -2.5 mm (the mouse brain atlas Paxinos and Watson, 1998). The tetrode configuration allows us to move each electrode individually, and prior to all recording I daily adjust their dorsoventral position by 50-100 $\mu$ m to reach the dorsal edge of the PFC.

**Electrophysiology recording.** For both implant types, extracellular activity was acquired using a mouse-adapted head-stage (ZIF-Clip® 16-Channel Microwire Array, TDT, Florida) and a Cheetah acquisition system (Neuralynx, Bozeman, USA). To avoid any constraint the rotation of the animals was compensated using an automated commutator (Saturn X, Neuralynx). Individual signal channels were acquired at 32KHz, prior to being band-pass filtered at 300-9000Hz and digitally stored. After a week of recovery, in a single-cage housing mode, all the mice were tested in the ID/ED Operon task to repeat the last habituation stage prior to surgery for habituating them to the head-stage. After this, they were tested through all the stages of the task and the PFC activity was recorded (*Figure 4*). At the end of the behavior test, a 500 $\mu$ A current was passed throughout each channel (electrolesions) and mice were deeply euthanized using urethane (2g/kg) before to be transcidentally perfused with phosphate buffer solution (PBS, 20-30ml) and paraformaldehyde (PFA, 4% in PBS, 20-30 ml). Brains were collected, conserved 24h in 4% PFA (post perfusion) and then conserved in a cryo-protective solution (30% sugar in PBS) before to be coronally slice using a microtome (50 $\mu$ m thick slice, VT1200 Leica). Brain tissue slices were then mounted on glass coverslips and stained with Nissl staining (Nissl based mounting medium) before to be examined on a fluorescent microscope (Nikon). A NeuroLucida system (MBF Bioscience, Vermont, USA ) was used to scan and reconstruct brain slice together with the exact localization of the recording site. Mice that present signs of infection, poor recovery to the surgery, poor implant stability or misplacement of the electrode/tetrodes were discarded of all further analyses.

**Data analysis of electrophysiology recording.** All recorded data were analyzed offline after the experiments. Each daily session of recordings was loaded on a personal computer with the data analyses software Spike2 15.0 (Cambridge electronic department, CED). Prior to analyses, signals were band-pass filtered at 300-5000Hz to remove any persistent movement artifact and action potentials were extracted using built-in functions. In order to obtain single units sorting, only action potential presenting a signal-ratio-noise (SNR) of their amplitude of more than 1/3 were analyzed (1.5 of the standard deviation of the overall signal), (Lewicki, 1998; Tolia *et al.*, 2007; Vyazovskiy *et al.*, 2009; Rey, Pedreira and Quian Quiroga, 2015). Action potentials (AP) were then further sorted using a semi-automatic approach based on the principal component analyses (PCA) using the AP waveform, a refractory period of 2ms, the variation of the AP waveform (<95% of the confident interval), the inter-spike-interval (ISI) distribution histogram and the PCA-cluster analyses. A recorded neuron was considered as a single unit if it was presenting all these parameters (Olcese, *et al.*, 2013) and was conserved on the same channel during the entire recording period.

Prior to any further analyses, the firing activity (express in Hz) and the variability of the firing activity (defined as the coefficient of variation, CV) during the recording session were used to further characterize the neurons into putative interneurons or putative pyramidal neurons.

Because the number of sessions and the number of single-unit recorded during each session present a very strong variability, I pooled together all the units recorded during each stage, without considering their individual location in the trial number. This allows me to not biased the results, considering that I could not be certain that two units recorded on the same electrode on two consecutive days were originating from the same neuron. Similarly, due to the low-firing activity of the principal cells in the PFC, I discarded all cells with a firing rate of  $<0.1$ Hz that could not be clearly identified due to an insufficient PCA and waveform comparison.

One major obstacle in my analyses was the variability in the latency to respond to the cue, that was apparently affected in genetically mutated mice. This leads me to use 6 behavioral events to normalized my data: response to the light stimulus (CUE), correct response (CORRECT), incorrect response (INCORRECT), collection of the reward (REWARD) and entry inside the food magazine in case of incorrect response (NO REWARD). The time period prior to the CUE and the REWARD/NO REWARD was then considered as the inter-trial interval (ITI).

Based on the distribution of each neuron using the firing activity and CV, I could distinguish 4 clusters: 1)Low Firing/low CV, 2)High firing/High CV, 3)Low firing/High CV and finally 4) High firing/Low CV. Once the action potential timestamp of each neuron was extracted and converted into Matlab, I performed two separate analyses. The first one based on the variation of the firing activity normalized to the ITI of each stage using z-score normalization, the second one using the average firing rate between each relevant period of the stage. The first one provides a higher time resolution, but is strongly dependent on the variability of the firing rate; the second allows a pairwise analysis for each neuron with a loss of time resolution. Changes in the neuronal activity were compared in the behaviorally relevant phases:

- the entire period of the latency to respond (defined as the time between the presentation of the cue and the response) plus 3 seconds of baseline;
- the entire period of latency to reward /no reward (defined as the time between the response and the entry inside the food magazine) plus 3 seconds of baseline.

The z-score was calculated as follow:

$$Z = \frac{\text{observed\#of spikes} - \text{mean}(\text{observed\#of spikes in the 3 seconds of baseline})}{\text{SD}(\text{observed\#of spikes in the 3 seconds of baseline})}$$

For each event, a 10 ms time bin was used for the analysis of the firing rate in the window considered.

The raw firing activity was extracted as a number of spike per second (Hz) during the entire period of the response or the reward/no reward.

**Chronic Oxygen Probes Implants and Brain ppO<sub>2</sub> measurements.** Brain partial pressure of oxygen (ppO<sub>2</sub>) was measured with an Oxylite system (Oxford Optronics, UK) using a fiber-optic probe designed for chronic implantation in mice brain tissues. The probes consist of a Teflon holder with a fiber optic of 1.8 mm in length and 250 µm in diameter. The Oxylite system detects the oxygen quenching of the fluorescence generated by a dye (platinum(II) meso-tetra-pentafluorophenyl-porphine) embedded into the tip of the probe by an optical pulse in an oxygen-dependent fashion. The probes are pre-calibrated by Oxford Optronics in solutions of multiple temperatures and PO<sub>2</sub> values (Ortiz-Prado *et al.*, 2010). The probe was implanted in medial PFC (X=+0,3; Y=+1,9; Z=-2,4 from Bregma) according to the Paxinos and Franklin mouse brain atlas coordinates using the similar surgical procedure as above. Healthy conditions were monitored daily for one week after surgery procedure, before starting tests.

PpO<sub>2</sub> was recorded in the ID/ED Operon task chamber during a daily session of 40 min of the test. Baseline oxygen level and resting oxygen levels were recorded in the home cage respectively for 15min and 10min, before and after the test session. PpO<sub>2</sub> was recorded every 2 s (2Hz) and digitized using the ANY-maze software (Stoelting Co.). There were no significant signs of inflammation or gliosis.

**Statistical analyses.** Results are expressed as mean±standard error of the mean (s.e.m.) throughout the thesis. Electrophysiology data of each genotype were analyzed using a one-way repeated measure ANOVA, followed by Tukey post hoc tests. The behaviors were analyzed using a two-sample t-test, followed by Bonferroni correction. The comparison of the behavior between different genotypes was analyzed using a two-sample t-test, followed by Bonferroni correction. Statistical analyses were performed using Origin.



## Results

### 1) Selective increase of oxygen consumption in mice mPFC during the extradimensional set shift stage of the Operon ID/ED

Similar to imaging data in humans, attentional set-shifting abilities and the dependence of PFC have been corroborated in non-human primates, rats, and mice using lesions, pharmacological and genetic studies (Berg, 1948; Milner, 1982; Roberts, Robbins and Everitt, 1988; Dias, Robbins and Roberts, 1996; Birrell and Brown, 2000; Nagahama *et al.*, 2001; Everett *et al.*, 2001; Bissonette *et al.*, 2008; Eling, Derckx and Maes, 2008; Nyhus and Barceló, 2009; Barnett *et al.*, 2010; Keeler and Robbins, 2011; Zhang *et al.*, 2015; Granseth, Andersson and Lindström, 2015). In the clinical setting, using fMRI analyses, it is commonly reported that a preponderant altered engagement of the PFC is evident and correlated with executive-function deficits in patients diagnosed with SCHIZOPHRENIA when tested in the IDS/EDS test of the CANTAB or in the analogous category shift of the WCST.

To study the mPFC activity in mice performing the ID/ED Operon task with some proxy measure of similar assessments done in fMRI human studies, I then first used an amperometry oxygen approach, implanting Carbon paste electrodes in the mPFC of wild-type mice (*Figure 5*). This method measuring oxygen consumption has been correlated with the blood-oxygen-level-dependent (BOLD) contrast imaging (Ortiz-Prado *et al.*, 2010) used in functional magnetic resonance imaging (fMRI) in humans.

Following similar MRI protocols in humans, I measured the partial pressure of oxygen (ppO<sub>2</sub>) during each stage of the ID/ED Operon task and compared this activity to the resting-state immediately after the test (*Figure 6*). Only the values of oxygen consumption in the EDS stage were significantly higher compared to its own resting state and all other stages (repeated measures ANOVA, interaction stages resting  $F(1,2)=28,957$ ;  $p=0.032$ ; post hoc  $p<0.05$  vs EDS Resting and other stages). Conversely, I did not find differences in the other stages vs resting state. These data confirmed with a similar measurement between humans and mice, that in the ID/ED Operon task there is a higher PFC engagement during the EDS stage, which requires major fatigue and activity.

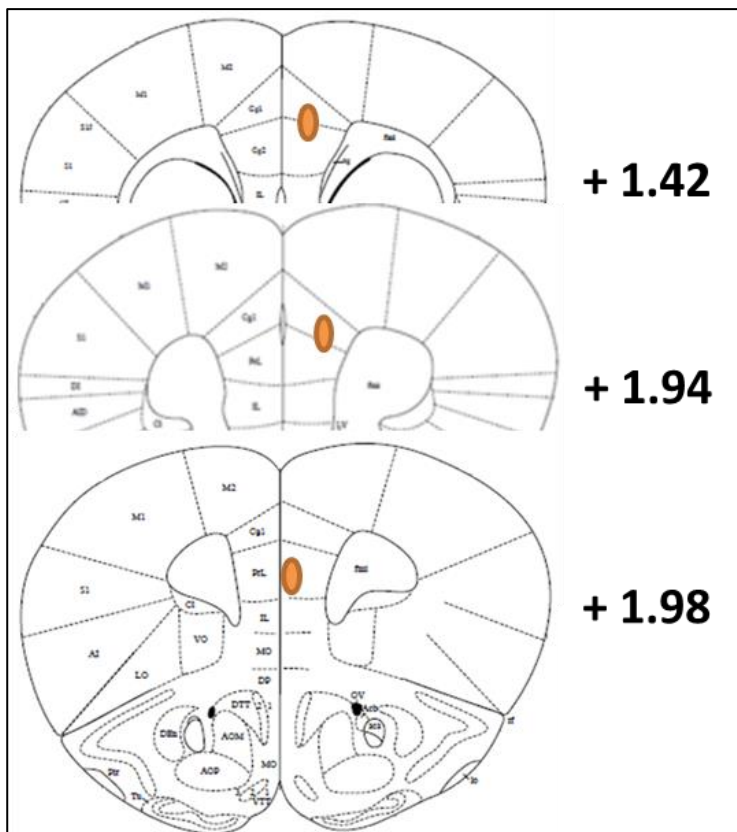


Figure 5. Stereotaxic positioning of the oxytometry carbon paste electrodes implanted in the mPFC of WT mice. The graphical representation is based on the dorsoventral coordinates on the Mice brain Atlas. N=3 mice.

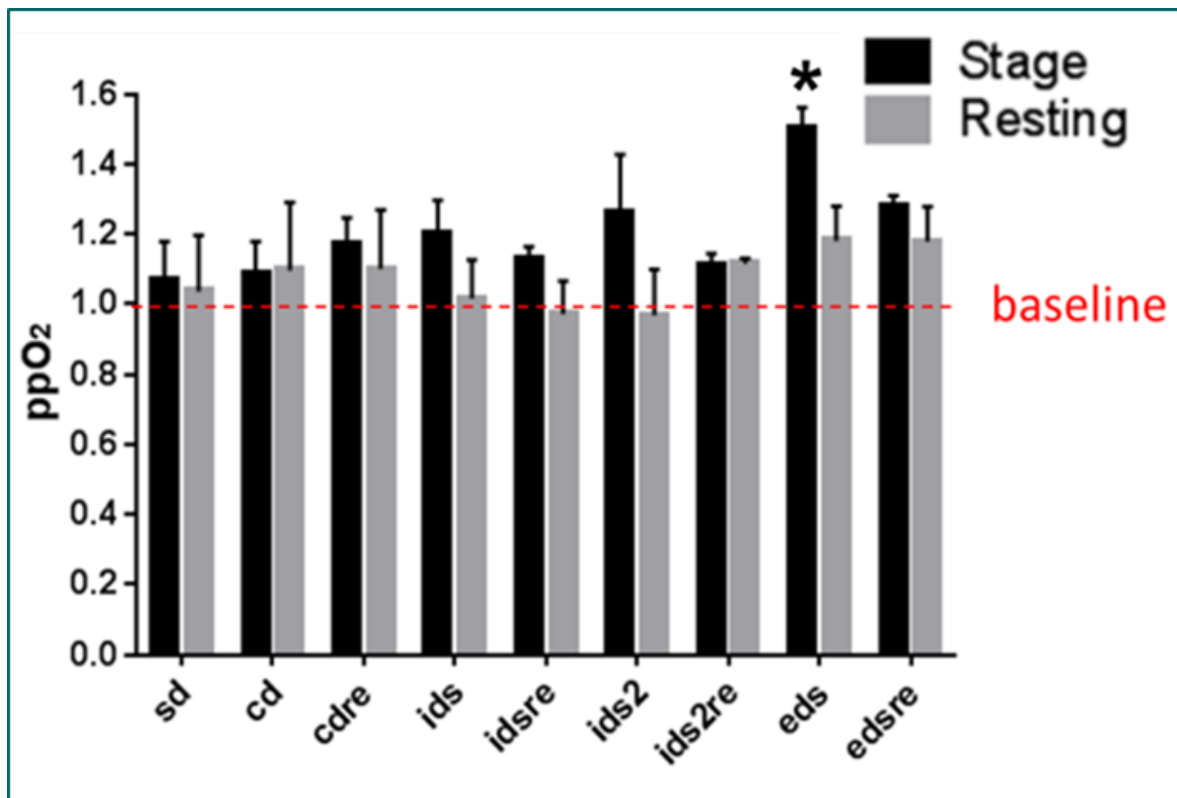


Figure 6. Consumption of oxygen in mPFC during the different stages of the task of WT mice. SD: Simple Discrimination; CD: Compound Discrimination; CDRe: Compound Discrimination Reversal; IDS: Intra-Dimensional Shift; IDSRe: Intra-Dimensional Shift Reversal; IDS2: Intra-Dimensional Shift 2; IDS2Re: Intra-Dimensional Shift 2 Reversal; EDS: Extra-Dimensional Shift; EDSRe: Extra-Dimensional Shift Reversal. Red dashed line: baseline recorded before the beginning of the task. Black bar: consumption of oxygen recorded during the performance of the task. Grey bar: consumption of oxygen recorded 10 minutes after the test when mice returned to the homecages. Statistics: \*  $p < 0.05$ , EDS Stage VS EDS Resting. Data are expressed like mean  $\pm$  SEM. N=3 mice.

## 2) The behavior of WT mice with silicon probes

Similar to what has been reported using imaging studies in humans, my data on the oxygen consumption supported an implication of the PFC in ID/ED set-shifting. However, two major limitations appear, the first one is the time resolutions (previously discussed) and the second is that oxytometry results are only an indirect indication of the neuronal population within the PFC. Thus, to directly investigate the neuronal activity of the mPFC during every single phase of the ID/ED Operon task, following training and implantation, I performed an *in vivo* extracellular recording of mPFC neurons activity in wild-type (wt) mice performing the ID/ED automated operon task.

I used a linear multi-site extracellular electrode, with a design containing 4x4shanks for a total of 16 recording sites: this design is sufficient to cover the entire mPFC (*see Material&Methods*).

My initial experiments involved 12 mice that were chronically implanted, and to reduce the number of experimental animals, all the mice were first pre-screened and trained on our protocol prior to undergoing the surgical implantation (*Figure 4*). The majority of tested mice (9/12, 75%) completed the test within a short period of time (10.88 $\pm$ 1.25 days) while the remaining mice (3/12, 25%) were not able to fully complete the

test (criterion <8/10 for 6 consecutive days). Following behavioral testing, posthoc analyses of the electrode placement were done using immunohistochemistry (*Figure 7*). Due to the misplacement of the electrode, I exclude one mouse from further analyses.

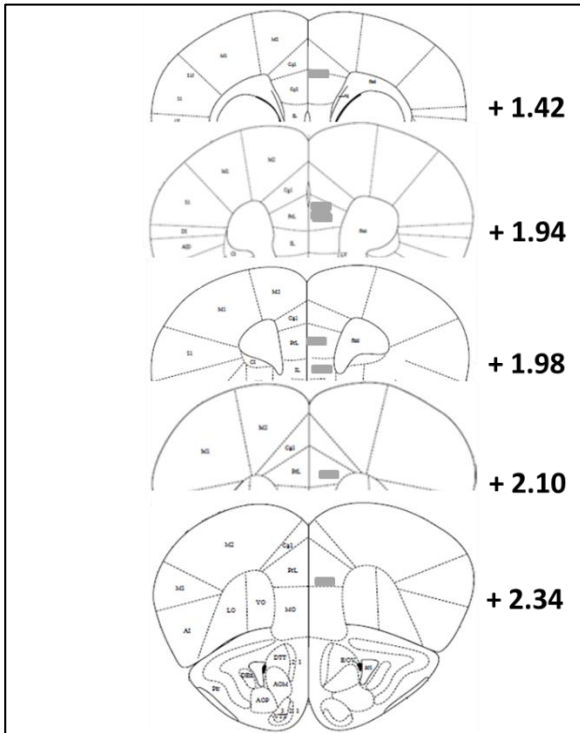


Figure 7. Stereotaxic positioning of the silicon probe electrodes implanted in the mPFC of WT mice. The graphical representation is based on the dorsoventral coordinates on the Mice brain Atlas. N=8 mice.

An initial analysis of the behavioral performance of the remaining mice (8/12) revealed an increase of the trial and time to reach criterion in the CDRe stage compare to the immediate previous stages (CD). These results are in agreement with our previous observations from naïve mice with no prior surgery or implant, and support the expected increase of difficulty to complete the first reversal stage (Scheggia *et al.*, 2014). Similarly, to our previous report using the ID/ED Operon, I found an improvement of the behavior, as reported by the number of trial to criterion, during the following reversal stages (IDSRe, IDS2Re, and EDSRe). These results confirm the ability to the tested mice to face repeated reversal following the first exposition. Following the completion of the CDRe stage, I found a decrease in the number of trials and time to reach the criterion using a stage by stage comparison. However, in contrast to what we observed in mice naïve to surgery/implant, I did not observe a significant increase in the number of trials required to solve the EDS stage compared to the previous IDS stages for both trials and time to reach criterion (*Figure 8, 9*).

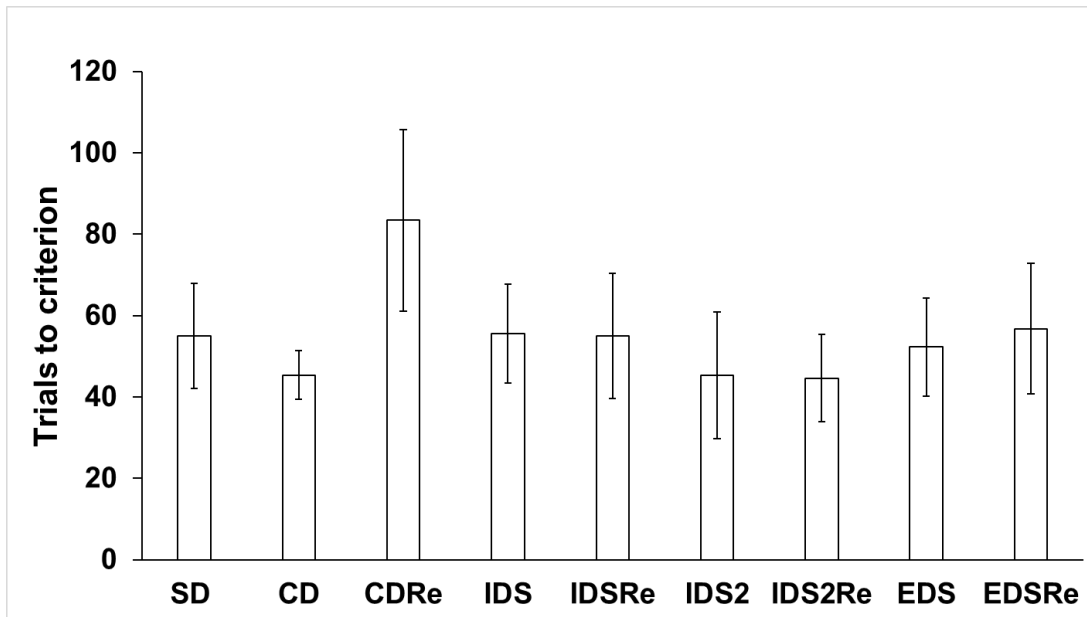


Figure 8. The number of trials to reach the criterion of WT mice. Following testing of mice implanted for extracellular recording, I obtained the number of trials to reach the behavioral predetermined criterion. SD: Simple Discrimination; CD: Compound Discrimination; CDRé: Compound Discrimination Reversal; IDS: Intra-Dimensional Shift; IDSRe: Intra-Dimensional Shift Reversal; IDS2: Intra-Dimensional Shift 2; IDS2Re: Intra-Dimensional Shift 2 Reversal; EDS: Extra-Dimensional Shift; EDSRe: Extra-Dimensional Shift Reversal. Data are expressed as Mean $\pm$ SEM. N=8 mice.

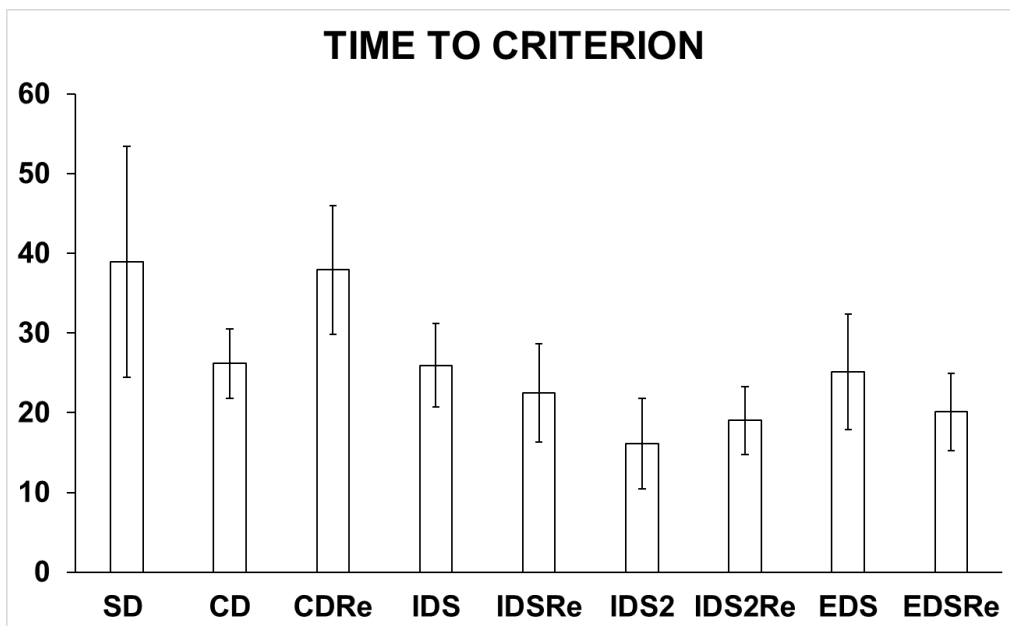


Figure 9. The time spent to reach the criterion of WT mice. Following testing of mice implanted for extracellular recording, I obtained the time spent to reach the behavioral predetermined criterion. SD: Simple Discrimination; CD: Compound Discrimination; CDRé: Compound Discrimination Reversal; IDS: Intra-Dimensional Shift; IDSRe: Intra-Dimensional Shift Reversal; IDS2: Intra-Dimensional Shift 2; IDS2Re: Intra-Dimensional Shift 2 Reversal; EDS: Extra-Dimensional Shift; EDSRe: Extra-Dimensional Shift Reversal. Data are expressed as Mean $\pm$ SEM. The time is in minutes. N=8 mice.

However, a more refined analysis revealed that half of these mice (4/8) were showing an increased number of trials and time needed to reach the criteria in the EDS stage, while the other half did not show it (*Figure 10*). The EDS stage is the most sensitive stage of this task, and it is the stage that has been consistently and selectively reported to depend on the proper functioning of the mPFC (Dias, Robbins and Roberts, 1996; Birrell and Brown, 2000; Bissonette *et al.*, 2008). Thus, while I did not observe any sign of infection or major lesions during the implantation, it remains possible that the surgery and/or the implantation of the silicon probes might be influencing the behavior in this specific stage. It will be interesting to see in further study, if low- to moderate-lesions of the PFC, similar to what I induced using the electrode implantation, affect the EDS stage. Because of the variability in the behavioral test, with half the mice showing difficulties during the EDS stage, I pooled together and then analyzed separately the two groups of mice, based on their behavior (*see paragraph 3, Extra Dimensional Shift (EDS)*). During the analyses of the electrophysiological recording, mice showing an abnormal behavior during the EDS stage can be then used to compare with the other stages without the potential confounding factor linked to the EDS increase of the number of trials and test duration. Interestingly, this comparison appears to be a condition paralleling equivalent cognitive human assessments with fMRI. In the cases of human imaging, comparing brain activity between two different periods require a similar design and conditions. Based on that, differences in brain activity might be interpreted as a different engagement of that particular brain region to achieve an equivalent level of behavioral performance.

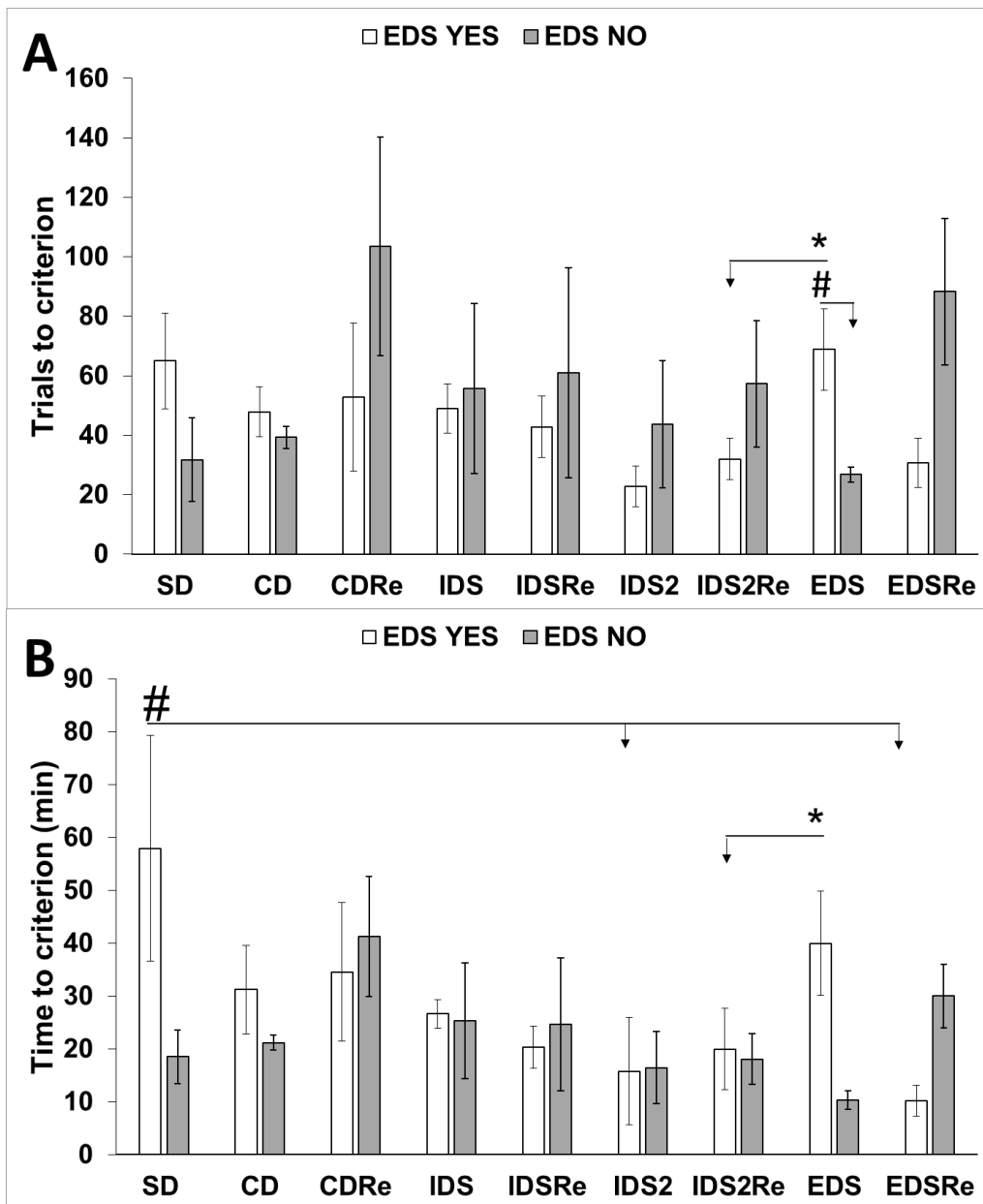


Figure 10. The number of trials and time to reach the criterion of two different groups of WT mice. A) Trials to criterion. B) Time to criterion. SD: Simple Discrimination; CD: Compound Discrimination; CDRe: Compound Discrimination Reversal; IDS: Intra-Dimensional Shift; IDSRe: Intra-Dimensional Shift Reversal; IDS2: Intra-Dimensional Shift 2; IDS2Re: Intra-Dimensional Shift 2 Reversal; EDS: Extra-Dimensional Shift; EDSRe: Extra-Dimensional Shift Reversal. EDS YES: mice that performed in a correct way EDS (n=4). EDS NO: mice that performed in a wrong way the EDS (n=4). White bars: trials to the criterion of WT with EDS YES. Gray bars: trials to the criterion of WT EDS NO. Statistics: A)\*  $p < 0.05$ , EDS WT EDS YES vs IDS2Re WT EDS YES. #  $p < 0.05$ , EDS WT EDS YES vs EDS WT EDS NO. B) #  $P < 0.05$ , SD wt EDS YES vs IDS2 WT EDS YES, EDSRe WT EDS YES. \*  $p < 0.05$ , EDS WT EDS YES vs IDS2Re WT EDS YES. Data are expressed as Mean $\pm$ SEM. Time is in minutes. N=4 for each group.

Following this preliminary observation, I hypothesized that the implantation of a rigid and immovable extracellular electrode composed of 4 shank of 50 $\mu$ m might affect the normal functioning of the PFC, due to potential lesions. To test that hypothesis, I tested a second cohort of animals (n=7 WT mice) using a custom-design Microdrive with 4 tetrodes that were individually mobile. Not only this tetrode design allows smaller

tetrodes (4x12 $\mu$ m), but also the custom-made drive allows me to slowly move in a dorsoventral axis the tetrodes, reducing the pressure on the brain during implantation and allowing to screen a much bigger surface of the PFC. Finally, considering the discomfort given by the head-implant, I also modified the food magazine of our apparatus. This new 3D-printed design was adjusted in order to have the pellet-collector extruding out of the apparatus wall, allowing the mice to collect the sugar pellet without touching the walls.

These experiments were performed more recently, so the electrophysiological analyses for these mice are still ongoing and not included in this thesis. Concerning the behavioral performance of these mice (tetrodes implanted mice), I found that their overall behavioral performance during CDR<sub>e</sub> was increased, similarly to our previous report (Scheggia *et al.*, 2014). Similarly, the performance of the mice during the following reversal stages was similar to classical results, and so confirmed the acquisition of the attentional set. Finally, during EDS, I found a significant increase in the trials and time to reach the criterion in a similar amplitude as the one previously reported (*Figure 11, 12*). In particular, the number of trials to reach the criterion was significantly higher in EDS compared to those in SD, CD, IDS, and EDS<sub>Re</sub> (ONE WAY repeated measure ANOVA,  $F(8,48)= 2.82329$ ,  $P= 0.01191$ , posthoc HSD TUKEY:  $P_{EDSvsSD}= 0.0038$ . Paired t-test, Bonferroni correction, ,  $P_{EDS\_vs\_CD}= 0.01469$ ;  $P_{EDS\_vs\_IDS}= 0.04411$ ;  $P_{EDS\_vs\_EDSRe}= 0.01669$ ). I next tested the time to reach criterion, and found a significant increase during EDS compared to SD, CD or IDS (ONE WAY repeated measure ANOVA,  $F(8,48)= 3.83169$ ,  $P= 0.00149$ , posthoc HSD TUKEY:  $P_{EDSvsSD}= 7,51213E-4$ ;  $P_{EDSvsCD}= 0.00875$ ;  $P_{EDSvsIDS}= 0.00224$ )

These findings confirm that implantation itself is not a problem for the correct performance of the task. However, I could not conclude if the restoration of the expected behavior was due to the size of the implant, the ability to move the electrode, or the novel design of the pellet magazine.



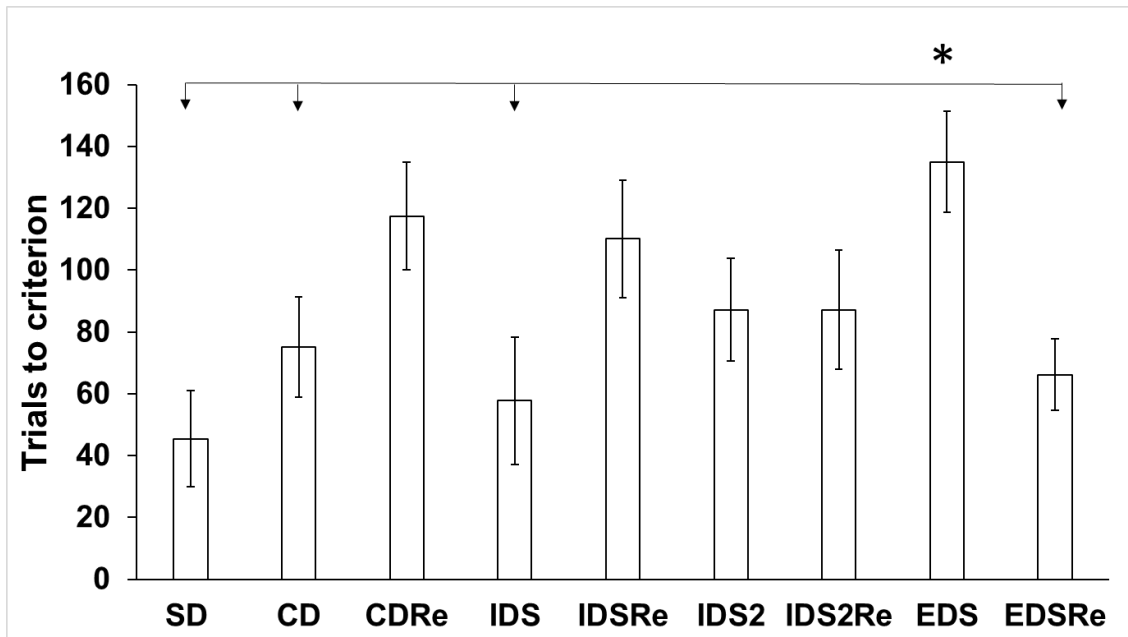


Figure 11. The number of trials to reach the criterion of WT mice. Following testing of mice implanted with Microdrives for extracellular recording, I obtained the number of trials to reach the behavioral predetermined criterion. SD: Simple Discrimination; CD: Compound Discrimination; CDRe: Compound Discrimination Reversal; IDS: Intra-Dimensional Shift; IDSRe: Intra-Dimensional Shift Reversal; IDS2: Intra-Dimensional Shift 2; IDS2Re: Intra-Dimensional Shift 2 Reversal; EDS: Extra-Dimensional Shift; EDSRe: Extra-Dimensional Shift Reversal. Statistics: \*  $p < 0.05$ , EDS vs SD, CD, IDS, and EDSRE. Data are expressed as Mean  $\pm$  SEM. N=7 mice.

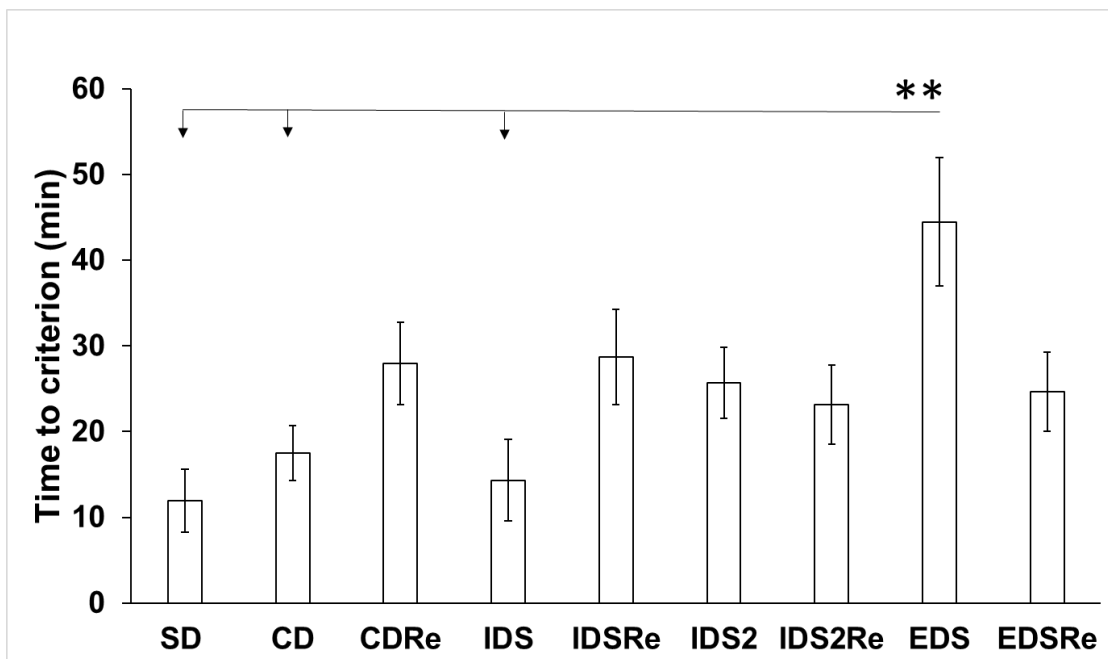


Figure 12. The time spent to reach the criterion of WT mice. Following testing of mice implanted mice with Microdrives for extracellular recording, I obtained the time spent to reach the behavioral predetermined criterion. SD: Simple Discrimination; CD: Compound Discrimination; CDRe: Compound Discrimination Reversal; IDS: Intra-Dimensional Shift; IDSRe: Intra-Dimensional Shift Reversal; IDS2: Intra-Dimensional Shift 2; IDS2Re: Intra-Dimensional Shift 2 Reversal; EDS: Extra-Dimensional Shift; EDSRe: Extra-Dimensional Shift Reversal. Statistics: \*\*  $p < 0.01$ , EDS vs SD, CD, and IDS. Data are expressed as Mean  $\pm$  SEM. Time is expressed in minutes. N=7 mice.

In order to better understand the behavioral output of the 1<sup>st</sup> group, I performed additional analyses. These analyses were not produced in our previous report and were expected to provide a better understanding of the mice's behavior during the different stages. In particular, I focused on the latency to respond, characterized as the time between the onset of the cue presentation and the onset of the nose poke, defined as the period of decisional processing. Based on the accuracy of the behavioral output, I could divide such latency as “latency to correct” or “latency to incorrect”. Overall, I found that the latency to make a choice was variable across stages, with the latency during SD greater than all other stages (*Figure 13*) (ONE WAY repeated measure ANOVA,  $F(8,120)= 8,84148$ ,  $P=0.01191$ , posthoc HSD TUKEY:  $P_{SDvCD}= 0,0038$ ;  $P_{SDvCDRe}= 5,63645E-5$ ;  $P_{SDvIDS}= 4,88415E-7$ ;  $P_{SDvIDSRe}= 1,99502E-7$ ;  $P_{SDvIDS2}= 6,1136E-7$ ;  $P_{SDvIDS2Re}= 8,74431E-6$ ;  $P_{SDvEDS}= 3,45381E-8$ ;  $P_{SDvEDSRe}= 3,92103E-7$ ). This adaptative latency seems to suggest an improvement over time of the animal response time and the possibility to develop a habituation behavior to the operant conditioning.

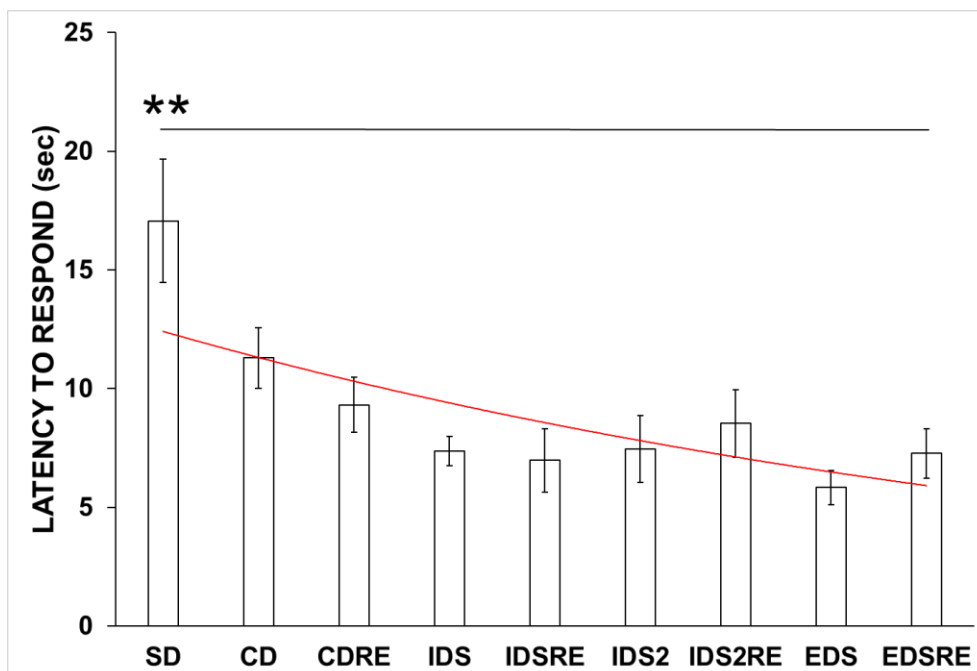


Figure 13. Latency to respond of WT mice. It represents the time, in seconds, between the delivery of the cues and the responses. SD: Simple Discrimination; CD: Compound Discrimination; CDRe: Compound Discrimination Reversal; IDS: Intra-Dimensional Shift; IDSRe: Intra-Dimensional Shift Reversal; IDS2: Intra-Dimensional Shift 2; IDS2Re: Intra-Dimensional Shift 2 Reversal; EDS: Extra-Dimensional Shift; EDSRe: Extra-Dimensional Shift Reversal. Red line: the exponential trend of the values across the different stages. Statistics:  $**p<0.01$ , SD vs CD,CDRe,IDS,IDSRe,IDS2,IDS2Re,EDS,EDSRe. Data are expressed as Mean $\pm$ SEM. N=7 mice.

I next separated each trial based on the accuracy of the response. I found that the latency decrease across stages for both correct and incorrect outcomes. In particular, the latency to correct choice was higher in the SD stage compared to IDS2Re or EDS (*Figure 14*) (ONE WAY repeated measure ANOVA,  $F(8,56)= 2,84081$ ,  $P= 0,01013$ , posthoc HSD TUKEY:  $P_{SDvIDS2Re}= 0,03707$ ;  $P_{SDvEDS}= 0,00302$ ); in the case of an incorrect decision making, the latency in SD was always higher than the latency for all the other stages (*Figure 14*) (ONE WAY repeated measure ANOVA,  $F(8,56)= 7,23162$ ,  $P= 1,53591E-6$ , posthoc HSD TUKEY:  $P_{SDvCD}= 0,00681$ ;

$P_{SDvCDRe} = 3,16176E-4$ ;  $P_{SDvIDS} = 9,61843E-6$ ;  $P_{SDvIDSRe} = 1,24851E-5$ ;  $P_{SDvIDS2} = 1,30061E-5$ ;  $P_{SDvIDS2Re} = 9,03645E-4$ ;  $P_{SDvEDS} = 1,03105E-5$ ;  $P_{SDvEDSRe} = 8,12079E-6$ ). Interestingly, I did not find any differences in the between stages latency for a correct or incorrect decision making (*Figure 14*).

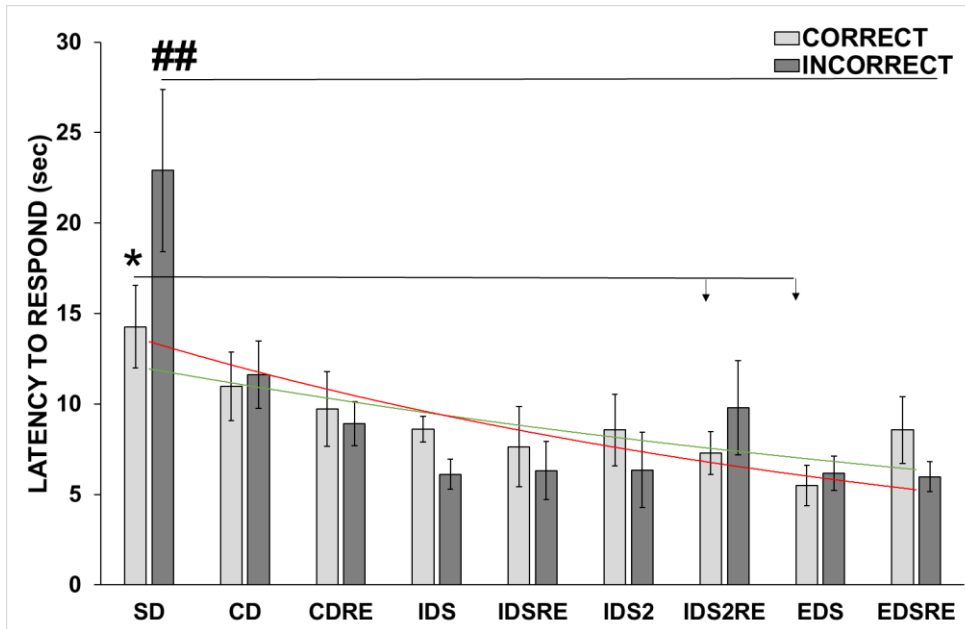


Figure 14. Latency to correct and incorrect responses of WT mice. They are the time, in seconds, between the delivery of the cues and the correct and incorrect responses. SD: Simple Discrimination; CD: Compound Discrimination; CDRe: Compound Discrimination Reversal; IDS: Intra-Dimensional Shift; IDSRe: Intra-Dimensional Shift Reversal; IDS2: Intra-Dimensional Shift 2; IDS2Re: Intra-Dimensional Shift 2 Reversal; EDS: Extra-Dimensional Shift; EDSRe: Extra-Dimensional Shift Reversal. Light gray bar: latency to correct responses. Dark gray bar: latency to incorrect responses. Green line: the exponential trend of the latency to correct responses across the different stages. Red line: the exponential trend of the latency to incorrect responses across the different stages. Statistics: \* $p < 0.05$ , SD correct vs IDS2Re correct, EDS correct. ##  $p < 0.01$ , SD incorrect vs CD incorrect, CDRe incorrect, IDS incorrect, IDSRe incorrect, IDS2 incorrect, IDS2Re incorrect, EDS incorrect, EDSRe incorrect. Data are expressed as Mean $\pm$ SEM. N=7 mice.

A second analysis that could provide a better understanding of the mice's behavior was the latency to collect the reward (in the case of correct outcome).

Interesting, I found that the latency to collect following correct trial was lower in the IDS2 compare to the previous IDS stages ( $P=0.03438$ ) (*Figure 15*). When the relevant dimension was changed (EDS), the latency to reward was significantly higher than previous stages, and in particular the immediately prior stage IDS2 ( $P=0.033$ ).

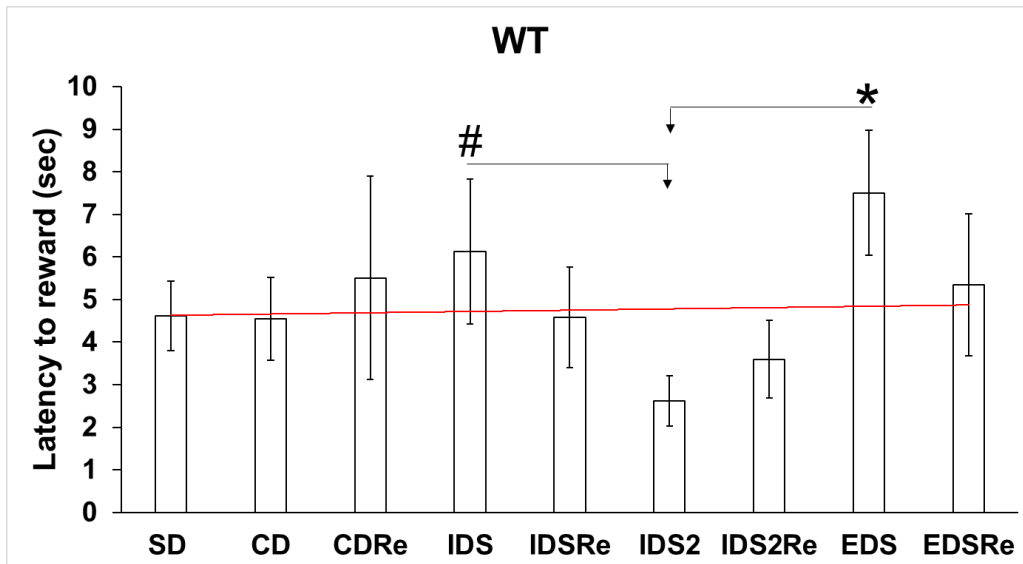


Figure 15. Latency to reward of WT mice. It is the time, in seconds, between a correct poke and the time of the first head entry to the food pellet magazine. SD: Simple Discrimination; CD: Compound Discrimination; CDR<sub>e</sub>: Compound Discrimination Reversal; IDS: Intra-Dimensional Shift; IDSR<sub>e</sub>: Intra-Dimensional Shift Reversal; IDS2: Intra-Dimensional Shift 2; IDS2Re: Intra-Dimensional Shift 2 Reversal; EDS: Extra-Dimensional Shift; EDSRe: Extra-Dimensional Shift Reversal. Red line: the exponential trend of the latency to reward across the different stages. Statistics: #  $p < 0.05$ , IDS vs IDS2. \*  $p < 0.05$ , EDS vs IDS2. Data are expressed as Mean  $\pm$  SEM. N=7 mice.

### 3) Electrophysiology of WT implanted with silicon probes

I recorded the neuronal activity of PFC using well-identified single units during the entire performance. The analyses reported here are based on all the mice implanted with silicon probes analyzed together in one pool or separated based on their performance during the EDS state (*see above in paragraph 2*).

For all stages, neurons were grouped independently of their position within the completion of the stage. As I show before, the period between the cue delivery and the decision making (1) and the period between the decision making and the reward collection (2) are highly affected in the different stages. And so, I decided to analyze the neuronal activity of the PFC during several behavioral events as set stimuli for the electrophysiology analysis (*Figure 16*).

In particular:

- **Cue event:** defined as the moment to which the visual/olfactory cues are delivered
- **Correct event:** defined as the moment to which the mouse produces a correct poke in response to the cue. Following that behavioral outcome, a delay of 10ms is generated before the sugar pellet delivery in the correct side and the reward falls down in the food magazine (latency 10ms);
- **Reward event:** defined as the moment to which the reward is delivered, this event is always associated to an auditory cue resulting from the pellet dispenser servo-motor and the pellet falling within the magazine
- **Incorrect event:** defined as the moment to which the mice produce an incorrect poke in response to the cue. Following that behavioral outcome, a 5s period where the house-light is turned On, as a signal for the incorrect response.

- **House-light event:** Defined as the entire period where the house light is turned ON in response to incorrect decision..

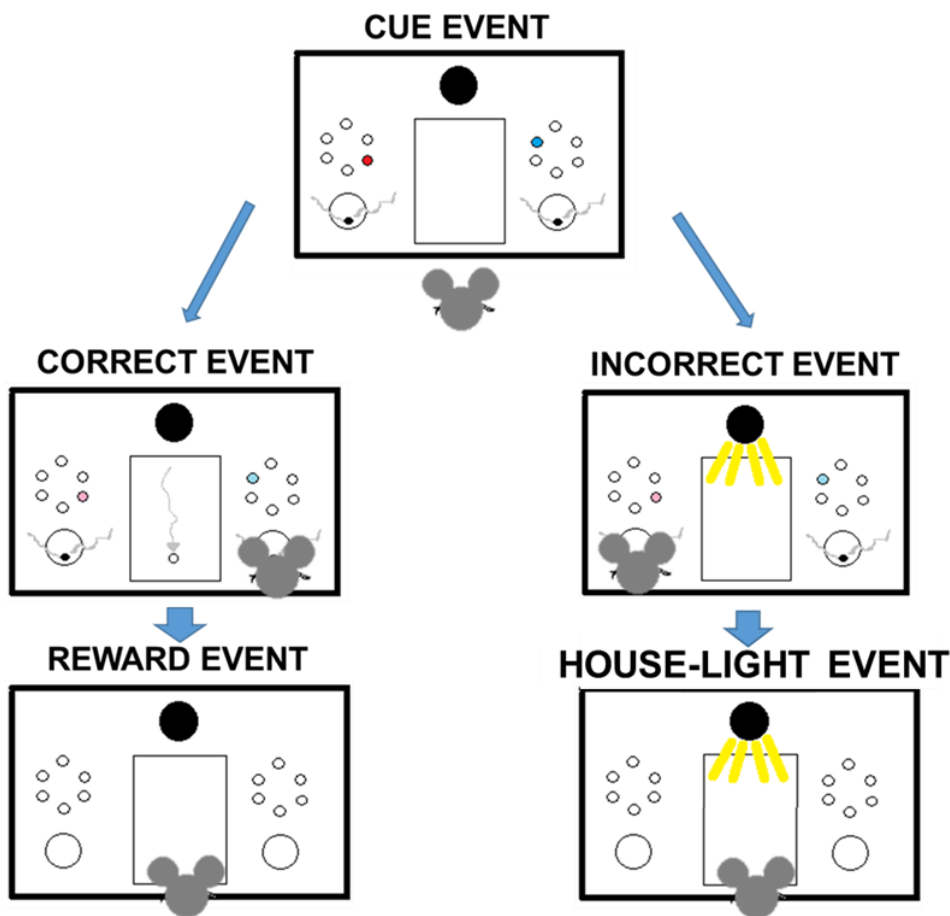


Figure 16. Behavioral events considered for electrophysiological analysis. These events are the main events of the task characterized a correct (CUE, CORRECT, REWARD) or incorrect (CUE, INCORRECT, HOUSE-LIGHT) trial.

One of the challenging aspects of in vivo electrophysiology recording of PFC neurons is the low firing activity of the principal neurons (Stark *et al.*, 2013; Blaaser, Connors and Nurmikko, 2017). Indeed, these neurons also called pyramidal neurons have a firing activity of less than 1 Hz when recorded in freely behaving mice (Lee *et al.*, 2016). Because the extraction of action potential (spike sorting) is based on the comparison of different components of the action potential shape (principal component analyses, PCA), a neuron with low firing will result in the oversampling (increase noise artifact) or downsampling (elimination action potential). Similarly, detection of variation in the firing rate of slow-firing neurons have often been shown to be challenging, and require careful sampling (Dautan *et al.*, 2016). Thus, I made the decision to extract only neurons that were clearly identified as single units and presenting a signal-ratio-noise higher than 3. While this approach does not allow me to analyse multi-unit activity (MUA) due to the low number of neurons sampled, it allows us to be confident that the units analyzed were clearly identified as single unit. Additionally, because the recordings were performed throughout different consecutive days, and I could not be certain that from day-to-day the

same neuron was conserved, I conservatively decided to analyze every single-unit individually without considering a possible conservation between stages or days.

During the spikes sorting, I had to discard an animal from the analysis for a large amount of noise in the traces, and therefore for the impossibility to obtain a clean neuronal signal.

From all animals recorded (n=7), a total of 172 single units were recorded across the entire behavioral testing. Because there are different types of neurons in the mPFC, I tried to distinguish them using classically defined clustering (Scheggia *et al.*, 2020) and see if there was an electrophysiological effect due to a specific type of neuron across stages. To classify neurons, I considered the average firing rates (Hz) and the coefficient of variation (CV). The CV is a standardized measure of the dispersion of a probability distribution or frequency distribution based on the formula:

$$CV = \frac{\text{STANDARD DEVIATION (Firing rate)}}{\text{MEAN (Firing rate)}}$$

Based on the previous report using optogenetic identification or large-scale recording, I decided to clusters my recorded unit based on their average firing rate and their CV:

- SLOW&REGULAR → average firing rate ≤ 0.6 Hz; CV ≤ 2;
- SLOW&BURSTY → average firing rate ≤ 0.6 Hz; CV > 2;
- FAST&REGULAR → average firing rate > 0.6 Hz; CV ≤ 2;
- FAST&BURSTY → average firing rate > 0.6 Hz; CV > 2.

As expected, in all the stages of the task, the great majority of the neurons that I recorded belong to the group of SLOW&REGULAR and SLOW&BURSTY neurons (*Figure 17*), considered as putative pyramidal neurons (Stark *et al.*, 2013). Indeed, a bursting factor is very difficult to identify based on the CV only, due to the use of the standard error in the formula, that introduce a firing rate effect. For that slow-firing neurons were considered as pyramidal.

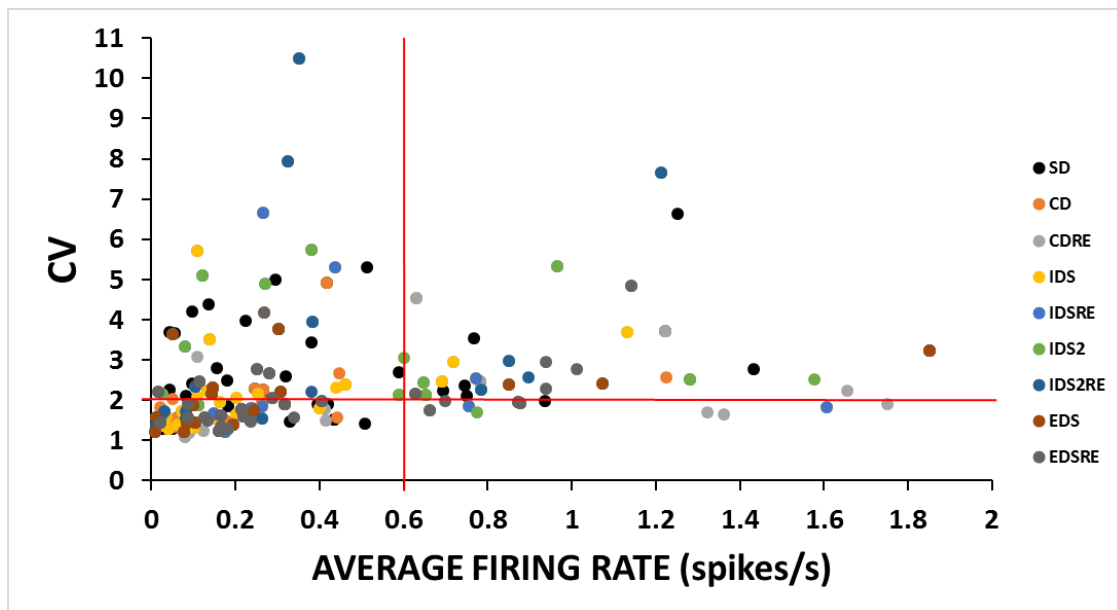


Figure 17. Type of single-unit recorded in WT mice. Each color represents a different stage of the task. SD: Simple Discrimination; CD: Compound Discrimination; CDRe: Compound Discrimination Reversal; IDS: Intra-Dimensional Shift; IDSRe: Intra-Dimensional Shift Reversal; IDS2: Intra-Dimensional Shift 2; IDS2Re: Intra-Dimensional Shift 2 Reversal; EDS: Extra-Dimensional Shift; EDSRe: Extra-Dimensional Shift Reversal. X-axis: average firing rate of the single units, expressed in the number of spikes per second. Y-axis: Coefficient of Variation: STANDARD DEVIATION (FIRING)/MEAN(FIRING). Red lines: delimitations for characterized the 4 different groups of single-units. N=7 mice.

For the successive analyses, I first focused on the variation of the firing activity in the proximity of specific events, and in particular the time of correct poke and the time of incorrect poke, using peristimulus time analyses, considering bin of 10ms amplitude, and using normalized z-score analyses. For proper analyses, I normalized the z-score to the firing rate during baseline. Due to the great number of neurons, and to previous reports in the PFC, I considered the firing rate variation as binomial distribution, that allowed me to consider a significant change to the baseline as presenting an increase of the z-score of  $<or>$  of 1.96. Because I could not be confident that neurons presenting a firing rate  $<0.1\text{Hz}$  were not oversampled, and due to limitations in the analyses, I discarded all units with an average firing activity  $<0.1\text{Hz}$  in the intervals considered.

The PSTH (peristimulus time histogram) were divided into different periods and normalized using z-score normalization for a 3s period defined as immediately preceding the mean + 2SD of the cue delivery time.

In case of correct choice to the cue delivery:

- 1) PRE-CUE DELIVERY: is defined as the period to which less than 40% of the cue has been delivered, and is considered as a period immediately before the cue is delivered for the majority of the trials ( $-2$  standard deviation from the mean cue delivery period).
- 2) CUE DELIVERY: is defined as the period to which for most of the trial (95%) the cue has been delivered and is defined as the mean  $\pm$ SEM.

- 3) **DECISION MAKING:** is defined as the period to which there were for less than 40% of trials the cue has to be presented, defined as mean +2SD. For the majority of the trials, this period will correspond to the decision-making period, where the animal is giving the choice to produce a correct or an incorrect response.
- 4) **POST-DECISION:** it is defined as the period to which the decision has been made and bordered by the mean+SEM of the reward collection (in the case of incorrect “and the food magazine entries”)
- 5) **REWARD:** is defined as the period to which the animals have been receiving the reward and collect it in more than 95% of the trials (mean  $\pm$ SEM).
- 6) **POST-REWARD:** is defined as the period to which for most of the trial (>95%) the animal has received the reward and is now considered as the inter-trial interval.

In case of incorrect choice to cue delivery:

- 1) **PRE-CUE DELIVERY:** is defined as the period to which less than 40% of the cue has been delivered, and is considered as a period immediately before the cue is delivered for the majority of the trials (-2 standard deviation from the mean cue delivery period).
- 2) **CUE DELIVERY:** is defined as the period to which for most of the trial (95%) the cue has been delivered and is defined as the mean  $\pm$ SEM.
- 3) **DECISION MAKING:** is defined as the period to which there were for less than 40% of trials the cue has to be presented, defined as mean +2SD. For the majority of the trials, it will correspond to the decision-making period, where the animal is giving the choice to produce a correct or an incorrect response.
- 4) **POST-DECISION/ HOUSE LIGHT:** is defined as the time period in which the house light is turned on as a sign of wrong response (5 seconds);
- 5) **POST HOUSE LIGHT:** it is the time period after the 5 seconds of house light. I decided to take 3 seconds, as the baseline before the PRE-CUE DELIVERY period.

Here, I will describe the variation of the firing activity in the 9 different stages of the task.

## 1. SIMPLE DISCRIMINATION (SD)

In the 7 recorded animals, I collected recordings for a total period of 16 days across all animals ( $1.17 \pm 0.18$ ). The number of neurons recorded was 52, and the number of neurons analyzed was 23.

During the intertrial interval, the firing rate was  $0.18 \pm 0.04$  Hz, and no significant difference was found for correct and incorrect trials (paired t-test,  $p=0.097$ ), so I pooled together the average activity. The activity decreased during the correct post-decision period ( $0.09 \pm 0.02$  Hz; paired t-test,  $p=0.02$ ) and the reward collection ( $0.05 \pm 0.02$  Hz; paired t-test,  $p=0.005$ ). But for the same period, no effect was found during incorrect trial (paired t-test,  $p>0.05$ ). For all other epochs in correct and incorrect trials, no significant differences in the average firing rate were observed (paired t-test,  $p>0.05$ ). Pairwise comparison of the variation of the firing rate



using paired t-test in correct and incorrect show that the firing was significantly higher during the cue period associated with correct trials compared to incorrect ( $p=0.036$ ). All other comparisons were not showing any significant differences ( $p>0.05$ ) (Figure 18).

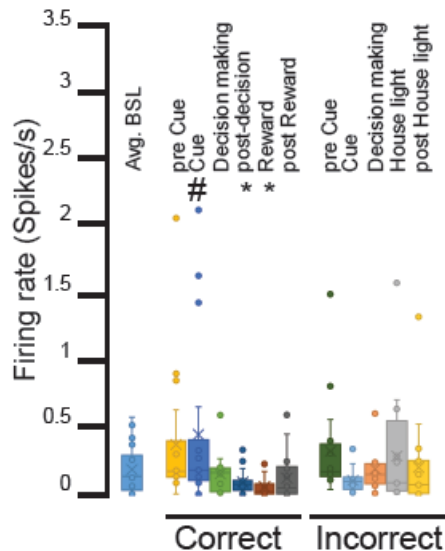


Figure 18. Firing rate of mPFC cells, recorded in WT mice, during SD stage. The firing rate is averaged for different periods around correct and incorrect choices. SD: Simple Discrimination. Statistics: \* AVG BSL vs all periods; # correct vs incorrect; \*  $p<0.05$ , AVG BSL vs post-decision correct, reward; #  $p<0.05$  cue correct VS cue incorrect. Data are expressed as Mean $\pm$ SEM. N=7 mice.

Following pairwise analyses of the individual firing rate during all periods, I focused on the PSTH of the firing rate during each trial. I found that the average latency between the cue delivery and the correct poke was  $14.27\pm 2.27$ s, while the latency between the correct poke and the reward was  $4.59\pm 0.92$ s. I used twice the standard deviation of the cue and reward to define the edge of the PSTH. I obtained a PSTH starting 26s prior to the cue response and ending 10s after. Before the onset and the offset, I considered 3 seconds of baseline activity (from -29s to -26s, from 10s to 13s). Immediately following cue delivery, I observed an increase in the z-score that quickly returned to the baseline (Figure 19). This effect could be associated with the cue delivery itself, as many studies demonstrated that the PFC responds to cue presentation associated with reward (Otis *et al.*, 2017) throughout dense inputs from the somatosensory, auditory or visual cortex. Concerning the remain time period, I did not find any significant change of the firing rate, at the exclusion of the post-reward delivery, where an increase was evident (Figure 19). These data might be in line with previous evidence, in humans or rodents, showing a marginal involvement of the mPFC in simple discrimination (Dias, Robbins and Roberts, 1996; Birrell and Brown, 2000; Bissonette *et al.*, 2008).

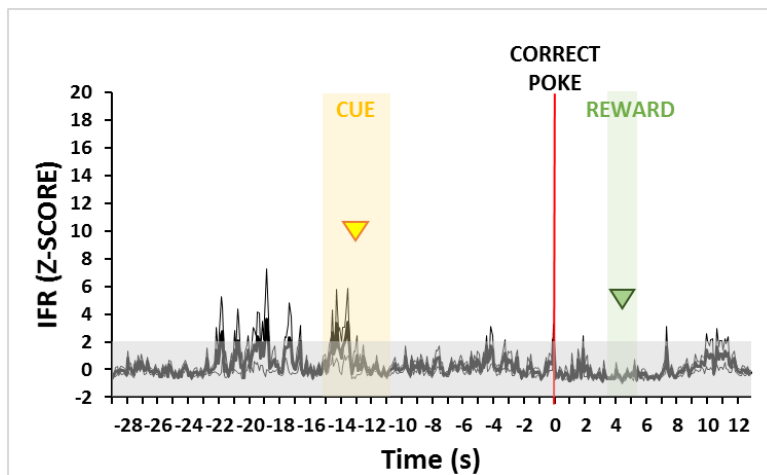


Figure 19. Instantaneous Firing Rate (IFR) of mPFC cells, recorded in WT mice, for the correct choice of SD stage. It represents the variation of the mPFC activity around a correct poke. X-axis: time, expressed in seconds. SD: Simple Discrimination. The axis is centered in the instant of the correct poke. Y-axis: z-score of the IFR. Gray square: represents the interval in which the firing is not significantly different from the baseline of 3 seconds in the beginning. Yellow arrow: it represents the average time of the cue delivery. Yellow square: represent the  $\pm$ SEM of the average time of cue delivery. Red line: the instant of correct poke. Green arrow: it represents the average time of the first entry in the food magazine. Green square: represent the  $\pm$ SEM of the average time of first entry in the food magazine. Data are expressed as Mean $\pm$ SEM. N=7 mice.

When testing incorrect outcome trials, the house light is turned on during 5 seconds as a sign of error. I used twice the standard deviation of the cue and period of the house light to define the edge of PSTH. Focusing on the PSTH of the incorrect poke, I found that the average latency between the cue delivery and the incorrect poke was  $22.90\pm 4.48$ s. I obtained a PSTH onset of -42s and an offset of +5s. Before the onset and after the offset, I considered 3 seconds of baseline activity (total studied period: from -45s to -42s; from 5s to 8s).

Interestingly, when I compared the firing activity during an incorrect poke, I found that the presentation of cues was delivered at much longer timescale than for correct poke, confirming the higher latency to incorrect. I then observed a similar increase in the z-score of the firing activity immediately before the cue delivery. I also found a change in the firing activity during the delivery of the cue, similar to the one observed following correct response. This might suggest a cortical expectation and reaction to the cue signal. In contrast, to correct choices, during the decision period, I observed a very strong increase of the firing activity, maintained while the decision was already made, both in the house-light period and post-house light period (*Figure 20*). This suggests that in my hands, the mPFC is mostly involved in response inhibition and the reward prediction error than for the correct choice. This confirms some reports in rats and mice showing that the PFC inputs to the dorsomedial striatum and the nucleus accumbens can be required for the maintenance of goal-directed behavior (Balleine and Dickinson, 1998; Goto and Grace, 2005; Gremel and Costa, 2013).

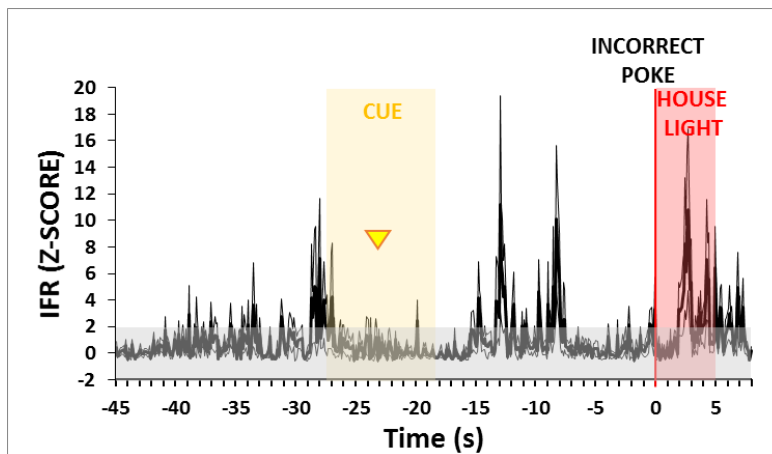


Figure 20. Instantaneous Firing Rate (IFR) of mPFC cells, recorded in WT mice, for the incorrect choice of SD stage. It represents the variation of the mPFC activity around an incorrect poke. X-axis: time, expressed in seconds. SD: Simple Discrimination. The axis is centered in the instant of the incorrect poke. Y-axis: z-score of the IFR. Gray square: represents the interval in which the firing is not significantly different from the baseline of 3 seconds in the beginning. Yellow arrow: it represents the average time of the cue delivery. Yellow square: represent the  $\pm$ SEM of the average time of cue delivery. Red line: the instant of correct poke. Red square: represent the duration of the house-light on. Data are expressed as Mean $\pm$ SEM. N=7 mice.

## 2. COMPOUND DISCRIMINATION (CD)

For the CD stage, I collected recordings for a total period of 13 days across all animals ( $1.63\pm 0.26$  day per animals). The number of neurons recorded was 29, and the number of neurons analyzed was 9.

During the intertrial interval, the firing rate was  $0.13\pm 0.05$  Hz, and no significant difference was found for correct and incorrect trials (paired t-test,  $p=0.308$ ), so I pooled together the average activity. The activity decreased during the reward collection ( $0.06\pm 0.03$  Hz; paired t-test,  $p=0.047$ ) and increased during the decision-making related to an incorrect choice ( $0.17\pm 0.05$  Hz;  $p=0.045$ ). But for the same period, no effect was found during correct trials (paired t-test,  $p=0.152$ ). For all other epochs in correct and incorrect trials, no significant differences in the average firing rate were observed (paired t-test,  $p>0.05$ ). Pairwise comparison of the variation of the firing rate using paired t-test in correct and incorrect show any significant differences ( $p>0.05$ ) (Figure 21).

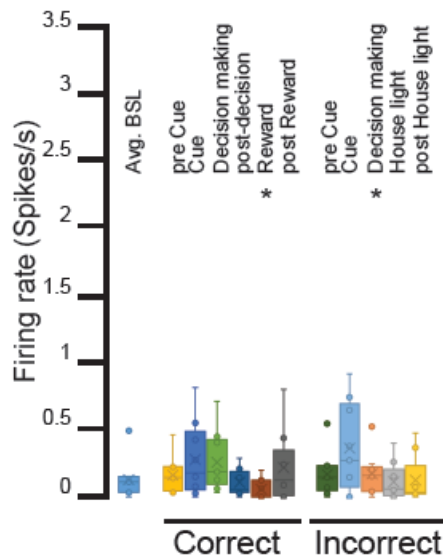


Figure 21. Firing rate of mPFC cells, recorded in WT mice, during CD stage. The firing rate is averaged for different periods around correct and incorrect choices. CD: Compound Discrimination. Statistics: \* AVG BSL vs all periods; \*  $p < 0.05$ , AVG BSL vs reward, decision-making incorrect. Data are expressed as Mean $\pm$ SEM. N=7 mice.

When focusing on the PSTH of the behavioral response towards the correct poke, I found that the average latency between the cue delivery and the correct poke was  $10.98 \pm 1.89$ s, while the latency between the correct poke and the reward was  $4.83 \pm 1.05$ s. I then obtained the PSTH with an onset positioned -22s before the correct behavioral outcome and an offset at +10s. Before the onset and after the offset, I considered 3 seconds of baseline activity (total studies period: from -25s to -22s; from 10s to 13s). Compared to the baseline, I observed a significant variation of the firing rate in the post-decision period, as described using the z-score. These observations suggest that PFC can play a role between the association cue-reward, which is similar to previous work suggesting participation in goal-directed (Locke and Braver, 2008). I also found a significant increase in the firing rate in the post-reward delivery (*Figure 22*).

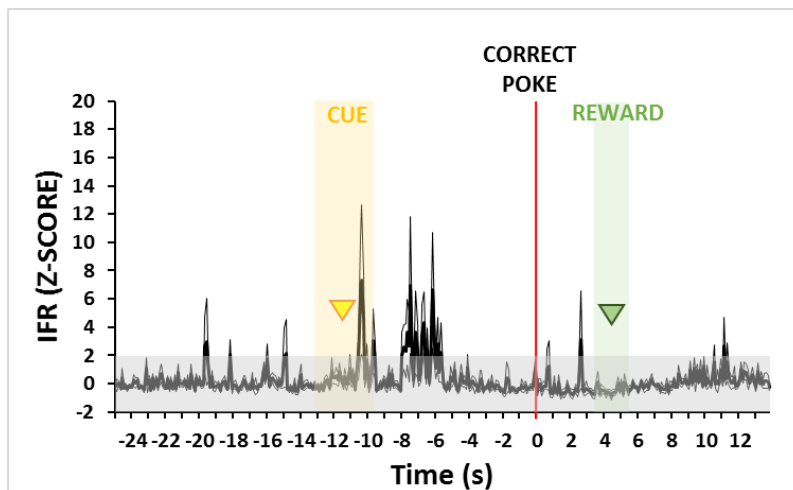


Figure 22. Instantaneous Firing Rate (IFR) of mPFC cells, recorded in WT mice, for the correct choice of CD stage. It represents the variation of the mPFC activity around a correct poke. X-axis: time, expressed in seconds. CD: Compound Discrimination. The axis is centered in the instant of the correct poke. Y-axis: z-score of the IFR. Gray square: represents the interval in which the firing is not significantly different from the baseline of 3 seconds in the beginning. Yellow arrow: it represents the average time of the cue delivery. Yellow square: represent the  $\pm$ SEM of the average time of cue delivery. Red line: the instant of correct poke. Green arrow: it represents the average time of the first entry in the food magazine. Green square: represent the  $\pm$ SEM of the average time of first entry in the food magazine. Data are expressed as Mean $\pm$ SEM. N=7 mice.

Next, I focused on the PSTH following an incorrect behavioral outcome (incorrect poke) and I found that the average latency between the cue delivery and the incorrect poke was  $11.61 \pm 1.86$ s. Similarly, the PSTH was obtained between -22s and +5s of the incorrect poke. Before the onset and after the offset, I considered 3 seconds of baseline activity (total studied period: from -25s to 8s).

When I compared the z-score of the firing activity during each individual trial with incorrect poke, I found an increase of the firing rate during the cue delivery, and the decision making period. This again seems to be confirmed, as found for the SD period, that the PFC might encode behavioral inhibition. I also found an increase of the firing activity when the light-house was turned ON (*Figure 23*).

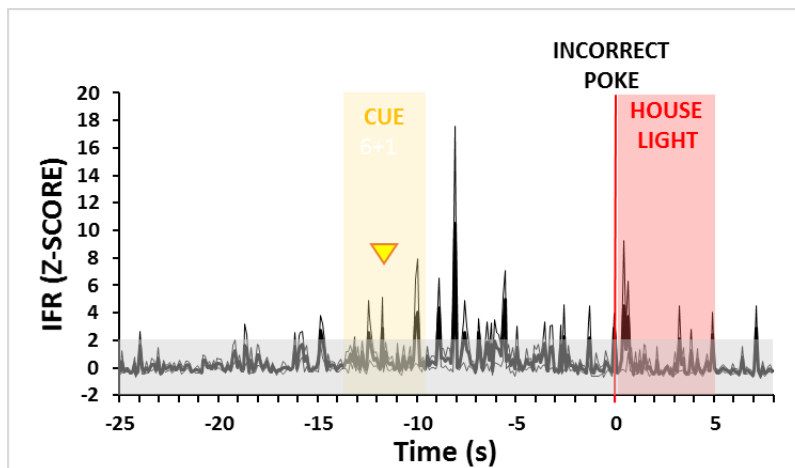


Figure 23. Instantaneous Firing Rate (IFR) of mPFC cells, recorded in WT mice, for the incorrect choice of CD stage. It represents the variation of the mPFC activity around an incorrect poke. X-axis: time, expressed in seconds. CD: Compound Discrimination. The axis is centered in the instant of the incorrect poke. Y-axis: z-score of the IFR. Gray square: represents the interval in which the firing is not significantly different from the baseline of 3 seconds in the beginning. Yellow arrow: it represents the average time of the cue delivery. Yellow square: represent the  $\pm$ SEM of the average time of cue delivery. Red line: the instant of correct poke. Red square: represent the duration of the house-light on. Data are expressed as Mean $\pm$ SEM. N=7 mice.

### 3.COMPOUND DISCRIMINATION REVERSAL (CDRe)

For the CDRe stage, I collected recordings for a total period of 17 days across all animals ( $2\pm 0.33$  days per animal). The number of neurons recorded was 45 and the number of neurons analyzed was 15.

During the intertrial interval, the firing rate was  $0.12\pm 0.02$  Hz, and no significant difference was found for correct and incorrect trials (paired t-test,  $p=0.474$ ), so I pooled together the average activity. The activity increased during the incorrect decision-making ( $0.28\pm 0.04$  Hz; paired t-test,  $p=0.006$ ) and the incorrect post-decision when the house light was turned on ( $0.20\pm 0.02$  Hz;  $p=0.021$ ). But for the same periods, no effects were found during correct trials (paired t-test,  $p>0.05$ ). For all other epochs in correct and incorrect trials, no significant differences in the average firing rate were observed (paired t-test,  $p>0.05$ ). Pairwise comparison of the variation of the firing rate using paired t-test in correct and incorrect show that the firing was significantly higher during the cue period associated with incorrect trials compared to correct ( $p=0.027$ ). All other comparisons were not showing any significant differences ( $p>0.05$ ) (Figure 24).

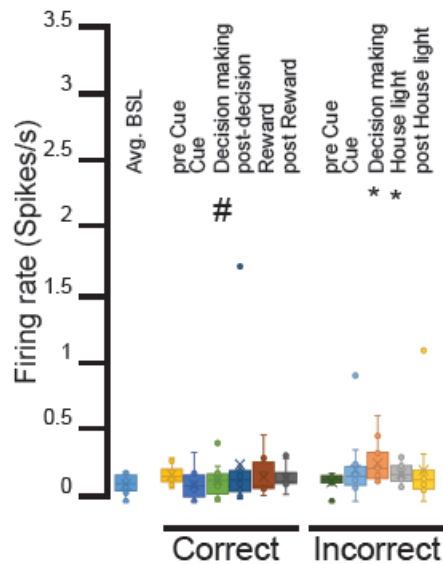


Figure 24. Firing rate of mPFC cells, recorded in WT mice, during CDRe stage. The firing rate is averaged for different periods around correct and incorrect choices. CDRe: Compound Discrimination Reversal. Statistics: \* AVG BSL vs all periods; # correct vs incorrect; \*  $p < 0.05$ , AVG BSL vs decision-making incorrect, house light; #  $p < 0.05$  decision-making correct VS decision-making incorrect. Data are expressed as Mean $\pm$ SEM. N=7 mice.

When focusing on the PSTH of the behavioral response towards the correct poke, I found that the average latency between the cue delivery and the correct poke is  $9.72 \pm 2.05$ s, while the latency between the correct poke and the reward is  $5.51 \pm 2.71$ s. I obtained a PSTH onset of -21s and an offset of +20s to the correct poke. Before the onset and after the offset, I considered 3 seconds of baseline activity (total studied period: from -24s to 23s). In this case, what I found is that in all the different periods of the PST, no significantly increased activity was observed compared to the baseline (*Figure 25*). This could be associated to the fact that the mPFC is not involved in the reversal learning (Dias, Robbins and Roberts, 1996; Birrell and Brown, 2000; Bissonette *et al.*, 2008)

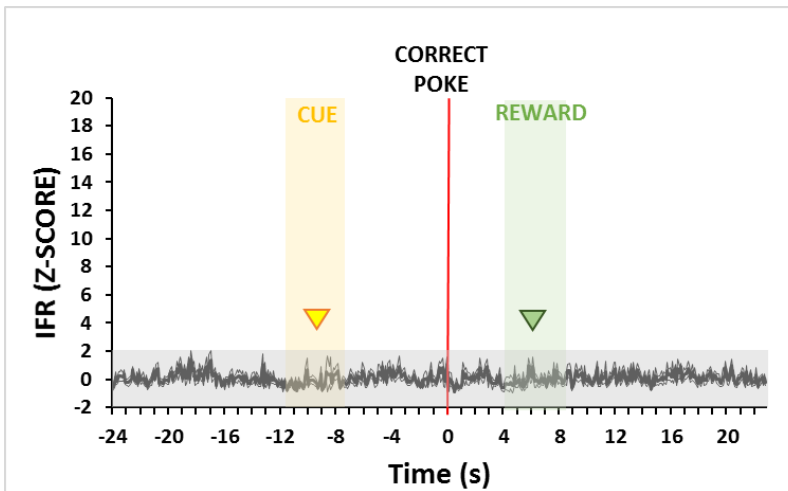


Figure 25. Instantaneous Firing Rate (IFR) of mPFC cells, recorded in WT mice, for the correct choice of CDR stage. It represents the variation of the mPFC activity around a correct poke. X-axis: time, expressed in seconds. CDR: Compound Discrimination Reversal. The axis is centered in the instant of the correct poke. Y-axis: z-score of the IFR. Gray square: represents the interval in which the firing is not significantly different from the baseline of 3 seconds in the beginning. Yellow arrow: it represents the average time of the cue delivery. Yellow square: represent the  $\pm$ SEM of the average time of cue delivery. Red line: the instant of correct poke. Green arrow: it represents the average time of the first entry in the food magazine. Green square: represent the  $\pm$ SEM of the average time of first entry in the food magazine. Data are expressed as Mean $\pm$ SEM. N=7 mice.

Next, I focused on the PSTH following an incorrect behavioral outcome (incorrect poke) and I found that the average latency between the cue delivery and the incorrect poke was  $8.92 \pm 1.23$ s. I obtained a PSTH onset of -17s and an offset of +5s to the incorrect poke. Before the onset and after the offset, I considered 3 seconds of baseline activity (total studied period: from -20s to 8s).

When I compared the z-score of the firing activity during each individual trial with incorrect poke, I found that the cue delivery was delivered at a similar timescale than for the correct poke. As for the correct choice, what I found was that in all the different periods of the PST, no significantly increased activity was observed compared to the baseline (*Figure 26*). This is in line with previous evidence indicating a scarce involvement of the mPFC in simple and initial reversal learning (Dias, Robbins and Roberts, 1996; Birrell and Brown, 2000; Bissonette *et al.*, 2008).



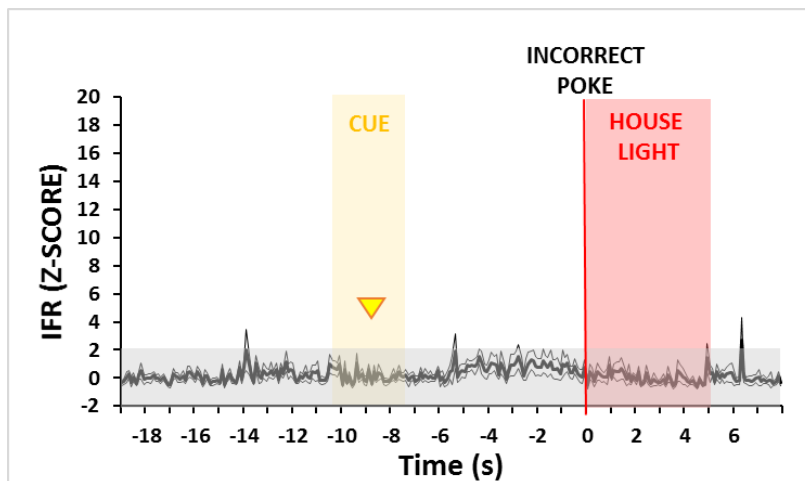


Figure 26. Instantaneous Firing Rate (IFR) of mPFC cells, recorded in WT mice, for the incorrect choice of CDRe stage. It represents the variation of the mPFC activity around an incorrect poke. X-axis: time, expressed in seconds. CDRe: Compound Discrimination Reversal. The axis is centered in the instant of the incorrect poke. Y-axis: z-score of the IFR. Gray square: represents the interval in which the firing is not significantly different from the baseline of 3 seconds in the beginning. Yellow arrow: it represents the average time of the cue delivery. Yellow square: represent the  $\pm$ SEM of the average time of cue delivery. Red line: the instant of correct poke. Red square: represent the duration of the house-light on. Data are expressed as Mean $\pm$ SEM. N=7 mice.

#### 4. INTRA-DIMENSIONAL SHIFT (IDS)

For the IDS stage, I collected recordings for a total period of 15 days across all animals ( $1.887\pm 0.20$ ). The number of neurons recorded was 43, and the number of neurons analyzed was 14.

During the intertrial interval, the firing rate was  $0.16\pm 0.08$  Hz, and no significant difference was found for correct and incorrect trials (paired t-test,  $p=0.234$ ), so I pooled together the average activity. The activity increased during the decision-making related to an incorrect choice ( $0.39\pm 0.11$  Hz; paired t-test,  $p=0.033$ ). But for the same period, no effect was found during correct trials (paired t-test,  $p=0.271$ ). For all other epochs in correct and incorrect trials, no significant differences in the average firing rate were observed (paired t-test,  $p>0.05$ ). Pairwise comparison of the variation of the firing rate using paired t-test in correct and incorrect show any significant differences ( $p>0.05$ ) (Figure 27).

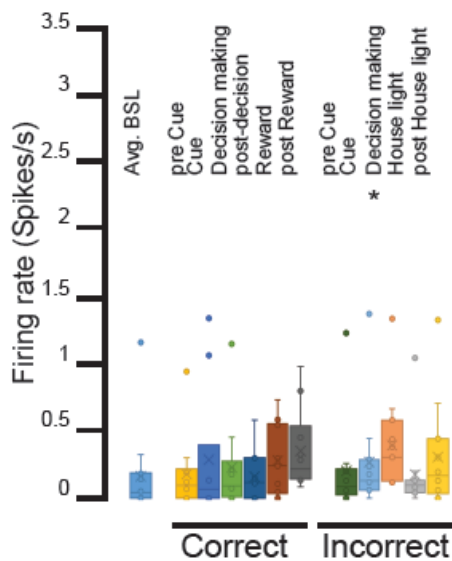


Figure 27. Firing rate of mPFC cells, recorded in WT mice, during IDS stage. The firing rate is averaged for different periods around correct and incorrect choices. IDS: Intra-Dimensional Shift. Statistics: \* AVG BSL vs all periods; \*  $p < 0.05$ , AVG BSL vs decision-making incorrect. Data are expressed as Mean  $\pm$  SEM. N=7 mice.

When focusing on the PSTH of the behavioral response towards the correct poke, I found that the average latency between the cue delivery and the correct poke is  $8.61 \pm 0.71$ s, while the latency between the correct poke and the reward is  $6.47 \pm 1.89$ s. I obtained a PSTH onset of -13s and an offset of +11s to the correct poke. Before the onset and after the offset, I considered 3 seconds of baseline activity (total studied period: from -16s to +14s). As for SD and CD (Figure 19, 22), but not for CDRe, during the immediate period preceding cue delivery and during the post-reward period, I observed a significant increase of the firing activity. Moreover, immediately during the cue delivery, I found an increase in the firing activity, which could again be associated with the cue delivery itself, which was maintained during the decision making period. This increase was maintained in the post-decision period and strongly increased in the reward collection, like CD (Figure 22), probably due to the collection of the reward (Figure 28) (Locke and Braver, 2008).

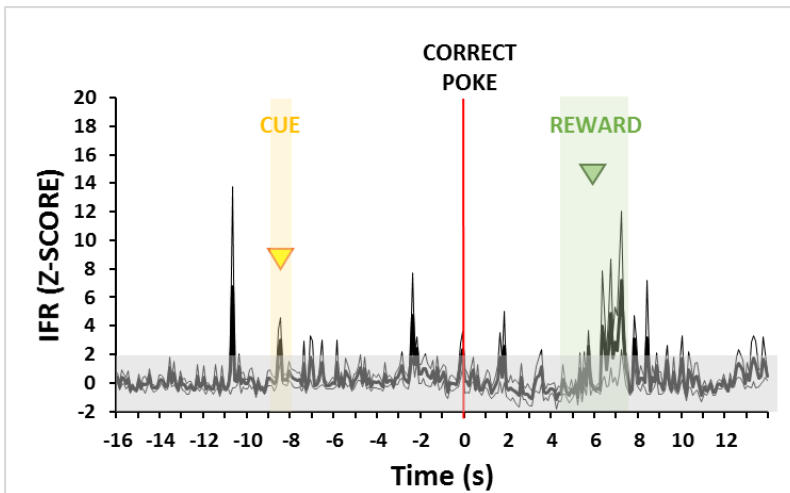


Figure 28. Instantaneous Firing Rate (IFR) of mPFC cells, recorded in WT mice, for the correct choice of IDS stage. It represents the variation of the mPFC activity around a correct poke. X-axis: time, expressed in seconds. IDS: Intra-Dimensional Shift. The axis is centered in the instant of the correct poke. Y-axis: z-score of the IFR. Gray square: represents the interval in which the firing is not significantly different from the baseline of 3 seconds in the beginning. Yellow arrow: it represents the average time of the cue delivery. Yellow square: represent the  $\pm$ SEM of the average time of cue delivery. Red line: the instant of correct poke. Green arrow: it represents the average time of the first entry in the food magazine. Green square: represent the  $\pm$ SEM of the average time of first entry in the food magazine. Data are expressed as Mean $\pm$ SEM. N=7 mice.

Next, I focused on the PSTH following an incorrect behavioral outcome (incorrect poke), and I found that the average latency between the cue delivery and the incorrect poke was  $6.12 \pm 0.83$ s.

I obtained a PSTH onset of -11s and an offset of +5s to the incorrect poke. Before the onset and after the offset, I considered 3 seconds of baseline activity (total studied period: from -14s to 8s).

When I compared the z-score of the firing activity during each individual trial with incorrect poke, I found that the cue delivery was delivered at a similar timescale than for the correct poke. I observed the same increase of the firing activity during the decision making period. In the case of a pre-cue period, delivery of the cue, post-decision, and post-house-light, there was no significant increase in the activity compared to the baseline (Figure 29), unlike SD and CD (Figure 20, 23).

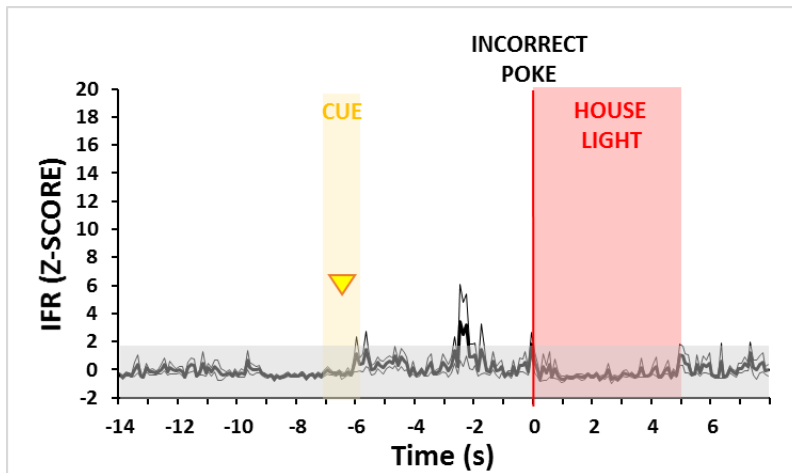


Figure 29. Instantaneous Firing Rate (IFR) of mPFC cells, recorded in WT mice, for the incorrect choice of IDS stage. It represents the variation of the mPFC activity around an incorrect poke. X-axis: time, expressed in seconds. IDS: Intra-Dimensional Shift. The axis is centered in the instant of the incorrect poke. Y-axis: z-score of the IFR. Gray square: represents the interval in which the firing is not significantly different from the baseline of 3 seconds in the beginning. Yellow arrow: it represents the average time of the cue delivery. Yellow square: represent the  $\pm$ SEM of the average time of cue delivery. Red line: the instant of correct poke. Red square: represent the duration of the house-light on. Data are expressed as Mean $\pm$ SEM. N=7 mice.

## 5. INTRA-DIMENSIONAL SHIFT REVERSAL (IDSRe)

For the IDSRe stage, I collected recordings for a total period of 13 days across all animals ( $1.63\pm 0.26$ ). The number of neurons recorded was 42, and the number of neurons analyzed was 11.

During the intertrial interval, the firing rate was  $0.20\pm 0.07$  Hz, and no significant difference was found for correct and incorrect trials (paired t-test,  $p=0.706$ ), so I pooled together the average activity. For all the epochs in correct and incorrect trials, no significant differences in the average firing rate were observed (paired t-test,  $p>0.05$ ). Pairwise comparison of the variation of the firing rate using paired t-test in correct and incorrect show any significant differences ( $p>0.05$ ) (Figure 30).

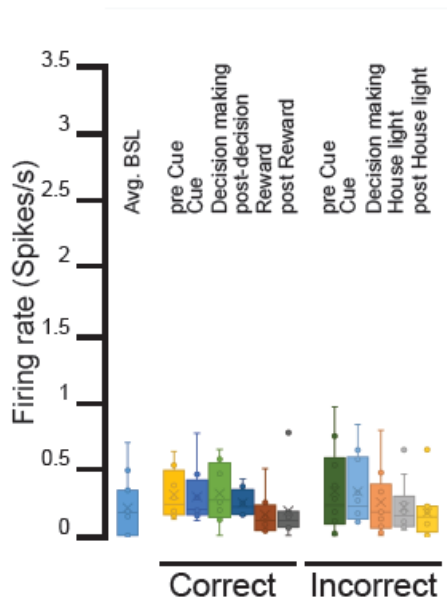


Figure 30. Firing rate of mPFC cells, recorded in WT mice, during IDSRe stage. The firing rate is averaged for different periods around correct and incorrect choices. IDSRe: Intra-Dimensional Shift Reversal. Data are expressed as Mean $\pm$ SEM. N=7 mice.

When focusing on the PSTH of the behavioral response towards the correct poke, I found that the average latency between the cue delivery and the correct poke is  $7.64\pm 2.23$ s, while the latency between the correct poke and the reward is  $4.95\pm 1.26$ s. I obtained a PSTH onset of -20s and an offset of +12s to the correct poke. Before the onset and after the offset, I considered 3 seconds of baseline activity (total studied period: from -23s to 15s). In this case, like for CDR<sub>e</sub> (Figure 25), no significantly increased activity was observed in all the other periods compared to the baseline (Figure 31). This could be associated to the fact that the mPFC is not involved in the reversal learning (Dias, Robbins and Roberts, 1996; Birrell and Brown, 2000; Bissonette *et al.*, 2008).

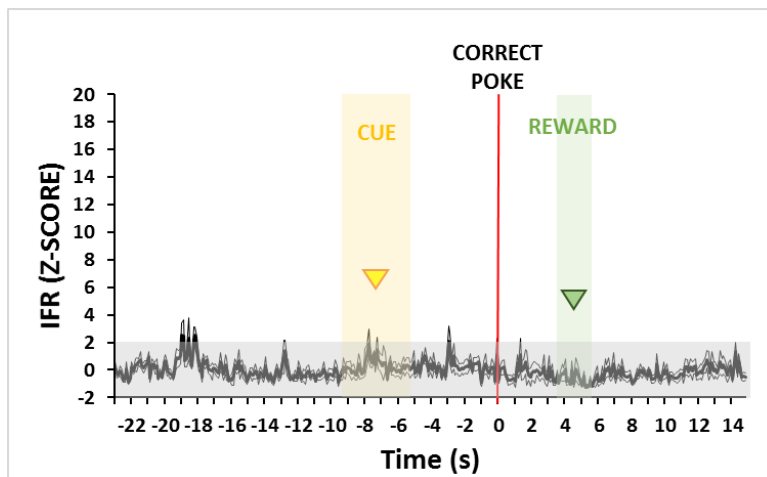


Figure 31. Instantaneous Firing Rate (IFR) of mPFC cells, recorded in WT mice, for the correct choice of IDSRe stage. It represents the variation of the mPFC activity around a correct poke. X-axis: time, expressed in seconds. IDSRe: Intra-Dimensional Shift Reversal. The axis is centered in the instant of the correct poke. Y-axis: z-score of the IFR. Gray square: represents the interval in which the firing is not significantly different from the baseline of 3 seconds in the beginning. Yellow arrow: it represents the average time of the cue delivery. Yellow square: represent the  $\pm$ SEM of the average time of cue delivery. Red line: the instant of correct poke. Green arrow: it represents the average time of the first entry in the food magazine. Green square: represent the  $\pm$ SEM of the average time of first entry in the food magazine. Data are expressed as Mean $\pm$ SEM. N=7 mice.

Next, I focused on the PSTH following an incorrect behavioral outcome (incorrect poke), and I found that the average latency between the cue delivery and the incorrect poke was  $6.32 \pm 1.61$ s.

I obtained a PSTH onset of -15s and an offset of +5s to the incorrect poke. Before the onset and after the offset, I considered 3 seconds of baseline activity (total studied period: from -18s to 8s).

When I compared the z-score of the firing activity during each individual trial with incorrect poke, I found that the cue delivery was delivered at a similar timescale than for the correct poke. I observed a strong increase of the firing activity immediately before the cue delivery. What I found is that in all the other different periods of the PST, no significantly increased activity was observed compared to the baseline (*Figure 32*), like CDRe (*Figure 26*), but not the stages with an introduction of new stimuli (SD, CD, IDS) (*Figure 20, 23, 29*).

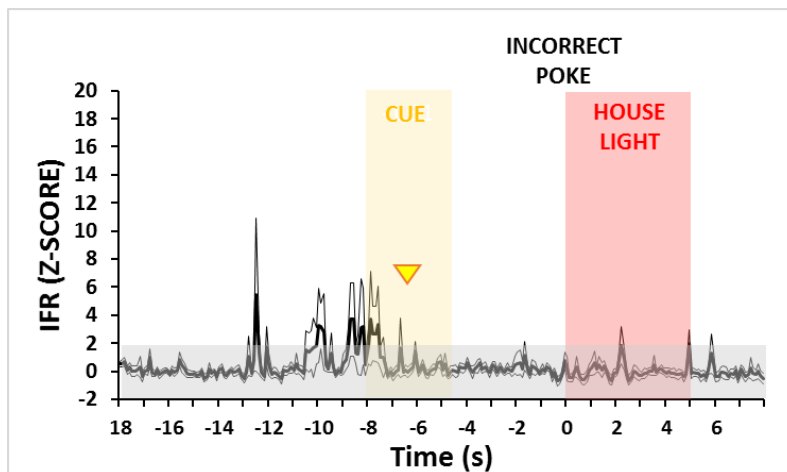


Figure 32. Instantaneous Firing Rate (IFR) of mPFC cells, recorded in WT mice, for the incorrect choice of IDSRe stage. It represents the variation of the mPFC activity around an incorrect poke. X-axis: time, expressed in seconds. IDSRe: Intra-Dimensional Shift Reversal. The axis is centered in the instant of the incorrect poke. Y-axis: z-score of the IFR. Gray square: represents the interval in which the firing is not significantly different from the baseline of 3 seconds in the beginning. Yellow arrow: it represents the average time of the cue delivery. Yellow square: represent the  $\pm$ SEM of the average time of cue delivery. Red line: the instant of correct poke. Red square: represent the duration of the house-light on. Data are expressed as Mean $\pm$ SEM. N=7 mice.

## 6. INTRA-DIMENSIONAL SHIFT 2 (IDS2)

The IDS2 is a stage introduced for reinforcing the attentional set developed through the previous stages. Here I collected recordings for a total period of 14 days across all animals ( $1.44 \pm 0.24$ ). The number of neurons recorded was 49, and the number of neurons analyzed was 20.

During the intertrial interval, the firing rate was  $0.17 \pm 0.03$  Hz, and no significant difference was found for correct and incorrect trials (paired t-test,  $p=0.059$ ), so I pooled together the average activity. The activity increased during almost all the epochs of correct choice: pre-cue ( $0.31 \pm 0.06$  Hz; paired t-test,  $p=0.027$ ), cue ( $0.24 \pm 0.04$  Hz; paired t-test,  $p=0.016$ ), decision-making ( $0.36 \pm 0.07$  Hz, paired t-test,  $p=0.027$ ), post-decision ( $0.28 \pm 0.05$  Hz; paired t-test,  $p=0.039$ ), and reward ( $0.34 \pm 0.07$  Hz; paired t-test,  $p=0.031$ ). This did not happen after the reward collection (paired t-test,  $p=0.838$ ). For all the epochs in incorrect trials, no significant differences of the average firing rate were observed (paired t-test,  $p>0.05$ ). Pairwise comparison of the variation of the firing rate using paired t-test in correct and incorrect show that the firing was significantly higher during the decision-making period associated with correct trials compared to incorrect ( $p=0.009$ ). All other comparisons were not showing any significant differences ( $p>0.05$ ) (Figure 33).

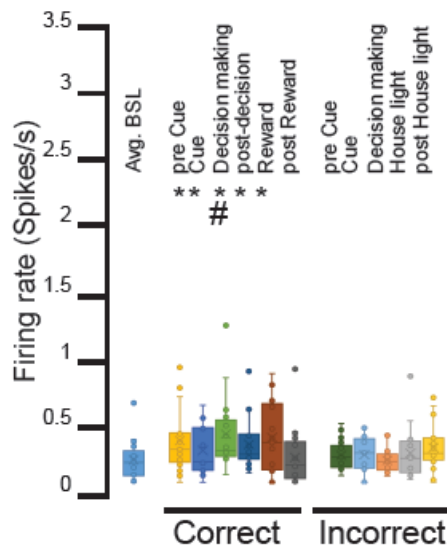


Figure 33. Firing rate of mPFC cells, recorded in WT mice, during IDS2 stage. The firing rate is averaged for different periods around correct and incorrect choices. IDS2: Intra-Dimensional Shift 2. Statistics: \* AVG BSL vs all periods; # correct vs incorrect; \*  $p < 0.05$ , AVG BSL vs pre-cue correct, cue correct, decision-making correct, post-decision correct, reward; #  $p < 0.05$  decision-making correct VS decision-making incorrect. Data are expressed as Mean  $\pm$  SEM. N=7 mice.

When focusing on the PSTH of the behavioral response towards the correct poke, I found that the average latency between the cue delivery and the correct poke is  $8.56 \pm 1.97$ s, while the latency between the correct poke and the reward is  $2.79 \pm 0.63$ s. I obtained a PSTH onset of -20s and an offset of +7s to the correct poke. Before the onset and after the offset, I considered 3 seconds of baseline activity (total studied period: from -23s to 10s).

Again, as for SD, CD, and IDS (Figure 19, 22, 28), but not for reversal stages, during the immediate period preceding cue delivery and during the post-reward period, I observed a significant increase of the firing activity. Moreover, immediately during the cue delivery, I found an increase in the firing activity, which could again be associated with the cue delivery itself, which was maintained during the decision making period. This increase was maintained in the post-decision period and strongly increased in the reward collection (Figure 34), like CD and IDS (Figure 22, 28).



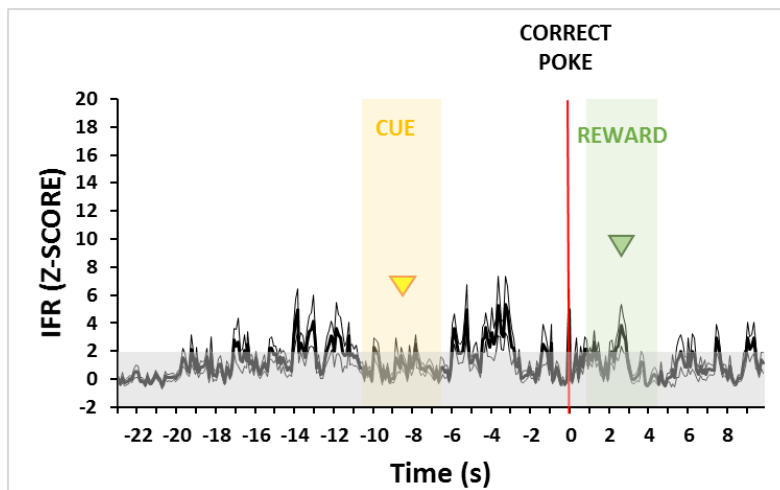


Figure 34. Instantaneous Firing Rate (IFR) of mPFC cells, recorded in WT mice, for the correct choice of IDS2 stage. It represents the variation of the mPFC activity around a correct poke. X-axis: time, expressed in seconds. IDS2: Intra-Dimensional Shift 2. The axis is centered in the instant of the correct poke. Y-axis: z-score of the IFR. Gray square: represents the interval in which the firing is not significantly different from the baseline of 3 seconds in the beginning. Yellow arrow: it represents the average time of the cue delivery. Yellow square: represent the  $\pm$ SEM of the average time of cue delivery. Red line: the instant of correct poke. Green arrow: it represents the average time of the first entry in the food magazine. Green square: represent the  $\pm$ SEM of the average time of first entry in the food magazine. Data are expressed as Mean $\pm$ SEM. N=7 mice.

Next, I focused on the PSTH following an incorrect behavioral outcome (incorrect poke), and I found that the average latency between the cue delivery and the incorrect poke was  $6.35 \pm 2.07$ s.

I obtained a PSTH onset of -19s and an offset of +5s to the incorrect poke. Before the onset and after the offset, I considered 3 seconds of baseline activity (total studied period: from -22s to 8s).

When I compared the z-score of the firing activity during each individual trial with incorrect poke, I found that the cue delivery was delivered at a similar timescale than for the correct poke. As for correct choice, I observed the same increase of the firing activity immediately before the cue delivery, and in the cue-delivery period, the cue delivery itself. In all the other periods, the activity didn't increase (*Figure 35*). This is different from what was found in SD, CD, and IDS (*Figure 20, 23, 29*), where the mPFC significantly increases the activity in the decision-making for an incorrect choice.

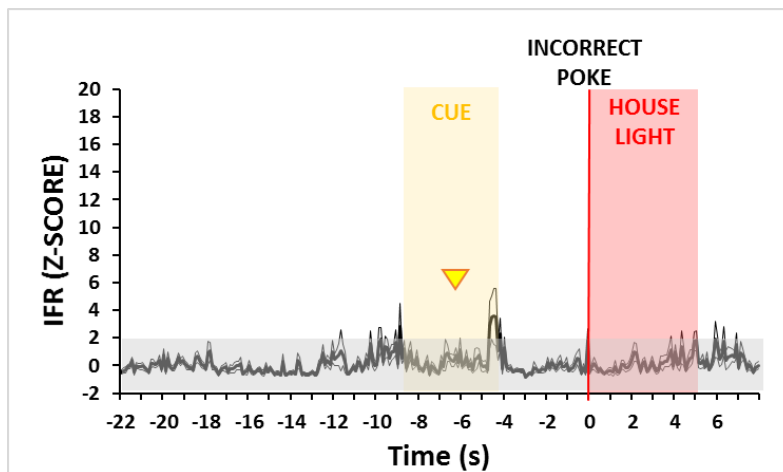


Figure 35. Instantaneous Firing Rate (IFR) of mPFC cells, recorded in WT mice, for the incorrect choice of IDS2 stage. It represents the variation of the mPFC activity around an incorrect poke. X-axis: time, expressed in seconds. IDS2: Intra-Dimensional Shift 2. The axis is centered in the instant of the incorrect poke. Y-axis: z-score of the IFR. Gray square: represents the interval in which the firing is not significantly different from the baseline of 3 seconds in the beginning. Yellow arrow: it represents the average time of the cue delivery. Yellow square: represent the  $\pm$ SEM of the average time of cue delivery. Red line: the instant of correct poke. Red square: represent the duration of the house-light on. Data are expressed as Mean $\pm$ SEM. N=7 mice.

## 7. INTRA-DIMENSIONAL SHIFT 2 REVERSAL (IDS2Re)

In the IDS2Re stage, I collect recordings for a total period of 13 days across all animals ( $1.63\pm 0.26$ ). The number of neurons recorded was 46 and the number of neurons analyzed was 19.

During the intertrial interval, the firing rate was  $0.18\pm 0.05$  Hz, and no significant difference was found for correct and incorrect trials (paired t-test,  $p=0.175$ ), so I pooled together the average activity. For all the epochs in correct and incorrect trials, no significant differences in the average firing rate were observed (paired t-test,  $p>0.05$ ). Pairwise comparison of the variation of the firing rate using paired t-test in the correct and incorrect trials show that the firing was significantly higher during the pre-cue period associated with correct trials compared to incorrect ( $p=0.04$ ). All other comparisons were not showing any significant differences ( $p>0.05$ ) (Figure 36).

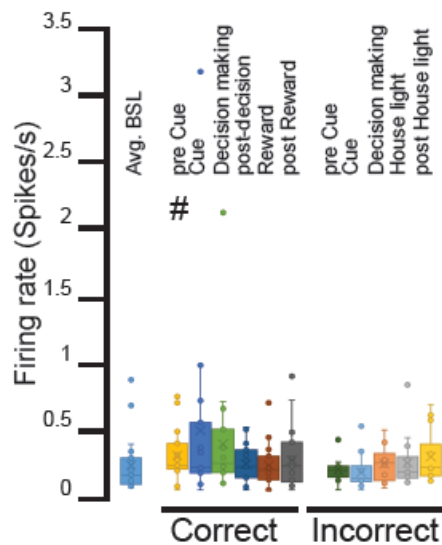


Figure 36. Firing rate of mPFC cells, recorded in WT mice, during IDS2Re stage. The firing rate is averaged for different periods around correct and incorrect choices. IDS2Re: Intra-Dimensional Shift 2 Reversal. Statistics: # correct vs incorrect; #  $p < 0.05$  pre-cue correct VS pre-cue incorrect. Data are expressed as Mean $\pm$ SEM. N=7 mice.

When focusing on the PSTH of the behavioral response towards the correct poke, I found that the average latency between the cue delivery and the correct poke is  $7.27 \pm 1.18$ s, while the latency between the correct poke and the reward is  $3.91 \pm 0.97$ s. I obtained a PSTH onset of -16s and an offset of +10s to the correct poke. Before the onset and after the offset, I considered 3 seconds of baseline activity (total studied period: from -19s to +13s). During the immediate period preceding cue delivery, I observed a significant strong increase of the firing activity (-22 to -16s, average z-score). Immediately during the cue delivery, this strong increase was maintained, which can again be associated with the cue delivery itself, also during the decision making period. This case is completely different from what happened for the other reversal stages (Figure 25, 31), where there was no involvement of the mPFC. The activity was quickly returning to baseline in the post-decision (Figure 37), like in the previous reversal stages (Figure 25, 31).

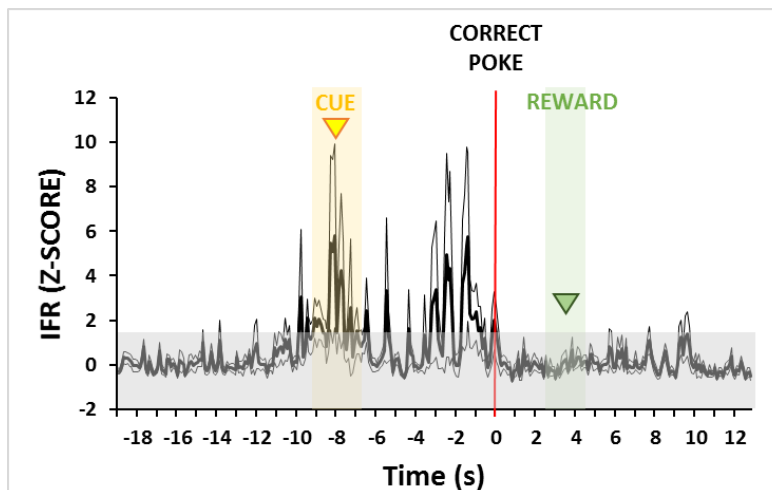


Figure 37. Instantaneous Firing Rate (IFR) of mPFC cells, recorded in WT mice, for the correct choice of IDS2Re stage. It represents the variation of the mPFC activity around a correct poke. X-axis: time, expressed in seconds. IDS2Re: Intra-Dimensional Shift 2 Reversal. The axis is centered in the instant of the correct poke. Y-axis: z-score of the IFR. Gray square: represents the interval in which the firing is not significantly different from the baseline of 3 seconds in the beginning. Yellow arrow: it represents the average time of the cue delivery. Yellow square: represent the  $\pm$ SEM of the average time of cue delivery. Red line: the instant of correct poke. Green arrow: it represents the average time of the first entry in the food magazine. Green square: represent the  $\pm$ SEM of the average time of first entry in the food magazine. Data are expressed as Mean $\pm$ SEM. N=7 mice.

Next, I focused on the PSTH following an incorrect behavioral outcome (incorrect poke), and I found that the average latency between the cue delivery and the incorrect poke  $9.80\pm 2.61$ s.

I obtained a PSTH onset of -22s and an offset of +5s to the incorrect poke. Before the onset and after the offset, I considered 3 seconds of baseline activity (total studied period: from -25s to 8s).

When I compared the z-score of the firing activity during each individual trial with incorrect poke, I found that the cue delivery was delivered at a similar timescale than for the correct poke. What I found is that in all the other different periods of the PSTH, no significantly increased activity was observed compared to the baseline (*Figure 38*), like reversal stages (*Figure 26, 32*), but not the stages with an introduction of new stimuli (SD, CD, IDS, IDS2) (*Figure 20, 23, 29, 35*).

The mPFC in case of correct choice in IDS2Re, a serial reversal stage, once reinforced the attentional set and becoming familiar with the reversal, behaved like in stages in the introduction of new stimuli, increasing the activity in the pre-responses periods.

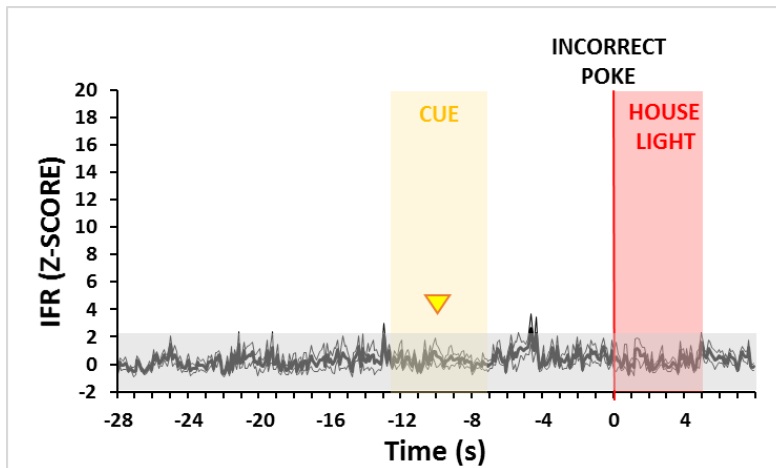


Figure 38. Instantaneous Firing Rate (IFR) of mPFC cells, recorded in WT mice, for the incorrect choice of IDS2Re stage. It represents the variation of the mPFC activity around an incorrect poke. X-axis: time, expressed in seconds. IDS2Re: Intra-Dimensional Shift 2 Reversal. The axis is centered in the instant of the incorrect poke. Y-axis: z-score of the IFR. Gray square: represents the interval in which the firing is not significantly different from the baseline of 3 seconds in the beginning. Yellow arrow: it represents the average time of the cue delivery. Yellow square: represent the  $\pm$ SEM of the average time of cue delivery. Red line: the instant of correct poke. Red square: represent the duration of the house-light on. Data are expressed as Mean $\pm$ SEM. N=7 mice.

## 8. EXTRA-DIMENSIONAL SHIFT (EDS)

This is the stage in which the relevant dimension change and in which the mPFC has been reported to be more involved. In this stage, I collected recordings for a total period of 16 days across all animals ( $1.75\pm 0.31$ ). The number of neurons recorded was 40, and the number of neurons analyzed was 11.

During the intertrial interval, the firing rate was  $0.21\pm 0.05$  Hz, but in this stage a significant difference was found for correct and incorrect trials (paired t-test,  $p=0.012$ ), so I didn't pool together the average activity. The firing rate in the intertrial interval before correct responses was  $0.18\pm 0.05$  Hz, and before incorrect responses was  $0.24\pm 0.05$  Hz. The activity decreased during the incorrect decision-making period ( $0.14\pm 0.03$  Hz; paired t-test,  $p=0.049$ ) and during the house light period ( $0.09\pm 0.01$  Hz; paired t-test,  $p=0.013$ ). For all other epochs in incorrect trials, and for all the epochs in correct trials no significant differences of the average firing rate were observed (paired t-test,  $p>0.05$ ). Pairwise comparison of the variation of the firing rate using paired t-test in correct and incorrect show that the firing was significantly higher during the post-decision period associated with correct trials compared to incorrect ( $p=0.013$ ). All other comparisons were not showing any significant differences ( $p>0.05$ ) (Figure 39).

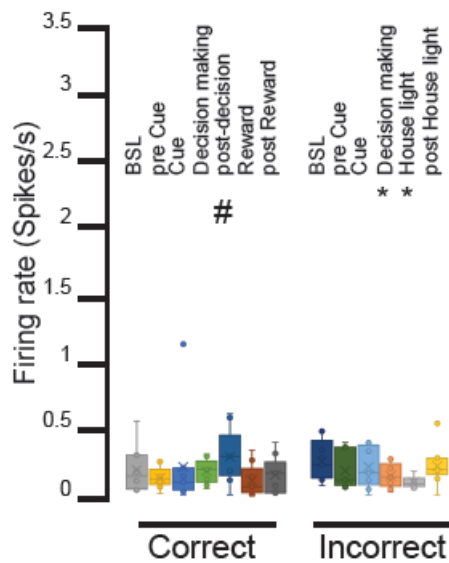


Figure 39. Firing rate of mPFC cells, recorded in WT mice, during EDS stage. The firing rate is averaged for different periods around correct and incorrect choices. EDS: Extra-Dimensional Shift. Statistics: \* AVG BSL vs all periods; # correct vs incorrect; \*  $p < 0.05$ , AVG BSL vs decision-making incorrect, house light; #  $p < 0.05$  post-decision correct VS post-decision incorrect (house light). Data are expressed as Mean $\pm$ SEM. N=7 mice.

When focusing on the PSTH of the behavioral response towards the correct poke, I found that the average latency between the cue delivery and the correct poke is  $5.49 \pm 1.13$ s, while the latency between the correct poke and the reward is  $6.76 \pm 1.56$ s. I used twice the standard deviation of the cue and reward delivery to define the edge of the PST. I obtained a PSTH onset of -12s and an offset of +11s to the correct poke. Before the onset and after the offset, I considered 3 seconds of baseline activity (total studied period: from -15s to +14s).

As for the previous IDS stages and IDS2Re (Figure 19, 22, 28, 34, 37) during the immediate period preceding cue delivery, I observed a significant increase in the firing activity which could be related to the learned expectancy of the cue. However, unlike the IDS stages and IDS2Re, the activity was quickly returning to baseline immediately during the cue delivery and the decision making period. However, it was evident a strong increase in the post-decision period after making the nose poke. This increase was maintained in reward-collection and post-reward collection periods (Figure 40).

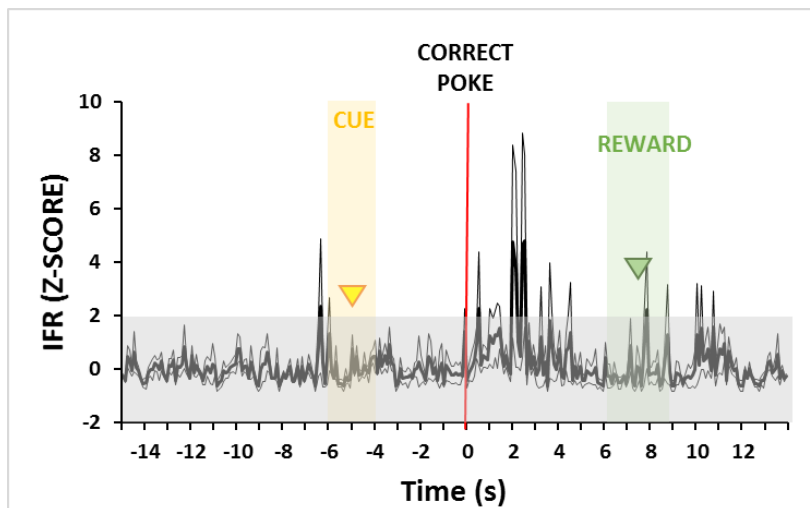


Figure 40. Instantaneous Firing Rate (IFR) of mPFC cells, recorded in WT mice, for the correct choice of EDS stage. It represents the variation of the mPFC activity around a correct poke. X-axis: time, expressed in seconds. EDS: Extra-Dimensional Shift. The axis is centered in the instant of the correct poke. Y-axis: z-score of the IFR. Gray square: represents the interval in which the firing is not significantly different from the baseline of 3 seconds in the beginning. Yellow arrow: it represents the average time of the cue delivery. Yellow square: represent the  $\pm$ SEM of the average time of cue delivery. Red line: the instant of correct poke. Green arrow: it represents the average time of the first entry in the food magazine. Green square: represent the  $\pm$ SEM of the average time of first entry in the food magazine. Data are expressed as Mean $\pm$ SEM. N=7 mice.

Next, I focused on the PSTH following an incorrect behavioral outcome (incorrect poke), and I found that the average latency between the cue delivery and the incorrect poke was  $6.17 \pm 0.95$ s.

I obtained a PSTH onset of -12s and an offset of +5s to the incorrect poke. Before the onset and after the offset, I considered 3 seconds of baseline activity (total studied period: from -15s to 8s).

When I compared the z-score of the firing activity during each individual trial with incorrect poke, I found that the cue delivery was delivered at a similar timescale than for the correct poke. As for the correct choice, I observed an increase in the firing activity in the decision-making period. In all the other periods, the activity did not increase (*Figure 41*). This pattern of activity was similar to the reversal stages, and differed to the previous IDS stages, in which there was an increase in the decision-making period. This confirms a specific and different implication of mPFC in the EDS stage (Dias, Robbins and Roberts, 1996; Birrell and Brown, 2000; Bissonette *et al.*, 2008).

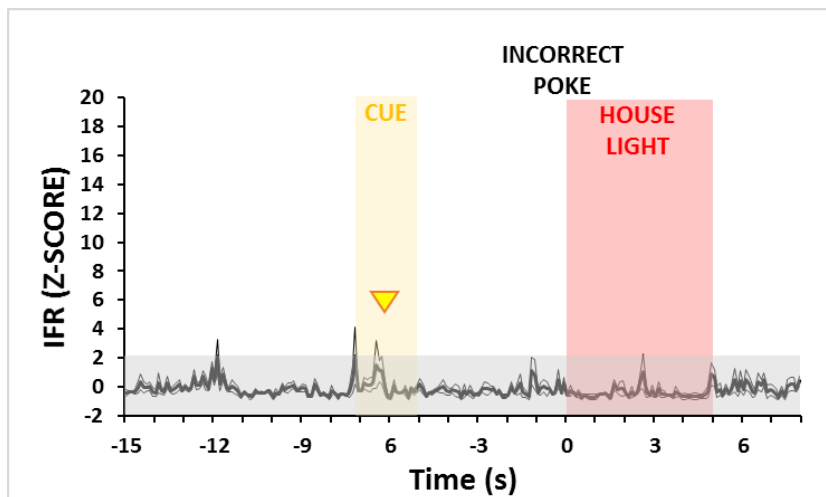


Figure 41. Instantaneous Firing Rate (IFR) of mPFC cells, recorded in WT mice, for the incorrect choice of EDS stage. It represents the variation of the mPFC activity around an incorrect poke. X-axis: time, expressed in seconds. EDS: Extra-Dimensional Shift. The axis is centered in the instant of the incorrect poke. Y-axis: z-score of the IFR. Gray square: represents the interval in which the firing is not significantly different from the baseline of 3 seconds in the beginning. Yellow arrow: it represents the average time of the cue delivery. Yellow square: represent the  $\pm$ SEM of the average time of cue delivery. Red line: the instant of correct poke. Red square: represent the duration of the house-light on. Data are expressed as Mean $\pm$ SEM. N=7 mice.

As said in paragraph 2, I divided the WT animal into two groups, based on the better or worst performance of EDS, to see if there were electrophysiological differences coming from these two groups of mice.

What I found, was that the activity pattern of the mPFC was similar in both groups, with an increase in the post-decision period (*Figure 42*).



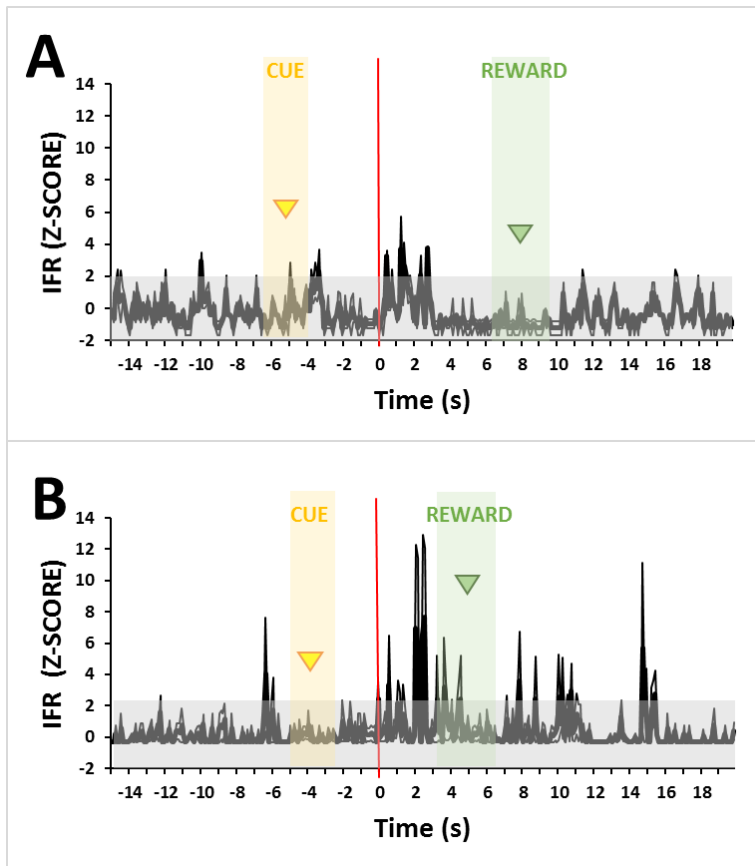


Figure 42. Instantaneous Firing Rate (IFR) of mPFC cells, recorded in WT mice, for the correct choice of EDS stage. It represents the variation of the mPFC activity around a correct poke. X-axis: time, expressed in seconds. EDS: Extra-Dimensional Shift. The axis is centered in the instant of the correct poke. Y-axis: z-score of the IFR. Gray square: represents the interval in which the firing is not significantly different from the baseline of 3 seconds in the beginning. Yellow arrow: it represents the average time of the cue delivery. Yellow square: represent the  $\pm$ SEM of the average time of cue delivery. Red line: the instant of correct poke. Green arrow: it represents the average time of the first entry in the food magazine. Green square: represent the  $\pm$ SEM of the average time of first entry in the food magazine. A) Z-score of IFR for WT that performed in a correct way the EDS (EDS YES). B) Z-score of IFR for WT that performs in an incorrect way the EDS (EDS NO). Data are expressed as Mean $\pm$ SEM. N=7 mice.

## 9. EXTRA-DIMENSIONAL SHIFT REVERSAL (EDSR<sub>e</sub>)

This stage is the first reversal with the new relevant dimensions.

For the EDSR<sub>e</sub> stage, I collected recordings for a total period of 16 days across all animals ( $1.75 \pm 0.37$ ). The number of neurons recorded was 35 and the number of neurons analyzed was 20.

During the intertrial interval, the firing rate was  $0.14 \pm 0.02$  Hz, and no significant difference was found for correct and incorrect trials (paired t-test,  $p=0.645$ ), so I pooled together the average activity. The activity increased during the post house light period ( $0.40 \pm 0.10$  Hz; paired t-test,  $p=0.018$ ). For all other epochs in incorrect trials, and for all the epochs in correct trials no significant differences of the average firing rate were observed (paired t-test,  $p>0.05$ ). Pairwise comparison of the variation of the firing rate using paired t-test in correct and incorrect show any significant differences ( $p>0.05$ ) (Figure 43).

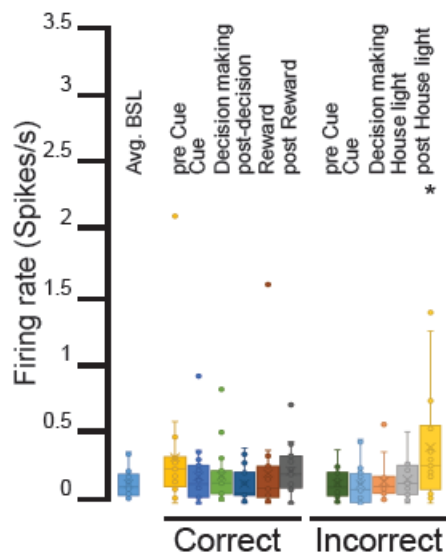


Figure 43. Firing rate of mPFC cells, recorded in WT mice, during EDSRe stage. The firing rate is averaged for different periods around correct and incorrect choices. EDSRe: Extra-Dimensional Shift Reversal. Statistics: \* AVG BSL vs all periods; \*  $p < 0.05$ , AVG BSL vs post-house light. Data are expressed as Mean $\pm$ SEM. N=7 mice.

When focusing on the PSTH of the behavioral response towards the correct poke, I found that the average latency between the cue delivery and the correct poke is  $8.56 \pm 1.85$ s, while the latency between the correct poke and the reward is  $5.85 \pm 1.81$ s. I used twice the standard deviation of the cue and reward delivery to define the edge of the PST. I obtained a PSTH onset of  $-19$ s and an offset of  $+16$ s to the correct poke. Before the onset and after the offset, I considered 3 seconds of baseline activity (total studied period: from  $-22$ s to  $19$ s). In this case, as for IDS2Re (Figure 37) what I found is that there is a significant increase during the immediate period preceding cue delivery. No significantly increased activity is observed in the following periods (Figure 44), as for the other reversal stages (Figure 25, 31, 37).

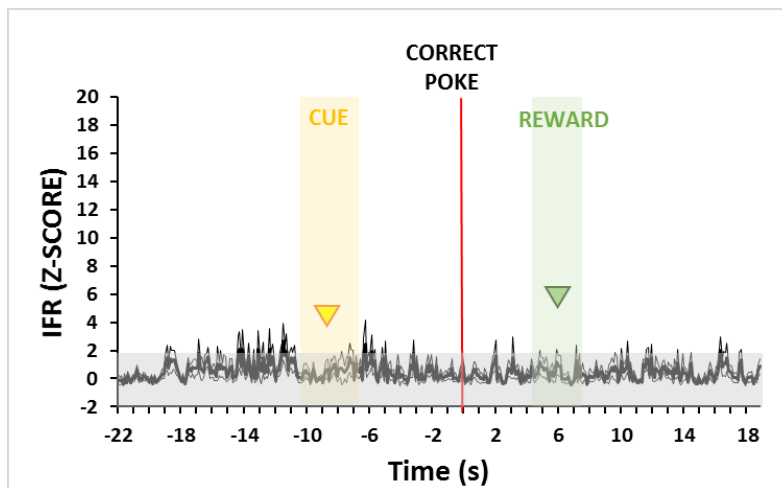


Figure 44. Instantaneous Firing Rate (IFR) of mPFC cells, recorded in WT mice, for the correct choice of EDSRe stage. It represents the variation of the mPFC activity around a correct poke. X-axis: time, expressed in seconds. EDSRe: Extra-Dimensional Shift Reversal. The axis is centered in the instant of the correct poke. Y-axis: z-score of the IFR. Gray square: represents the interval in which the firing is not significantly different from the baseline of 3 seconds in the beginning. Yellow arrow: it represents the average time of the cue delivery. Yellow square: represent the  $\pm$ SEM of the average time of cue delivery. Red line: the instant of correct poke. Green arrow: it represents the average time of the first entry in the food magazine. Green square: represent the  $\pm$ SEM of the average time of first entry in the food magazine. Data are expressed as Mean $\pm$ SEM. N=7 mice.

Next, I focused on the PSTH following an incorrect behavioral outcome (incorrect poke), and I found that the average latency between the cue delivery and the incorrect poke was  $5.98 \pm 0.83$ s.

I obtained a PSTH onset of -11s and an offset of +5s to the incorrect poke. Before the onset and after the offset, I considered 3 seconds of baseline activity (total studied period: from -14s to 8s).

When I compared the z-score of the firing activity during each individual trial with incorrect poke, I found that the cue delivery is delivered at a similar timescale than for the correct poke. As for the previous reversal stages CDRe, IDSRe, IDS2Re (Figure 26, 32, 38), what I found is that in all the other different periods of the PST, no significantly increased activity was observed compared to the baseline, except for the post house light period (Figure 45).

The mPFC in case of correct choice in EDSRe, being the reversal rule familiar, behaved like IDS stages and IDS2Re, increasing the activity in the pre-responses periods.

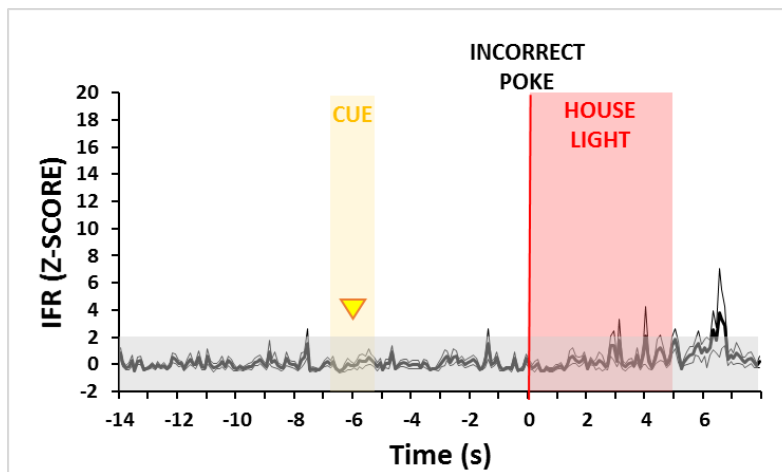


Figure 45. Instantaneous Firing Rate (IFR) of mPFC cells, recorded in WT mice, for the incorrect choice of EDSRe stage. It represents the variation of the mPFC activity around an incorrect poke. X-axis: time, expressed in seconds. EDSRe: Extra-Dimensional Shift Reversal. The axis is centered in the instant of the incorrect poke. Y-axis: z-score of the IFR. Gray square: represents the interval in which the firing is not significantly different from the baseline of 3 seconds in the beginning. Yellow arrow: it represents the average time of the cue delivery. Yellow square: represent the  $\pm$ SEM of the average time of cue delivery. Red line: the instant of correct poke. Red square: represent the duration of the house-light on. Data are expressed as Mean $\pm$ SEM. N=7 mice.

#### 4) D2L +/- mice show cognitive deficits in serial reversal learning compared to WT mice

The in vivo characterization of behavioral and electrophysiological readouts related to PFC-related executive functions in wild-type mice set up the ground for exploring how clinically-relevant genetic variants could impact PFC encoding of these cognitive processes. I started assessing D2L heterozygous mice with a variation altering the ratio between the short and long-form of dopamine D2 receptors. As for WT mice, I used a linear multi-site extracellular electrode, with a design containing 4 shanks of 4 recording sites for a total of 16 sites, that was sufficient to cover the entire PFC (*see Material&Methods*). I trained 7 D2L $\pm$  mice in the first habituation phases of the task. After two days from this initial pre-screening (*Figure 4*), mice were implanted in the prelimbic/ infralimbic region, and after a week of recovery, they were habituated to the cable and tested through the entire test.

I found that all D2L $\pm$  tested mice (7/7, 100%) were completing the test within a short period of time ( $13.14 \pm 1.55$  days), Following behavioral testing, posthoc analyses of the electrode placement were done using immunohistochemistry (*Figure 46*) (*see Material&Methods*).

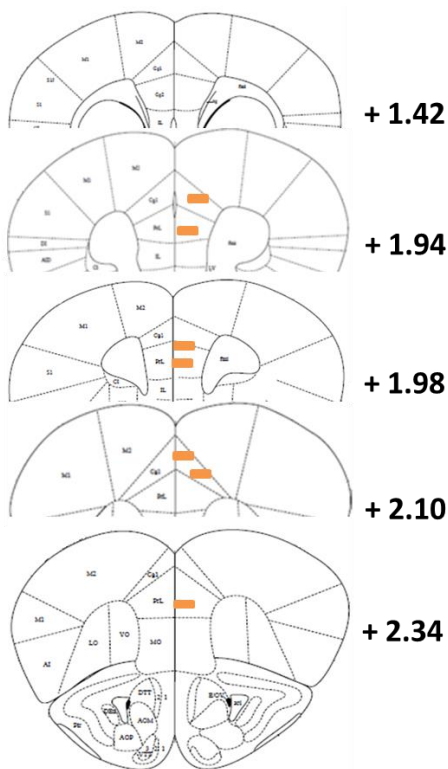


Figure 46. Stereotaxic positioning of the silicon probes electrodes implanted in the mPFC of D2L $\pm$  mice. The graphical representation is based on the dorsoventral coordinates on the Mice brain Atlas. N=7 mice.

Next, I analyzed the behavioral performance.

The main behavioral difference I found for D2L  $\pm$  was related to their serial reversal learning. In particular, no difference were evident compared to WT mice in the CDRe and IDSRe, while they needed more trial to solve the IDS2Re compared to WT mice (two-sample t-test, Bonferroni correction,  $t(13)=3.10348$ ,  $p=0.00839$ , trials; two-sample t-test, Bonferroni correction,  $t(13)=2.59085$ ,  $p=0.02239$ , time) (Figure 47, 48).

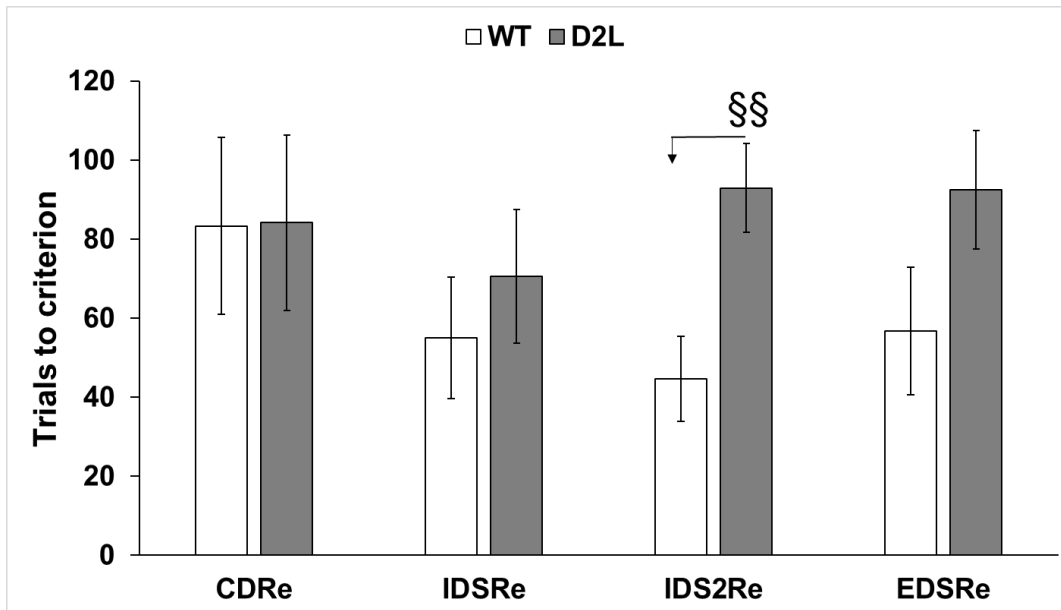


Figure 47. The number of trials to reach the criterion in the reversal stages of the task, obtained from WT and D2L<sup>+/-</sup> mice. CDR<sub>e</sub>: Compound Discrimination Reversal; IDS<sub>Re</sub>: Intra-Dimensional Shift Reversal; IDS2<sub>Re</sub>: Intra-Dimensional Shift 2 Reversal; EDS<sub>Re</sub>: Extra-Dimensional Shift Reversal. White bars: trials to criterion of WT mice. Dark gray bars: trials to criterion of D2L<sup>+/-</sup> mice. Statistics: § p<0.01, IDS2<sub>Re</sub> D2L<sup>+/-</sup> vs IDS2<sub>Re</sub> wt. Data are expressed as Mean±SEM. N WT=8 mice. N D2L<sup>+/-</sup> = 7 mice.

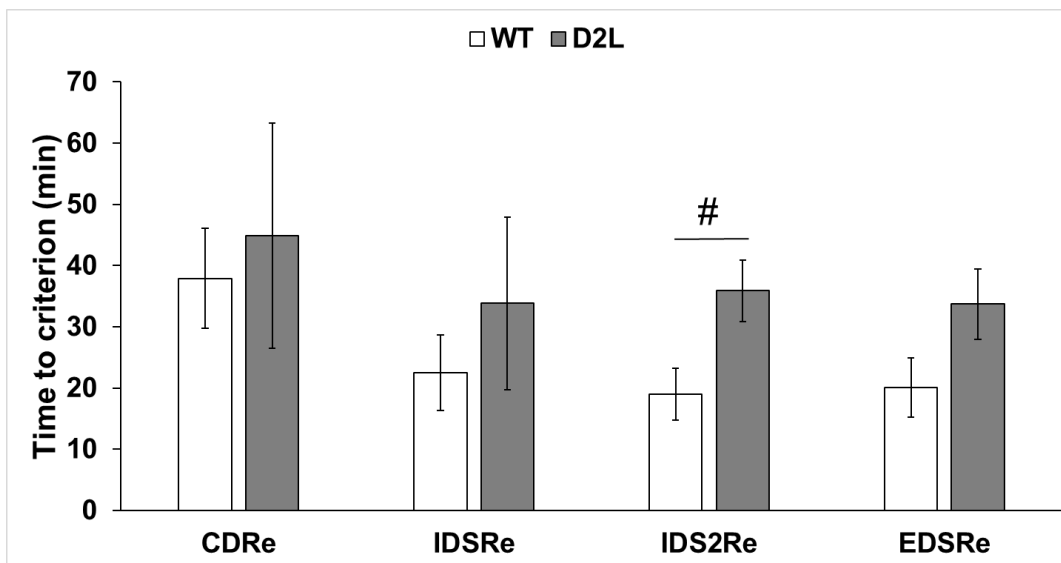


Figure 48. Time spent to reach the criterion in the reversal stages of the task, obtained from WT and D2L<sup>+/-</sup> mice. CDR<sub>e</sub>: Compound Discrimination Reversal; IDS<sub>Re</sub>: Intra-Dimensional Shift Reversal; IDS2<sub>Re</sub>: Intra-Dimensional Shift 2 Reversal; EDS<sub>Re</sub>: Extra-Dimensional Shift Reversal. White bars: time to criterion of WT mice. Dark gray bars: times to criterion of D2L<sup>+/-</sup> mice. Statistics: # p<0.05, IDS2<sub>Re</sub> D2L<sup>+/-</sup> vs IDS2<sub>Re</sub> wt. Data are expressed as Mean±SEM. N WT=8 mice. N D2L<sup>+/-</sup> =7 mice.

Latency to respond decreases for D2L<sup>+/-</sup> groups during the progression of the task as for wt. In SD the latency is statistically different from those of IDS2<sub>Re</sub>, EDS, and EDS<sub>Re</sub> (ONE WAY repeated measure ANOVA, F(8,64)= 4.58485, P= 1.881E-4, posthoc HSD TUKEY: P<sub>SDvIDS2Re</sub>= 0.02854; P<sub>SDvEDS</sub> 0.00247; P<sub>SDvEDSRe</sub>= 0.0148); in CD with those of EDS (ONE WAY repeated measure ANOVA, F(8,64)= 4.58485, P= 1.881E-4,

posthoc HSD TUKEY:  $P_{CD \vee EDS} = 0.02239$ ); in CDRe with those in EDS, and EDSRe (ONE WAY repeated measure ANOVA,  $F(8,64) = 4.58485$ ,  $P = 1.881E-4$ , posthoc HSD TUKEY:  $P_{CDRe \vee EDS} = 0.00769$ ;  $P_{CDRe \vee EDSRe} = 0.04022$ ). For what concern the EDS mice didn't increase the latency (*Figure 49*).

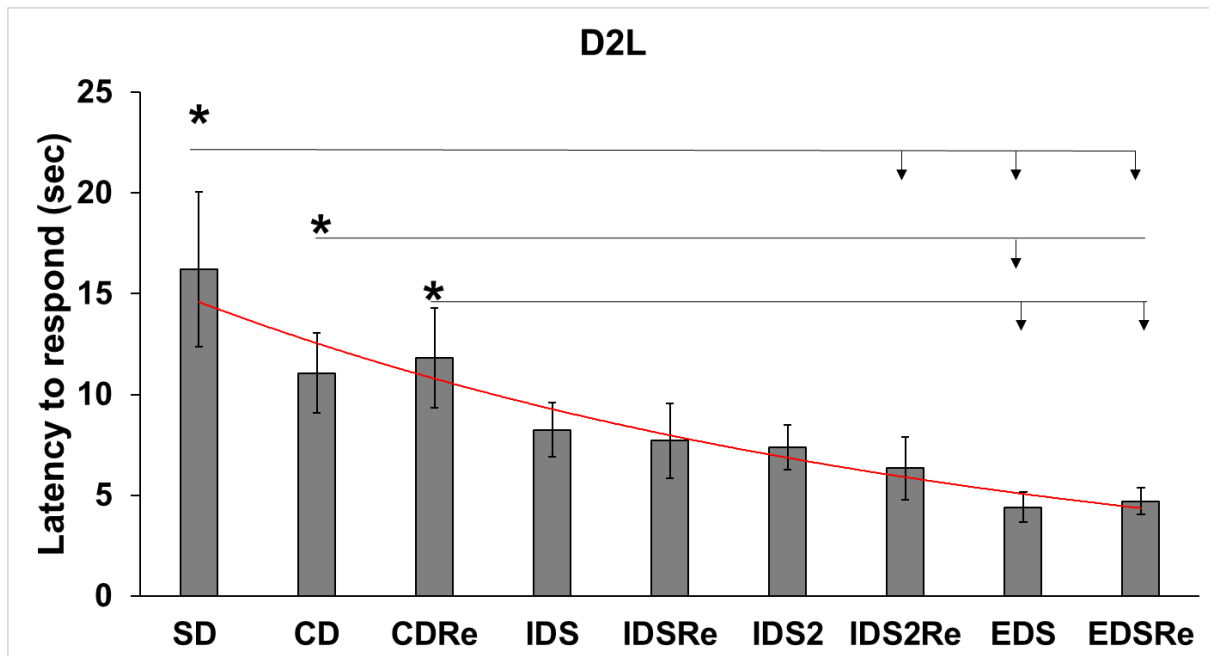


Figure 49. Latency to respond of D2L $_{+/-}$  mice. It represents the time, in seconds, between the delivery of the cues and the responses. SD: Simple Discrimination; CD: Compound Discrimination; CDRe: Compound Discrimination Reversal; IDS: Intra-Dimensional Shift; IDSRe: Intra-Dimensional Shift Reversal; IDS2: Intra-Dimensional Shift 2; IDS2Re: Intra-Dimensional Shift 2 Reversal; EDS: Extra-Dimensional Shift; EDSRe: Extra-Dimensional Shift Reversal. Red line: the exponential trend of the values across the different stages. Statistics:  $*p < 0.05$ , SD vs IDSRe, EDS, EDSRe. Statistics:  $*p < 0.05$ , SD vs IDS2Re, EDS, EDSRe; CD vs EDS; CDRe vs EDS, EDSRe. Data are expressed as Mean  $\pm$  SEM. N=7 mice.

I then compare the latency to correct with the latency to incorrect responses.

For what concern D2L $_{+/-}$  mice, what I found is a decrease of this latency across stages in both cases. In particular, in the case of correct choice, I found that the latency is statistically greater in SD compared to those in EDS and EDSRE (ONE WAY repeated measure ANOVA,  $F(8,32) = 3.47583$ ,  $P = 0.00541$ , posthoc HSD TUKEY:  $P_{SD \vee EDS} = 0.021$ ;  $P_{SD \vee EDSRE} = 0.03971$ ). In case of incorrect choice, the latency is statistically higher in SD compared to those in EDS (paired t-test, Bonferroni correction,  $P = 0.03901$ ). I found no significant effect across different stages between latency to correct and latency to incorrect responses (*Figure 50*). This suggests that the mice might present some difficulties to discriminate between the different cues.

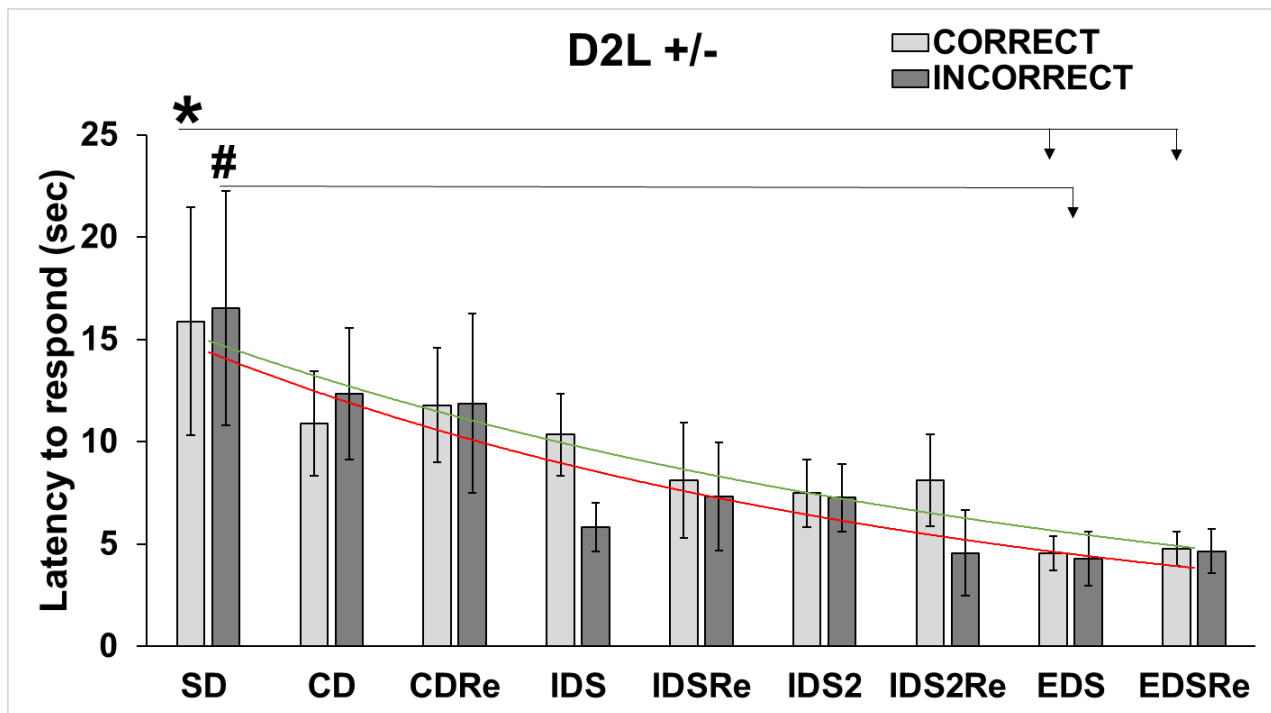


Figure 50. Latency to correct and incorrect responses of D2L<sup>+/-</sup> mice. They are the time, in seconds, between the delivery of the cues and the correct and incorrect responses, obtained from 7 D2L<sup>+/-</sup> mice. SD: Simple Discrimination; CD: Compound Discrimination; CDRe: Compound Discrimination Reversal; IDS: Intra-Dimensional Shift; IDSR: Intra-Dimensional Shift Reversal; IDS2: Intra-Dimensional Shift 2; IDS2Re: Intra-Dimensional Shift 2 Reversal; EDS: Extra-Dimensional Shift; EDSRe: Extra-Dimensional Shift Reversal. Light gray bar: latency to correct responses. Dark gray bar: latency to incorrect responses. Green line: the exponential trend of the latency to correct responses across the different stages. Red line: the exponential trend of the latency to incorrect responses across the different stages. Statistics: \* $p < 0.05$ , SD correct vs EDS correct, EDSRe correct. #  $p < 0.01$ , SD incorrect vs EDS incorrect. Data are expressed as Mean $\pm$ SEM. N=7 mice.

Paying attention to the latency to reward, in D2L <sup>+/-</sup> mice, I found a higher latency to collect the reward at the beginning of the task, in SD, CD, and CDRe, meaning that probably they are low motivated. Then, there is a decrease through the different stages, meaning that mice, when developed the attentional set, become more and more motivated. The increase of the latency to reward when the relevant dimension change is not present, meaning that although the rule change, the attentional set that they developed before is too strong to create another one (Figure 51).



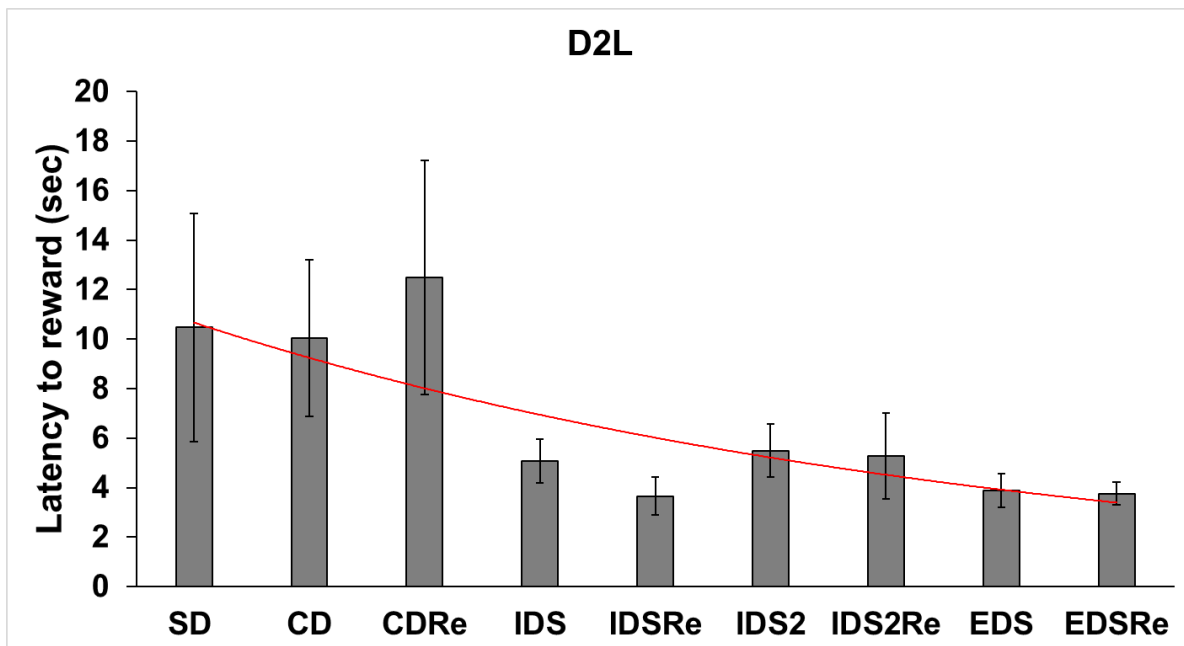


Figure 51. Latency to reward of D2L<sup>+/-</sup> mice. It is the time, in seconds, between a correct poke and the time of the first head entry to the food pellet magazine, obtained from 7 D2L<sup>+/-</sup> mice. SD: Simple Discrimination; CD: Compound Discrimination; CDRe: Compound Discrimination Reversal; IDS: Intra-Dimensional Shift; IDSRe: Intra-Dimensional Shift Reversal; IDS2: Intra-Dimensional Shift 2; IDS2Re: Intra-Dimensional Shift 2 Reversal; EDS: Extra-Dimensional Shift; EDSRe: Extra-Dimensional Shift Reversal. Red line: the exponential trend of the latency to reward across the different stages. Data are expressed as Mean±SEM. N=7 mice.

## 5) Electrophysiology of D2L<sup>+/-</sup> mice

During the entire performance of the task, the neural activity of the mPFC of dys<sup>+/-</sup> mice was recorded through single-unit multielectrode.

As for WT mice, I used the same behavioral events as stimuli for electrophysiology: CUE EVENT, CORRECT EVENT, REWARD EVENT, INCORRECT EVENT, HOUSE LIGHT EVENT (*Figure 16*).

During the spikes sorting, I had to discard two animals from the analysis for a large amount of noise in the traces, and therefore for the impossibility of obtaining a clean neuronal signal.

From all animals recorded (n=5), a total of 110 single units were recorded across the entire task.

Because there are different types of neurons in the mPFC, based on the previous reports using optogenetic identification or large scale recording, I decided to clusters my recorded unit based on their average firing rate and their CV: SLOW&REGULAR, SLOW&BURSTY, FAST&REGULAR, FAST&BURSTY.

As expected, in all the stages of the task, the great majority of the neurons that I recorded belong to the group of SLOW&REGULAR and SLOW&BURSTY neurons, considered as putative pyramidal neurons (*Figure 52*).

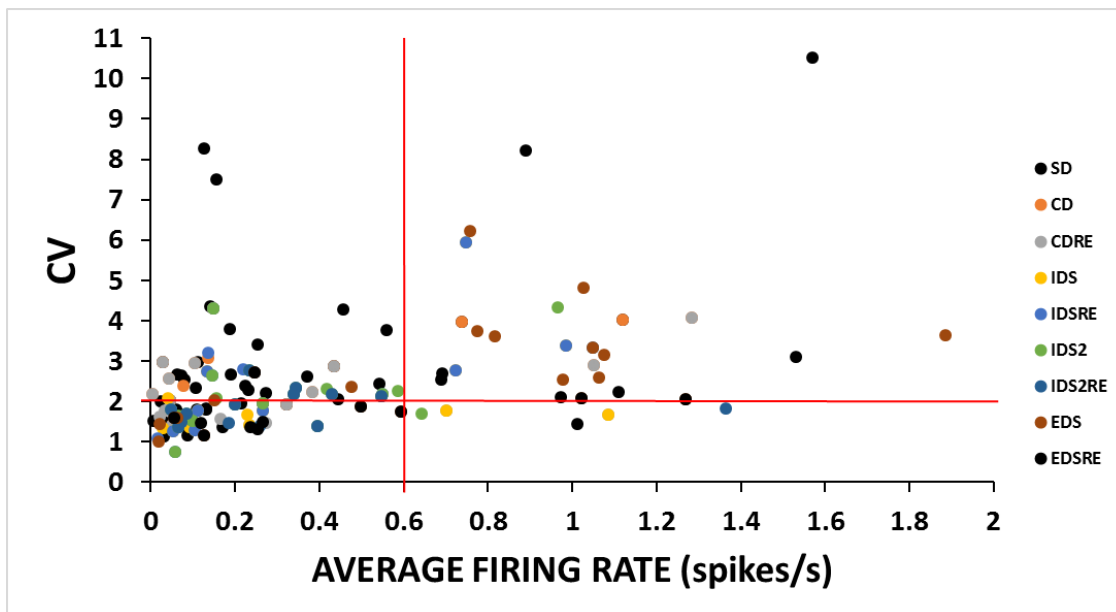


Figure 52. Type of single-unit recorded in D2L<sup>+/−</sup> mice. Each color represents a different stage of the task. SD: Simple Discrimination; CD: Compound Discrimination; CDRe: Compound Discrimination Reversal; IDS: Intra-Dimensional Shift; IDSRe: Intra-Dimensional Shift Reversal; IDS2: Intra-Dimensional Shift 2; IDS2Re: Intra-Dimensional Shift 2 Reversal; EDS: Extra-Dimensional Shift; EDSRe: Extra-Dimensional Shift Reversal. X-axis: average firing rate of the single units, expressed in the number of spikes per second. Y-axis: Coefficient of Variation: STANDARD DEVIATION (FIRING)/MEAN(FIRING). Red lines: delimitations for characterized the 4 different groups of single-units. N=5 mice.

For the same reason as for WT mice, I discarded all units with an average firing activity <math><0.1\text{Hz}</math>.

I first focused on the variation of the firing activity in the vicinity of specific events, and in particular the time of correct poke and the time of incorrect poke, using peristimulus time analyses and normalized using z-score analyses. Due to the great number of neurons, and to previous reports in the PFC, I consider the firing rate variation as binomial, that allows me to consider a significant change to the baseline as presenting an increase of the z-score of <math>\langle \text{or} \rangle</math> of 1.96.

In order to carefully analyses the behavior, I decided to divide the PSTH (peristimulus time histogram) into different periods, the same consideration for wt.

In case of correct choice: PRE-CUE DELIVERY, CUE DELIVERY, DECISION MAKING, POST-DECISION, REWARD, POST-REWARD.

In case of incorrect choice: PRE-CUE DELIVERY, CUE DELIVERY, DECISION MAKING, HOUSE-LIGHT, POST-HOUSE LIGHT.

I focused my attention on the IDS2Re stage, in which D2L<sup>+/−</sup> showed deficits in the performance of the stage.

During the intertrial interval, the firing rate was  $0.25 \pm 0.12$  Hz, and no significant difference was found for correct and incorrect trials (paired t-test,  $p=0.413$ ), so I pooled together the average activity. For all the epochs in correct and incorrect trials, no significant differences in the average firing rate were observed (paired t-test,

$p > 0.05$ ). Pairwise comparison of the variation of the firing rate using paired t-test in correct and incorrect show any significant differences ( $p > 0.05$ ) (Figure 53B).

I compared the results with those of WT mice, to see if there are possible alterations in mPFC which lead to performance deficits in IDS2Re.

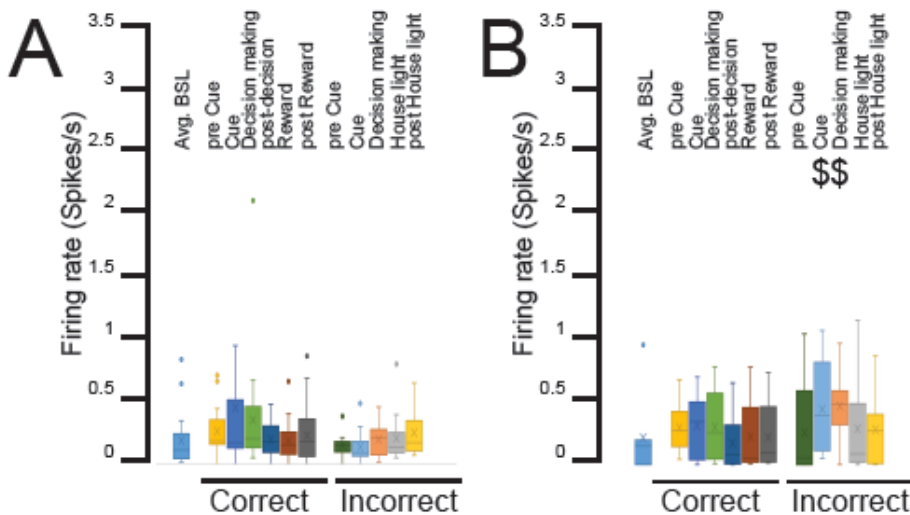


Figure 53. Firing rate of mPFC cells, recorded in WT and D2L<sup>+/-</sup> mice, during IDS2Re stage. The firing rate is averaged for different periods around correct and incorrect choices. IDSRe: Intra Dimensional Shift 2. A) WT mice. B) D2L<sup>+/-</sup> mice. Statistics: \$ WT vs D2L<sup>+/-</sup>; \$  $p < 0.05$ , cue WT vs cue D2L<sup>+/-</sup>, decision-making WT vs decision-making D2L<sup>+/-</sup>. Data are expressed as Mean $\pm$ SEM. N WT=7 mice. N D2L<sup>+/-</sup> =7 mice.

Looking at the firing rate of mPFC, I found that D2L<sup>+/-</sup> mice increased the firing activity during the cue (paired t-test,  $p = 0.012$ ) and decision-making period of an incorrect choice (paired t-test,  $p = 0.0051$ ), compared to WT mice (Figure 53).

What I found, comparing the IFR of mPFC cells, is that for D2L<sup>+/-</sup> the mPFC didn't increase the firing rate in the decision-making period of a correct choice, like for WT. Moreover, although for incorrect choice the mPFC of WT didn't increase in any period, in D2L<sup>+/-</sup> it increased in the decision-making period (Figure 54).

This suggests that in D2L<sup>+/-</sup> mice in the IDS2Re the mPFC encodes the decision making of incorrect choices, instead of correct choices like wt, causing probably the worst performance of mice in this stage.

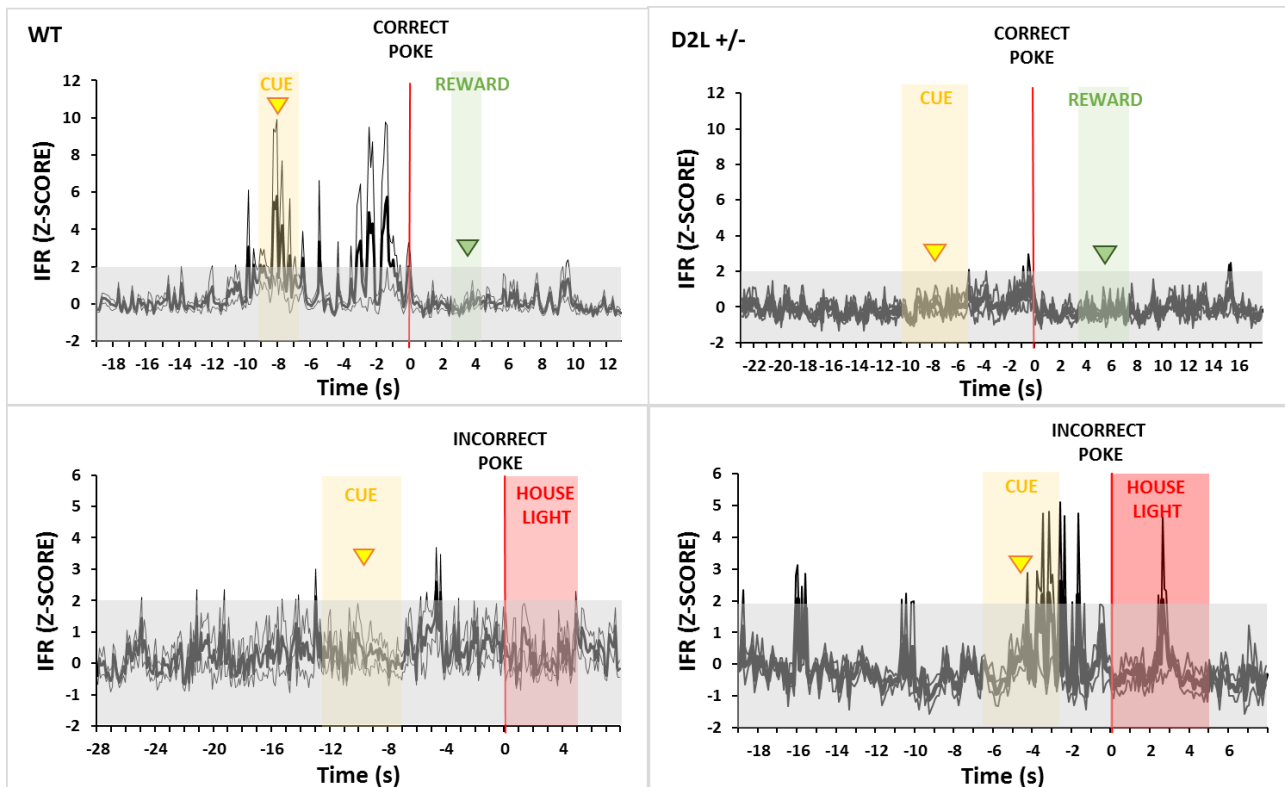


Figure 54. Instantaneous Firing Rate (IFR) of mPFC cells, recorded in WT and D2L<sup>+/-</sup> mice, for the correct and incorrect choices of IDS2Re stage. It represents the variation of the mPFC activity around a correct (top) or incorrect (bottom) poke. X-axis: time, expressed in seconds. IDS2Re: Intra-Dimensional Shift 2 Reversal. The axis is centered in the instant of the correct poke. Y-axis: z-score of the IFR. Gray square: represents the interval in which the firing is not significantly different from the baseline of 3 seconds in the beginning. Yellow arrow: it represents the average time of the cue delivery. Yellow square: represent the  $\pm$ SEM of the average time of cue delivery. Red line: the instant of correct/incorrect poke. Green arrow: it represents the average time of the first entry in the food magazine. Green square: represent the  $\pm$ SEM of the average time of first entry in the food magazine. Red square: represent the duration of the house-light on. Data are expressed as Mean $\pm$ SEM. N WT=7 mice. N D2L<sup>+/-</sup> =5 mice.

## 6) Dys <sup>+/-</sup> mice show deficits in the EDS, compared to WT mice

As for WT and D2L<sup>+/-</sup>-mice, I used a linear multi-site extracellular electrode, with a design containing 4 shanks of 4 recording sites for a total of 16 sites, that was sufficient to cover the entire PFC (see *Material&Methods*). I trained 7 dys<sup>+/-</sup> mice in the first habituation phases of the task. After two days from this initial pre-screening (Figure 4), mice were implanted in the prelimbic/ infralimbic region, and after a week of recovery, they were habituated to the cable and tested through the entire test.

I found that the great majority of dys<sup>+/-</sup> tested mice (6/7, 85.71%) were completing the test within a short period of time ( $10.50 \pm 1.57$  days), while the remaining dys <sup>+/-</sup> tested mice (1/7, 14.29%) were not able to complete the test (criterion <8/10 for 6 consecutive days). Following behavioral testing, posthoc analyses of the electrode placement were done using immunohistochemistry (Figure 55) (see *Material&Methods*).

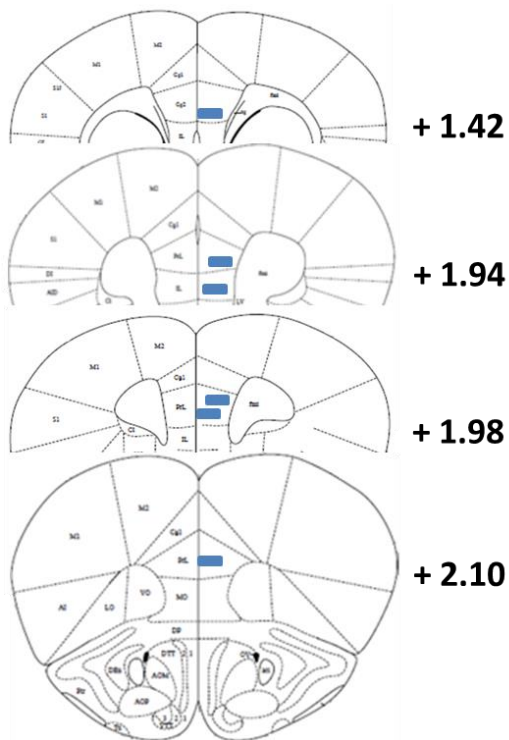


Figure 55. Stereotaxic positioning of the silicon probes electrodes implanted in the mPFC of *dys*<sup>+/-</sup> mice. The graphical representation is based on the dorsoventral coordinates on the Mice brain Atlas. N=6 mice.

I found that *dys*<sup>+/-</sup> mice increased the number of trials and the time to reach the criterion in EDS compared to the previous stages (*Figure 55, 56*). In particular, trials in EDS were significantly higher compared to those in IDS2Re (paired t-test, Bonferroni correction,  $t(5)=3,57091$ ;  $P=0,01603$ ).

Compared them with WT mice, I found that *dys*<sup>+/-</sup> had a deficit in EDS, in which the number of trials significantly increased (*Figure 56, 57*) (two-sample t-test,  $p=0.04145$ ). this was in agreement with evidence from probe-naïve mice (Scheggia *et al.*, 2018).

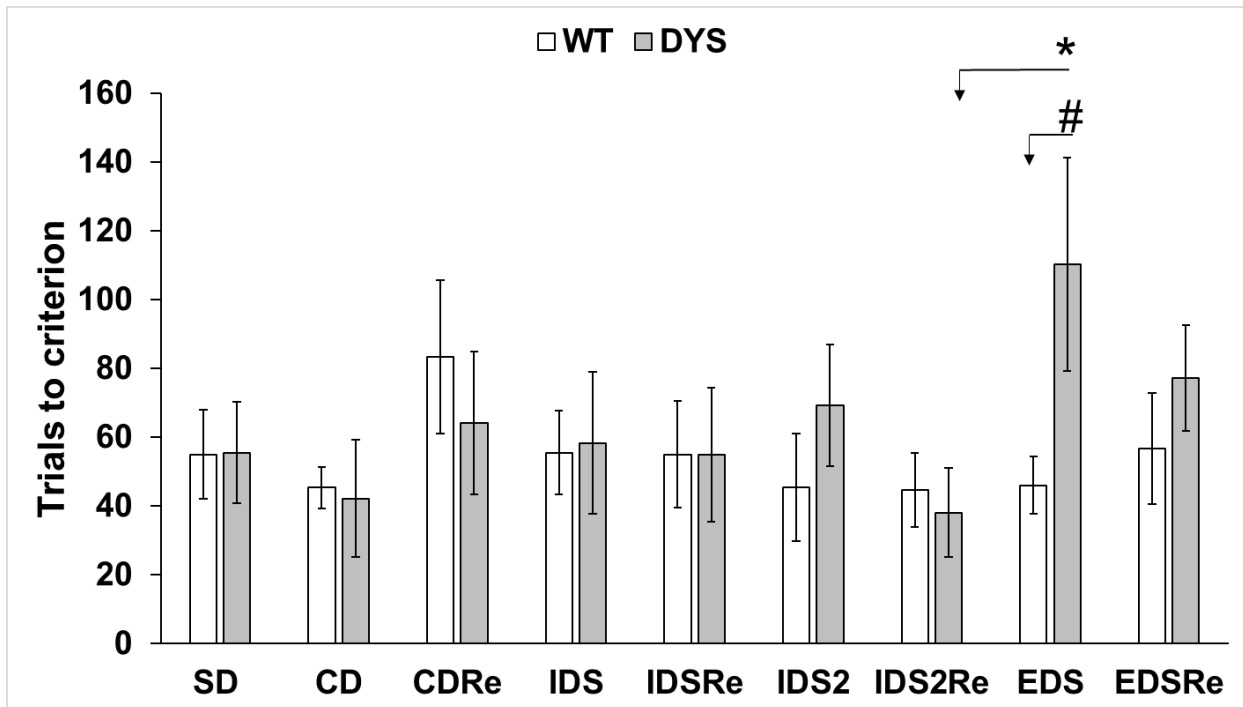


Figure 56. The number of trials to reach the criterion in all the stages of the task, obtained from WT and *dys*<sup>+/-</sup> mice. SD: Simple Discrimination; CD: Compound Discrimination; CDR<sub>e</sub>: Compound Discrimination Reversal; IDS: Intra-Dimensional Shift; IDS<sub>Re</sub>: Intra-Dimensional Shift Reversal; IDS<sub>2</sub>: Intra-Dimensional Shift 2; IDS<sub>2Re</sub>: Intra-Dimensional Shift 2 Reversal; EDS: Extra-Dimensional Shift; EDS<sub>Re</sub>: Extra-Dimensional Shift Reversal. White bars: trials to criterion of WT mice. Light gray bars: trials to criterion of *dys*<sup>+/-</sup> mice. Statistics: \**p*<0.05, EDS *dys*<sup>+/-</sup> vs IDS<sub>2Re</sub> *dys*<sup>+/-</sup>. #*p*<0.05, EDS *dys*<sup>+/-</sup> vs EDS wt. Data are expressed as Mean±SEM. N WT=8 mice. N *dys*<sup>+/-</sup> =6 mice.

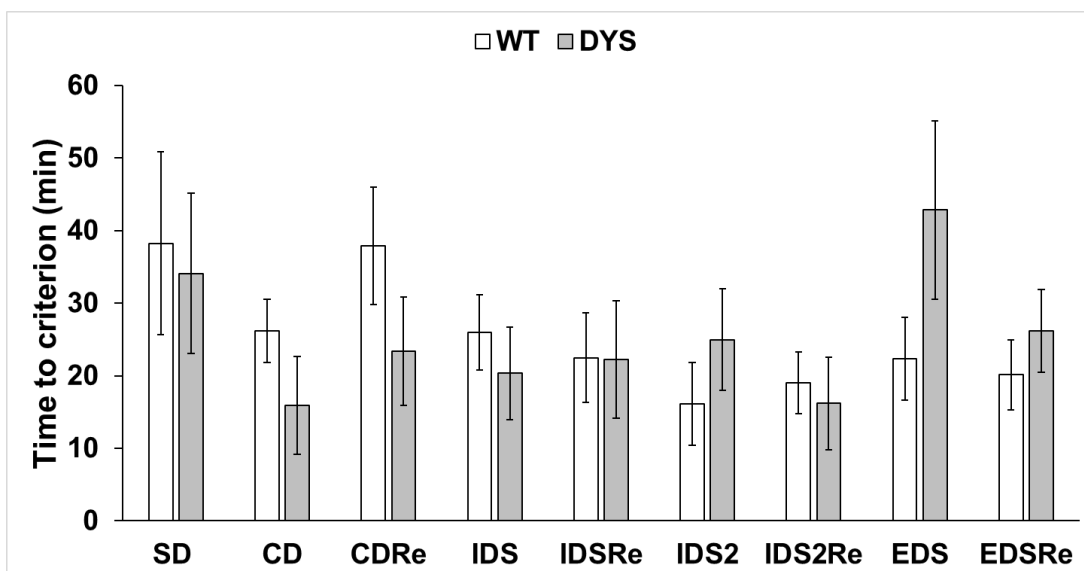


Figure 57. Time spent to reach the criterion in all the stages of the task, obtained from WT and *dys*<sup>+/-</sup> mice. SD: Simple Discrimination; CD: Compound Discrimination; CDR<sub>e</sub>: Compound Discrimination Reversal; IDS: Intra-Dimensional Shift; IDS<sub>Re</sub>: Intra-Dimensional Shift Reversal; IDS<sub>2</sub>: Intra-Dimensional Shift 2; IDS<sub>2Re</sub>: Intra-Dimensional Shift 2 Reversal; EDS: Extra-Dimensional Shift; EDS<sub>Re</sub>: Extra-Dimensional Shift Reversal. White bars: time to criterion of WT mice. Light gray bars: time to the criterion of *dys*<sup>+/-</sup> mice. Data are expressed as Mean±SEM. N WT=8 mice. N *dys*<sup>+/-</sup> = 6 mice.

Looking at the latency to respond, the time between the presentation of the cues and the response that represents an index of the decisional processing, I found that across the entire stage there was a trend to decrease the time to respond to the cue (*Figure 58*). Indeed I found that the time to respond in SD was higher than the time to respond in IDS2Re and EDS2Re (ONE WAY repeated measure ANOVA,  $F(8,72)= 2.47487$ ,  $P=0.0198$ , posthoc HSD TUKEY:  $P_{SDvIDSRe}= 0.03654$ ;  $P_{SDvEDSRe}= 0.02968$ ).

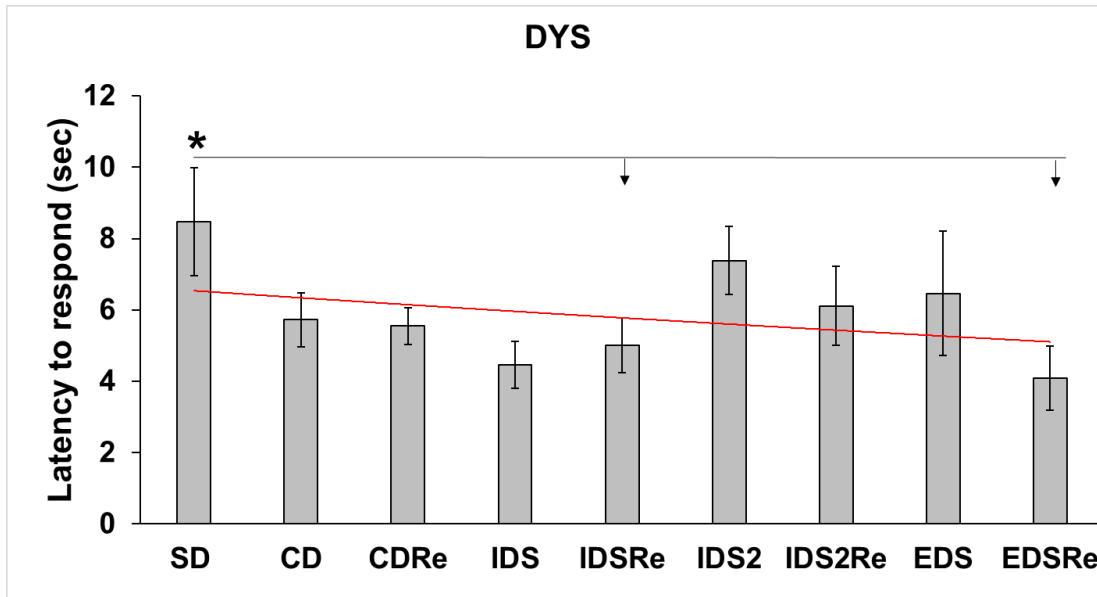


Figure 58. Latency to respond of dys+/- mice. It represents the time, in seconds, between the delivery of the cues and the responses, obtained from 5 dys+/- mice. SD: Simple Discrimination; CD: Compound Discrimination; CDRe: Compound Discrimination Reversal; IDS: Intra-Dimensional Shift; IDSRe: Intra-Dimensional Shift Reversal; IDS2: Intra-Dimensional Shift 2; IDS2Re: Intra-Dimensional Shift 2 Reversal; EDS: Extra-Dimensional Shift; EDSRe: Extra-Dimensional Shift Reversal. Red line: the exponential trend of the values across the different stages. Statistics: \* $p<0.05$ , SD vs IDSRe ,EDSRe. Data are expressed as Mean $\pm$ SEM. N=6 mice.

I then compared the latency to correct with the latency to incorrect responses.

What I found for dys+/- mice was a decrease of this latency across stages in both cases. I found no significant effect across different stages between latency to correct and latency to incorrect responses (*Figure 59*).

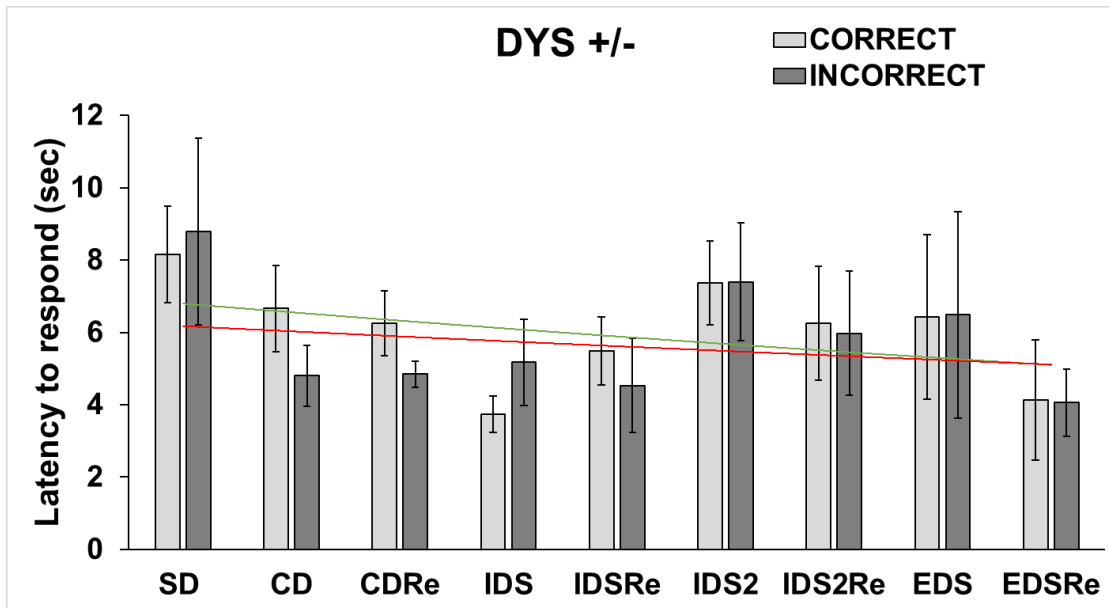


Figure 59. Latency to correct and incorrect responses of dys $\pm$  mice. They are the time, in seconds, between the delivery of the cues and the correct and incorrect responses, obtained from 5 dys $\pm$  mice. SD: Simple Discrimination; CD: Compound Discrimination; CDR<sub>e</sub>: Compound Discrimination Reversal; IDS: Intra-Dimensional Shift; IDS<sub>Re</sub>: Intra-Dimensional Shift Reversal; IDS<sub>2</sub>: Intra-Dimensional Shift 2; IDS<sub>2Re</sub>: Intra-Dimensional Shift 2 Reversal; EDS: Extra-Dimensional Shift; EDS<sub>Re</sub>: Extra-Dimensional Shift Reversal. Light gray bar: latency to correct responses. Dark gray bar: latency to incorrect responses. Green line: the exponential trend of the latency to correct responses across the different stages. Red line: the exponential trend of the latency to incorrect responses across the different stages. Statistics: \* $p < 0.05$ , SD correct vs IDS<sub>2Re</sub> correct, EDS correct. ##  $p < 0.01$ , SD incorrect vs CD incorrect, CDR<sub>e</sub> incorrect, IDS incorrect, IDS<sub>Re</sub> incorrect, IDS<sub>2</sub> incorrect, IDS<sub>2Re</sub> incorrect, EDS incorrect, EDS<sub>Re</sub> incorrect. Data are expressed as Mean $\pm$ SEM. N=6 mice.

Paying attention to the latency to reward, in dys  $\pm$  mice it didn't change through the days. There was a decrease in IDS<sub>2Re</sub>, probably due to the fact that they developed the attentional set. When changing the relevant dimension, it increased a little bit, because mice had to develop a new attentional set, and probably when they made a correct choice, they couldn't understand to have done it, and they couldn't expect the reward. After EDS, it started to decrease, because they started to develop the attentional set for the new dimension (Figure 60).



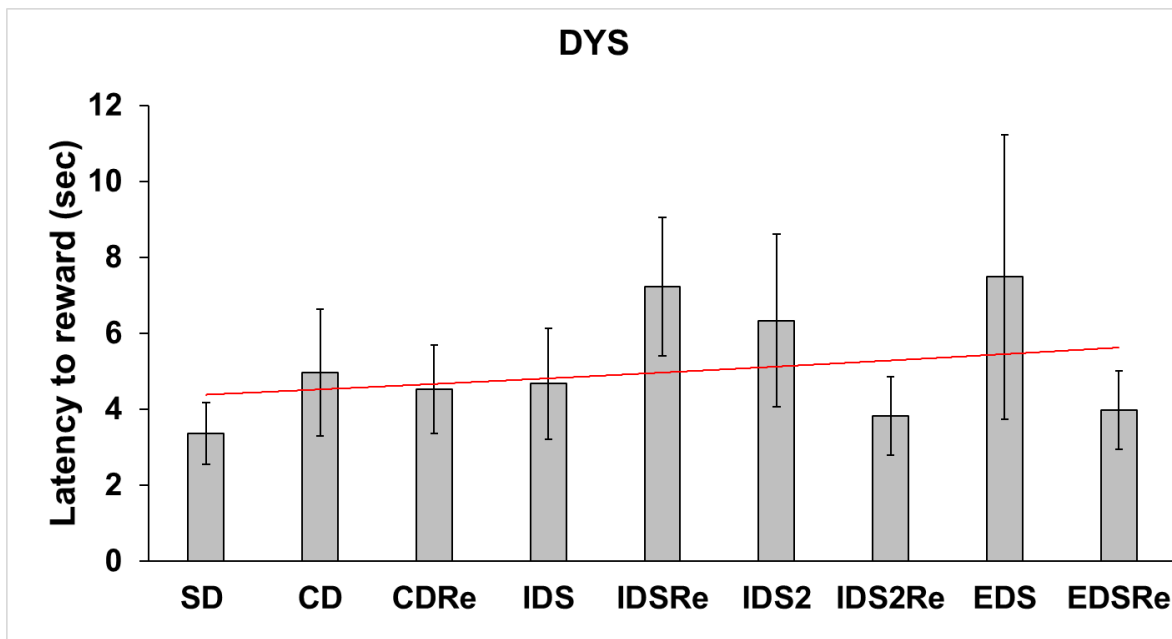


Figure 60. Latency to reward of dys<sup>+/-</sup> mice. It is the time, in seconds, between a correct poke and the time of the first head entry to the food pellet magazine, obtained from 5 dys<sup>+/-</sup> mice. SD: Simple Discrimination; CD: Compound Discrimination; CDRé: Compound Discrimination Reversal; IDS: Intra-Dimensional Shift; IDSRe: Intra-Dimensional Shift Reversal; IDS2: Intra-Dimensional Shift 2; IDS2Re: Intra-Dimensional Shift 2 Reversal; EDS: Extra-Dimensional Shift; EDSRe: Extra-Dimensional Shift Reversal. Red line: the exponential trend of the latency to reward across the different stages. Data are expressed as Mean±SEM. N=6 mice.

This suggests that there wasn't a difference between all the genotypes in the motivation during the task.

## 7) Electrophysiology of dys<sup>+/-</sup> mice

During the entire performance of the task, the neural activity of the mPFC of dys<sup>+/-</sup> mice was recorded through single-unit multielectrode.

As for WT mice, I used the same behavioral events as stimuli for electrophysiology: CUE EVENT, CORRECT EVENT, REWARD EVENT, INCORRECT EVENT, HOUSE LIGHT EVENT (*Figure 16*).

During the spikes sorting, I had to discard two animals from the analysis for a large amount of noise in the traces, and therefore for the impossibility of obtaining a clean neuronal signal.

From all animals recorded (n=4), a total of 111 single units were recorded across the entire task.

Because there are different types of neurons in the mPFC, based on the previous reports using optogenetic identification or large scale recording, I decided to clusters my recorded unit based on their average firing rate and their CV: SLOW&REGULAR, SLOW&BURSTY, FAST&REGULAR, FAST&BURSTY.

As expected, in all the stages of the task, the great majority of the neurons that I recorded belong to the group of SLOW&REGULAR and SLOW&BURSTY neurons, considered as putative pyramidal neurons (*Figure 61*).

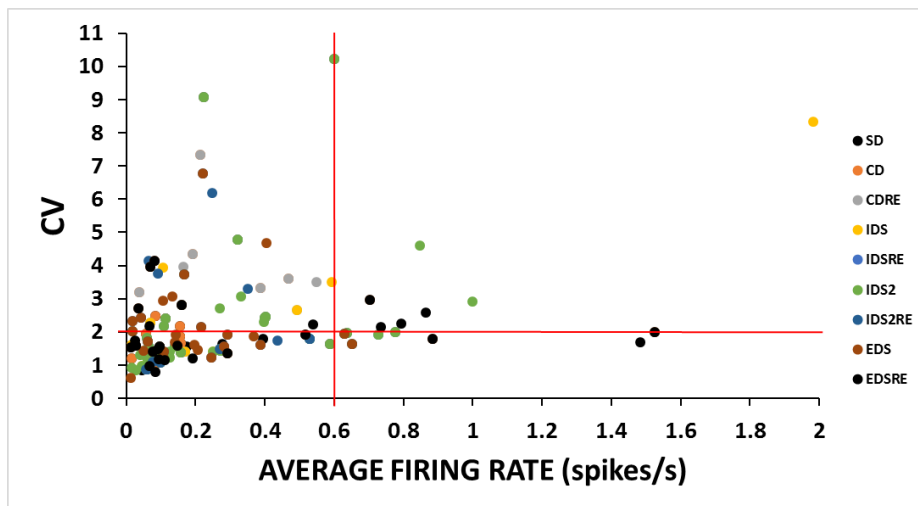


Figure 61. Type of single-unit recorded in dys+/- mice. Each color represents a different stage of the task. SD: Simple Discrimination; CD: Compound Discrimination; CDRE: Compound Discrimination Reversal; IDS: Intra-Dimensional Shift; IDSRe: Intra-Dimensional Shift Reversal; IDS2: Intra-Dimensional Shift 2; IDS2Re: Intra-Dimensional Shift 2 Reversal; EDS: Extra-Dimensional Shift; EDSRe: Extra-Dimensional Shift Reversal. X-axis: average firing rate of the single units, expressed in the number of spikes per second. Y-axis: Coefficient of Variation: STANDARD DEVIATION (FIRING)/MEAN(FIRING). Red lines: delimitations for characterized the 4 different groups of single-units. N=4 mice.

For the same reason as for WT mice, discarded all units with an average firing activity  $<0.1$ Hz.

I first focused on the variation of the firing activity in the vicinity of specific events, and in particular the time of correct poke and the time of incorrect poke, using peristimulus time analyses and normalized using z-score analyses. Due to the great number of neurons, and to previous reports in the PFC, I consider the firing rate variation as binomial, that allows me to consider a significant change to the baseline as presenting an increase of the z-score of  $<or>$  of 1.96.

In order to carefully analyses the behavior, I decided to divide the PSTH (peristimulus time histogram) into different periods, the same consideration for wt.

In case of correct choice: PRE-CUE DELIVERY, CUE DELIVERY, DECISION MAKING, POST-DECISION, REWARD, POST-REWARD.

In case of incorrect choice: PRE-CUE DELIVERY, CUE DELIVERY, DECISION MAKING, HOUSE-LIGHT, POST-HOUSE LIGHT.

During the intertrial interval, the firing rate was  $0.19 \pm 0.07$  Hz, and no significant difference was found for correct and incorrect trials (paired t-test,  $p=0.812$ ), so I pooled together the average activity. The activity increased during the incorrect decision-making period ( $0.39 \pm 0.10$  Hz; paired t-test,  $p=0.049$ ) and during the house light period ( $0.51 \pm 0.15$  Hz; paired t-test,  $p=0.013$ ). For all other epochs in incorrect trials, and for all the epochs in correct trials no significant differences of the average firing rate were observed (paired t-test,  $p>0.05$ ). Pairwise comparison of the variation of the firing rate using paired t-test in correct and incorrect show that the firing was significantly higher during the post-decision period associated with incorrect trials (house-

light period) compared to correct ( $p=0.013$ ). All other comparisons were not showing any significant differences ( $p>0.05$ ) (Figure 62B).

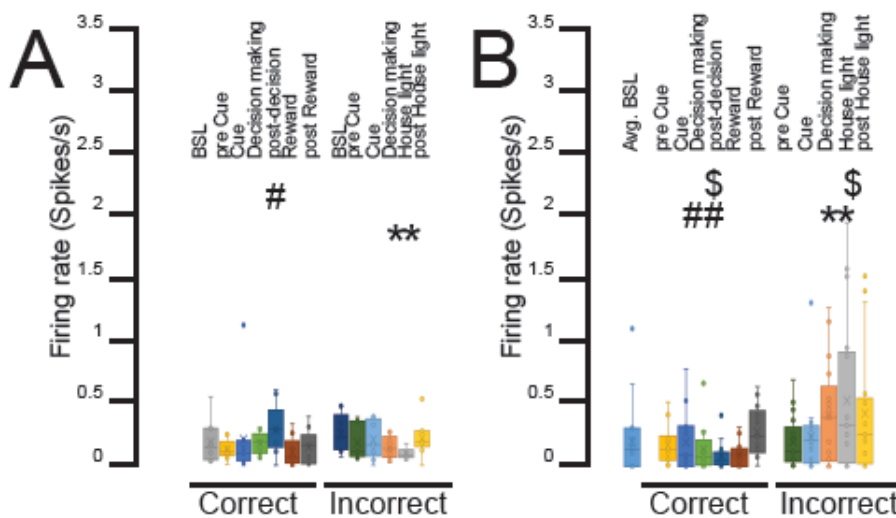


Figure 62. Firing rate of mPFC cells, recorded in WT and *dys*<sup>+/-</sup> mice, during EDS stage. The firing rate is averaged for different periods around correct and incorrect choices. EDS: Extra Dimensional Shift. A) WT mice. B) *dys*<sup>+/-</sup> mice. Statistics: \* AVG BSL vs all periods; # correct vs incorrect; \$ WT vs *dys*<sup>+/-</sup>; \* $p<0.05$ , WT, *dys*<sup>+/-</sup>: AVB BSL vs decision-making incorrect, house light. #  $p<0.05$ , *dys*<sup>+/-</sup>: decision-making correct vs decision-making incorrect, post-decision correct vs post-decision incorrect (house light). \$  $p<0.05$ , post-decision correct WT vs post-decision correct *dys*<sup>+/-</sup>, house light WT vs house light *dys*<sup>+/-</sup>. Data are expressed as Mean $\pm$ SEM. N WT=7 mice. N *dys*<sup>+/-</sup> =4 mice.

I compared the results with those of WT mice, to see if there are possible alterations in mPFC which lead to performance deficits in EDS.

Looking at the firing rate of mPFC, I found that *dys*<sup>+/-</sup> mice decreased the firing activity during the post-decision period related to a correct choice (paired t-test,  $p=0.008$ ), and increased the firing after a correct choice (paired t-test,  $p=0.049$ ), during the house light period, compared to WT mice (Figure 62).

What I found, comparing the IFRs of mPFC cells, for *dys*<sup>+/-</sup> is that the mPFC anticipated the increase of activity in the decision-making period of a correct choice, unlike WT where the increase was in the post-decision period. Moreover, although for incorrect choice the mPFC of WT didn't increase in any period, in *dys*<sup>+/-</sup> it increased in the decision-making and post-decision period (Figure 63).

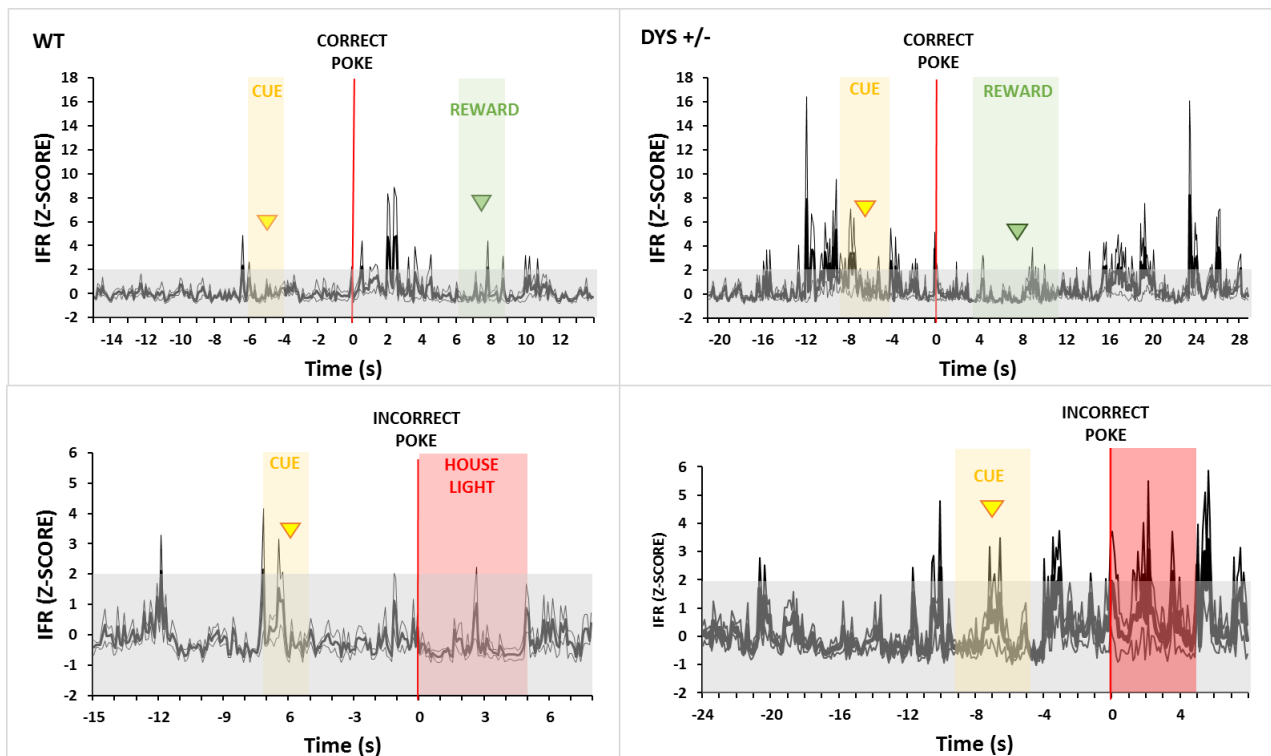


Figure 63. Instantaneous Firing Rate (IFR) of mPFC cells, recorded in WT and *dys*<sup>+/-</sup> mice, for the correct and incorrect choices of EDS stage. It represents the variation of the mPFC activity around a correct (top) or incorrect (bottom) poke. X-axis: time, expressed in seconds. EDS: Extra-Dimensional Shift. The axis is centered in the instant of the correct poke. Y-axis: z-score of the IFR. Gray square: represents the interval in which the firing is not significantly different from the baseline of 3 seconds in the beginning. Yellow arrow: it represents the average time of the cue delivery. Yellow square: represent the  $\pm$ SEM of the average time of cue delivery. Red line: the instant of correct/incorrect poke. Green arrow: it represents the average time of the first entry in the food magazine. Green square: represent the  $\pm$ SEM of the average time of first entry in the food magazine. Red square: represent the duration of the house-light on. Data are expressed as Mean $\pm$ SEM. N WT=7 mice. N *dys*<sup>+/-</sup>=4 mice.

This suggests that in *dys*<sup>+/-</sup> mice seems that mPFC, instead codified the post-decision of a correct choice, encodes the post-decision of an incorrect choice, and moreover the decision-making period of a correct choice, like all the IDS stages, causing probably the worst performance of mice in this stage.

## 8) *Dys*<sup>+/-</sup>-*D2L*<sup>+/-</sup> mice show a restored behavioral performance

In a recent work of my group (Scheggia *et al.*, 2018), it has been discovered that a shift in the ratio between the short and long-form of dopamine D2 receptors in the context of dysbindin-1 reduced expression might be associated with better executive functions abilities measured in the EDS stage of the ASST or the Wisconsin Card Sorting Task (WCST) (Figure 1A). Thus I investigate the extracellular activity of mPFC of *DYS*-*D2L* double-heterozygous mice by in vivo electrophysiology as performed in wt, *D2L*, and *dys* mutants.

8 *dys*<sup>+/-</sup>-*D2L*<sup>+/-</sup> mice performed the three habituation of the task. After two days from this initial pre-screening (Figure 4), mice were implanted in the prelimbic/ infralimbic region, and after a week of recovery, they were habituated to the cable and tested through the entire test.

I found that the majority of tested mice (7/8, 87.5%) were completing the test within a short period of time (10.88 $\pm$ 1.25 days) while one single mouse (1/8, 12.5%) did not complete the test (criterion <8/10 for 6 consecutive days). Following behavioral testing, posthoc analyses of the electrode placement were done using immunohistochemistry (Figure 64) (see Material&Methods).

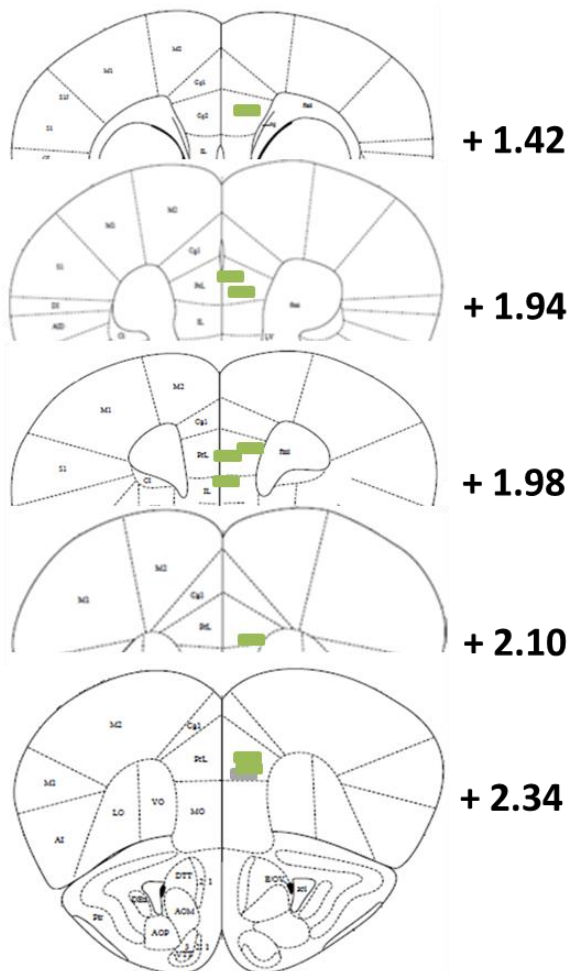


Figure 64. Stereotaxic positioning of the silicon probes electrodes implanted in the mPFC of *dys+/- D2L+/-* mice. The graphical representation is based on the dorsoventral coordinates on the Mice brain Atlas. N=7 mice.

Next, I analyzed the behavioral performance of the remaining mice (7/8 *dys+/-D2L+/-*).

*Dys+/-D2L+/-* mice restored the performance of EDS, in which *dys+/-* had an impairment, and restored also the performance of IDS2Re, where there was the impairment of *D2L+/-* mice. (Figure 65)

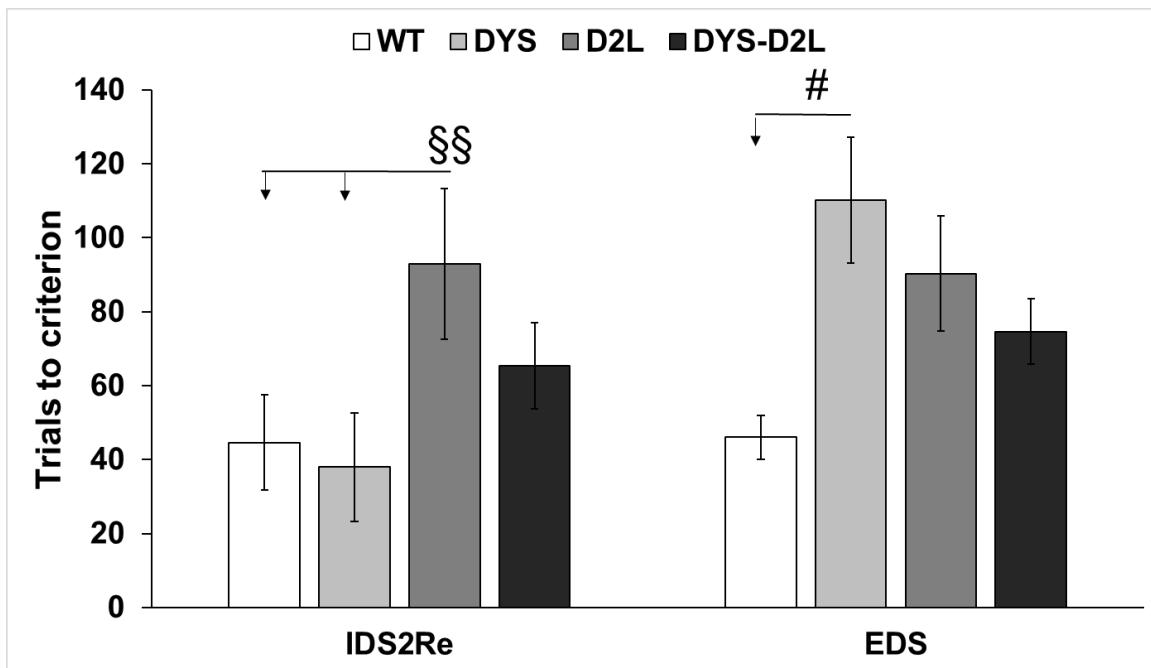


Figure 65. The number of trials to reach the criterion in IDS2Re and EDS, obtained from WT, *dys*<sup>+/-</sup>, *D2L*<sup>+/-</sup> and *dys*<sup>+/-</sup>-*D2L*<sup>+/-</sup> mice. IDS2Re: Intra-Dimensional Shift 2 Reversal; EDS: Extra-Dimensional Shift. White bars: trials to criterion of WT mice. Light gray bars: trials to criterion of *dys*<sup>+/-</sup> mice. Dark gray bars: trials to criterion of *D2L*<sup>+/-</sup> mice. Black bars: trials to criterion of *dys*<sup>+/-</sup>-*D2L*<sup>+/-</sup> mice. Statistics: #  $p < 0.05$ , EDS *dys*<sup>+/-</sup> vs EDS wt. §§  $p < 0.01$ , IDS2Re *D2L*<sup>+/-</sup> vs IDS2Re *dys*<sup>+/-</sup>, IDS2Re wt. Data are expressed as Mean $\pm$ SEM. N WT =8 mice. N *dys*<sup>+/-</sup> =6 mice. N *D2L*<sup>+/-</sup> =7 mice. N *dys*<sup>+/-</sup>-*D2L*<sup>+/-</sup> =7 mice.

*Dys*<sup>+/-</sup>-*D2L*<sup>+/-</sup> mice decreased the time in EDS, compared to *dys*<sup>+/-</sup> mice, and decreased also the time in SD, CD, and IDS2Re, compared to *D2L*<sup>+/-</sup> mice (Figure 66).

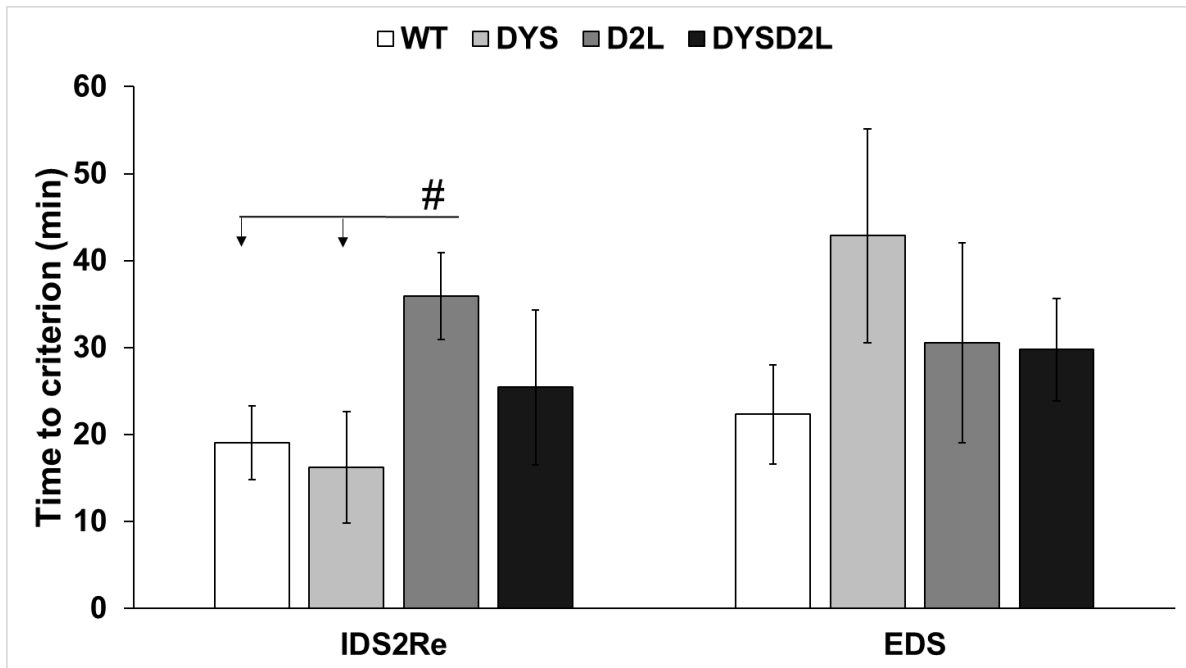


Figure 66. Time spent to reach the criterion in IDS2Re and EDS stages of the task, obtained from WT, *dys*<sup>+/-</sup>, *D2L*<sup>+/-</sup> and *dys*<sup>+/-</sup>*-D2L*<sup>+/-</sup> mice. IDS2Re: Intra-Dimensional shift 2 Reversal; EDS: Extra-Dimensional Shift. White bars: time to criterion of WT mice. Light gray bars: time to criterion of *dys*<sup>+/-</sup> mice. Dark gray bars: time to criterion of *D2L*<sup>+/-</sup> mice. Black bars: time to criterion of *dys*<sup>+/-</sup>*-D2L*<sup>+/-</sup> mice. Statistics: #  $p < 0.05$ , IDS2Re *D2L*<sup>+/-</sup> vs IDS2Re *dys*<sup>+/-</sup>, IDS2Re wt. Data are expressed as Mean $\pm$ SEM. N WT=8 mice. N *dys*<sup>+/-</sup>=6 mice. N *D2L*<sup>+/-</sup>=7 mice. N *dys*<sup>+/-</sup>*-D2L*<sup>+/-</sup>=7 mice.

Looking at the latency to respond, that is the time between the presentation of the cues and the response that represents an index of the decisional processing, I found that *dys*<sup>+/-</sup>*-D2L*<sup>+/-</sup> mice decreased the latency to respond stage by stage. The latency was higher in SD and CD; then it decreased stage by stage, significantly in IDS, IDSRe, IDS2, IDS2Re, compared to those in CD (*Figure 67*) (ONE WAY repeated measure ANOVA,  $F(8,88) = 3.28906$ ,  $P = 0.00249$ , posthoc HSD TUKEY:  $P_{CDvIDS} = 0.03688$ ;  $P_{CDvIDSRe} = 0.00585$ ;  $P_{CDvIDS2} = 0.00544$ ;  $P_{CDvIDS2Re} = 0.04676$ ).

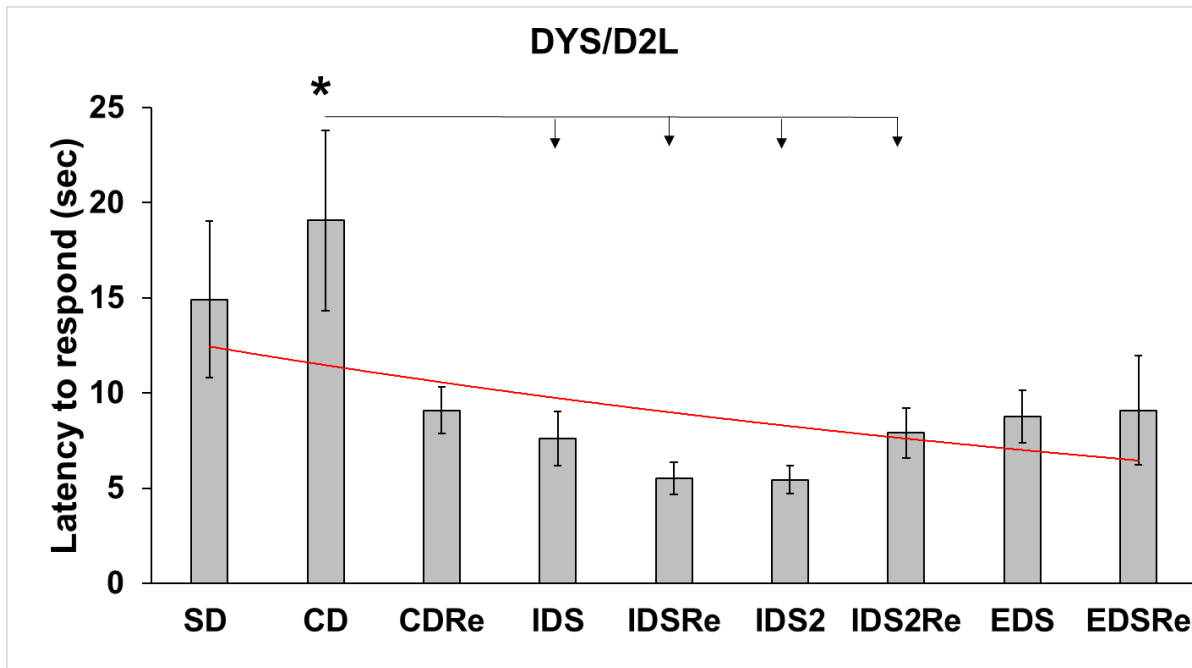


Figure 67. Latency to respond of dys<sup>±</sup>-D2L<sup>±</sup> mice. It represents the time, in seconds, between the delivery of the cues and the responses, obtained from 7 dys<sup>±</sup>-D2L<sup>±</sup> mice. SD: Simple Discrimination; CD: Compound Discrimination; CDRé: Compound Discrimination Reversal; IDS: Intra-Dimensional Shift; IDSRe: Intra-Dimensional Shift Reversal; IDS2: Intra-Dimensional Shift 2; IDS2Re: Intra-Dimensional Shift 2 Reversal; EDS: Extra-Dimensional Shift; EDSRe: Extra-Dimensional Shift Reversal. Red line: the exponential trend of the values across the different stages. Statistics: \*p<0.05, CD vs IDS,IDSRe ,IDS2,IDS2Re. Data are expressed as Mean±SEM. N=7 mice.

I considered then latency to correct and incorrect responses separately.

What I found for dys<sup>±</sup>-D2L<sup>±</sup> mice was a decrease in the latency to correct across stages in both cases. I found no significant effect across different stages between latency to correct and latency to incorrect responses (Figure 68).



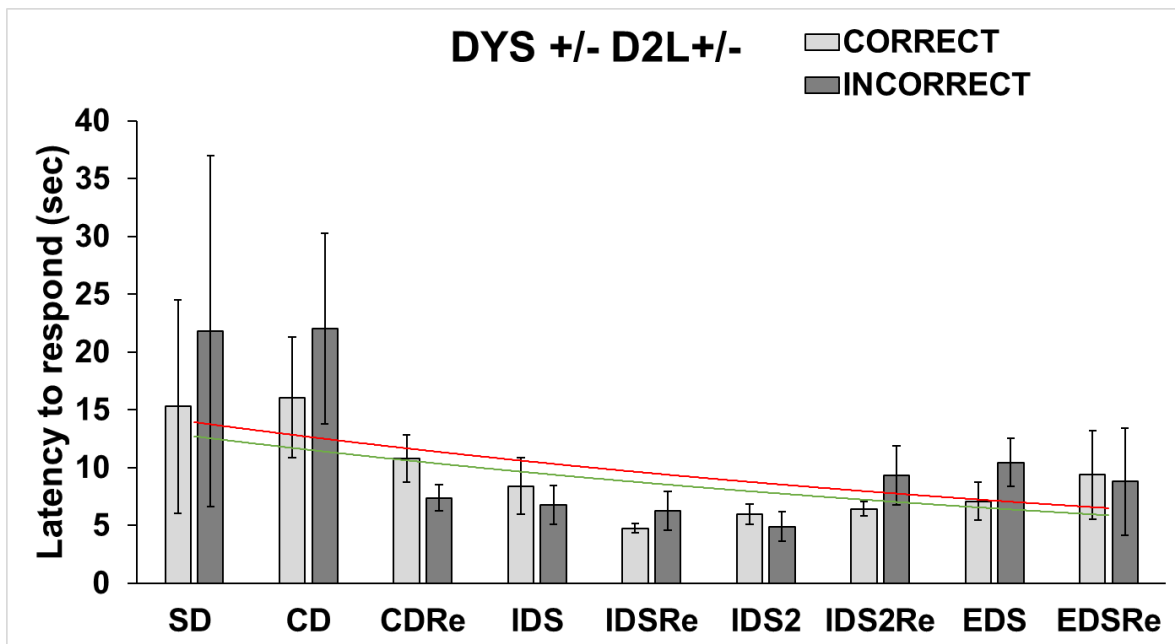


Figure 68. Latency to correct and incorrect responses of  $dys^{+/-}D2L^{+/-}$  mice. They are the time, in seconds, between the delivery of the cues and the correct and incorrect responses, obtained from 7  $dys^{+/-}D2L^{+/-}$  mice. SD: Simple Discrimination; CD: Compound Discrimination; CDR<sub>e</sub>: Compound Discrimination Reversal; IDS: Intra-Dimensional Shift; IDSRe: Intra-Dimensional Shift Reversal; IDS2: Intra-Dimensional Shift 2; IDS2Re: Intra-Dimensional Shift 2 Reversal; EDS: Extra-Dimensional Shift; EDSRe: Extra-Dimensional Shift Reversal. Light gray bar: latency to correct responses. Dark gray bar: latency to incorrect responses. Green line: the exponential trend of the latency to correct responses across the different stages. Red line: the exponential trend of the latency to incorrect responses across the different stages. Data are expressed as Mean $\pm$ SEM. N=7 mice.

Finally, I analyzed the latency to collect the reward, defined as the time between a correct poke and the time of the first head entry to the food pellet magazine. What I found is a significant decrease in the latency to reward from CD to IDSRe (ONE WAY repeated measure ANOVA,  $F(8,40) = 2.16254$ ,  $P = 0.05178$ , posthoc HSD TUKEY:  $P_{CD \text{ vs } IDS} = 0.04584$ ;  $P_{CD \text{ vs } IDSRe} = 0.04147$ ), meaning that mice seem to develop the attentional set, becoming more and more motivated in receiving the reward. From IDS2 the latency increases. This could mean that once developed the attentional set, probably mice lose a little bit the motivation in eating the reward, but they continue to perform the task because they are habituated to do it. When changing the relevant dimension, the latency is stabilized, and doesn't increase, and seems to decrease during the first reversal with the new relevant dimension, probably due to the fact that they have to develop a new attentional set and are motivated in learning the new rule (Figure 69).

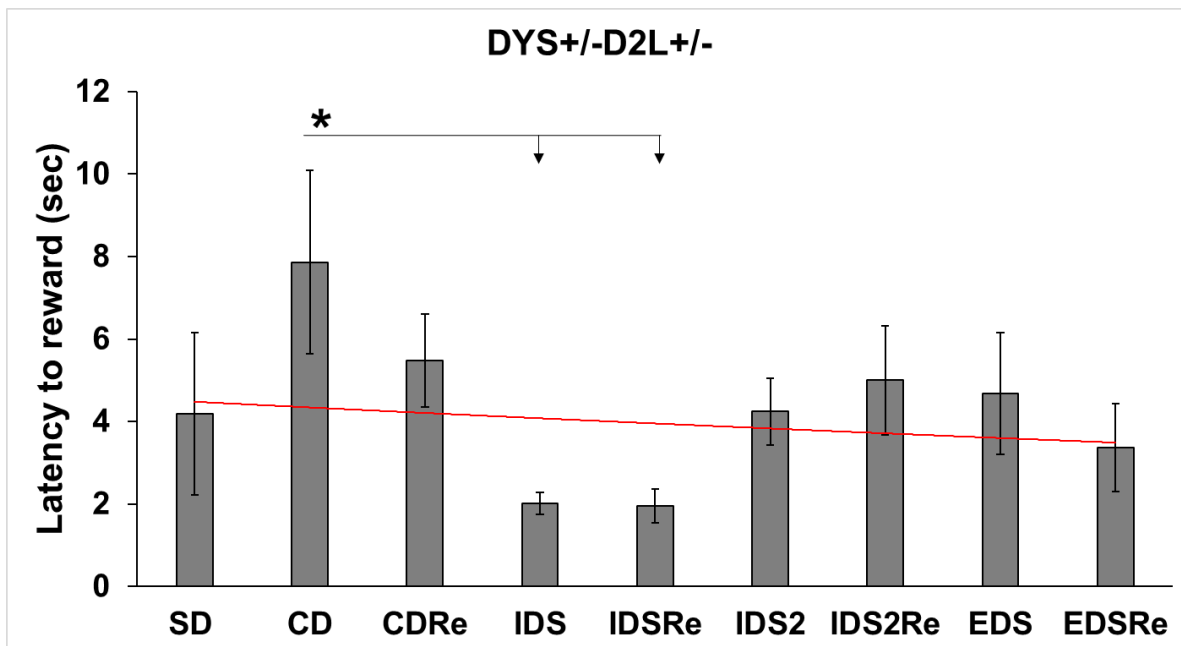


Figure 69. Latency to reward of  $dys^{+/-}D2L^{+/-}$  mice. It is the time, in seconds, between a correct poke and the time of the first head entry to the food pellet magazine, obtained from 7  $dys^{+/-}D2L^{+/-}$  mice. SD: Simple Discrimination; CD: Compound Discrimination; CDRe: Compound Discrimination Reversal; IDS: Intra-Dimensional Shift; IDSRe: Intra-Dimensional Shift Reversal; IDS2: Intra-Dimensional Shift 2; IDS2Re: Intra-Dimensional Shift 2 Reversal; EDS: Extra-Dimensional Shift; EDSRe: Extra-Dimensional Shift Reversal. Red line: the exponential trend of the latency to reward across the different stages. Statistics: \*  $p < 0.05$ , CD vs IDS, IDSRe. Data are expressed as Mean  $\pm$  SEM. N=7 mice.

This means that  $dys^{+/-}D2L^{+/-}$  mice develop faster the attentional set and start to lose the motivation in collecting the reward, until the changing of relevant dimensions.

## 9) Electrophysiology of $dys^{+/-}D2L^{+/-}$ mice

During the entire performance of the task, the neural activity of the mPFC of  $dys^{+/-}$  mice was recorded through single-unit multielectrode.

As for WT mice, I used the same behavioral events as stimuli for electrophysiology: CUE EVENT, CORRECT EVENT, REWARD EVENT, INCORRECT EVENT, HOUSE LIGHT EVENT (Figure 16).

During the spikes sorting, I had to discard three animals from the analysis for a large amount of noise in the traces, and therefore for the impossibility of obtaining a clean neuronal signal.

From all animals recorded (n=4), a total of 132 single units were recorded across the entire task.

Because there are different types of neurons in the mPFC, based on the previous reports using optogenetic identification or large scale recording, I decided to clusters my recorded unit based on their average firing rate and their CV: SLOW&REGULAR, SLOW&BURSTY, FAST&REGULAR, FAST&BURSTY.

As expected, in all the stages of the task, the great majority of the neurons that I recorded belong to the group of SLOW&REGULAR and SLOW&BURSTY neurons, considered as putative pyramidal neurons (Figure 70).

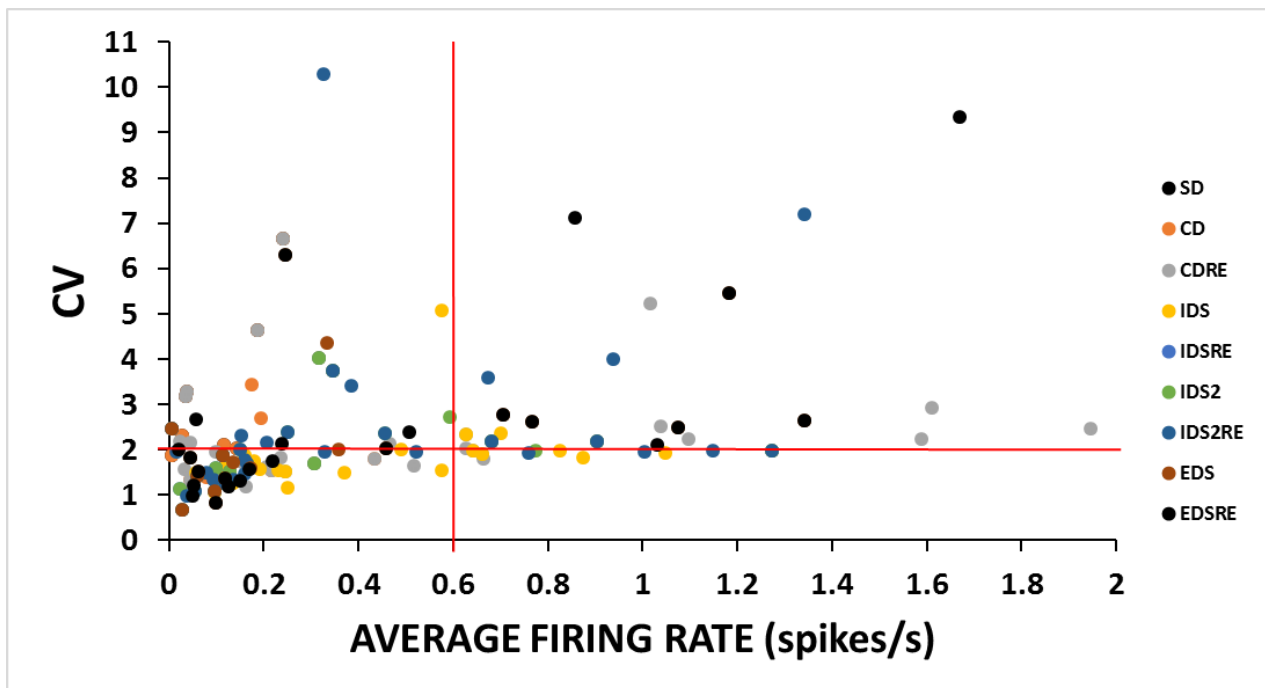


Figure 70. Type of single-unit recorded in *dys<sup>±</sup>-D2L<sup>±</sup>* mice. Each color represents a different stage of the task. SD: Simple Discrimination; CD: Compound Discrimination; CDRe: Compound Discrimination Reversal; IDS: Intra-Dimensional Shift; IDSRe: Intra-Dimensional Shift Reversal; IDS2: Intra-Dimensional Shift 2; IDS2Re: Intra-Dimensional Shift 2 Reversal; EDS: Extra-Dimensional Shift; EDSRe: Extra-Dimensional Shift Reversal. X-axis: average firing rate of the single units, expressed in the number of spikes per second. Y-axis: Coefficient of Variation: STANDARD DEVIATION (FIRING)/MEAN(FIRING). Red lines: delimitations for characterized the 4 different groups of single-units. N=4 mice.

For the same reason as for WT mice, discarded all units with an average firing activity <math><0.1\text{Hz}</math>.

I first focused on the variation of the firing activity in the vicinity of specific events, and in particular the time of correct poke and the time of incorrect poke, using peristimulus time analyses and normalized using z-score analyses. Due to the great number of neurons, and to previous reports in the PFC, I consider the firing rate variation as binomial, that allows me to consider a significant change to the baseline as presenting an increase of the z-score of <math><or></math> of 1.96.

In order to carefully analyses the behavior, I decided to divide the PSTH (peristimulus time instogram) into different periods, the same consideration for wt.

In case of correct choice: PRE-CUE DELIVERY, CUE DELIVERY, DECISION MAKING, POST-DECISION, REWARD, POST-REWARD.

In case of incorrect choice: PRE-CUE DELIVERY, CUE DELIVERY, DECISION MAKING, HOUSE-LIGHT, POST-HOUSE LIGHT.

I focused first on the EDS stage, the introduction of *D2L<sup>±</sup>* in *dys<sup>±</sup>* mice led to the restoration of the performance of the stage.

During the intertrial interval, the firing rate was  $0.32 \pm 0.09$  Hz, and no significant difference was found for correct and incorrect trials (paired t-test,  $p=0.188$ ), so I pooled together the average activity. The activity increased during the post-house light period related to an incorrect choice ( $0.54 \pm 0.10$  Hz; paired t-test,  $p=0.046$ ). For all other epochs in incorrect trials, and for all the epochs in correct trials no significant differences of the average firing rate were observed (paired t-test,  $p>0.05$ ). Pairwise comparison of the variation of the firing rate using paired t-test in correct and incorrect show that the firing was significantly higher during the pre-cue period associated with correct trials compared to incorrect ( $p=0.036$ ). All other comparisons were not showing any significant differences ( $p>0.05$ ) (Figure 71C).

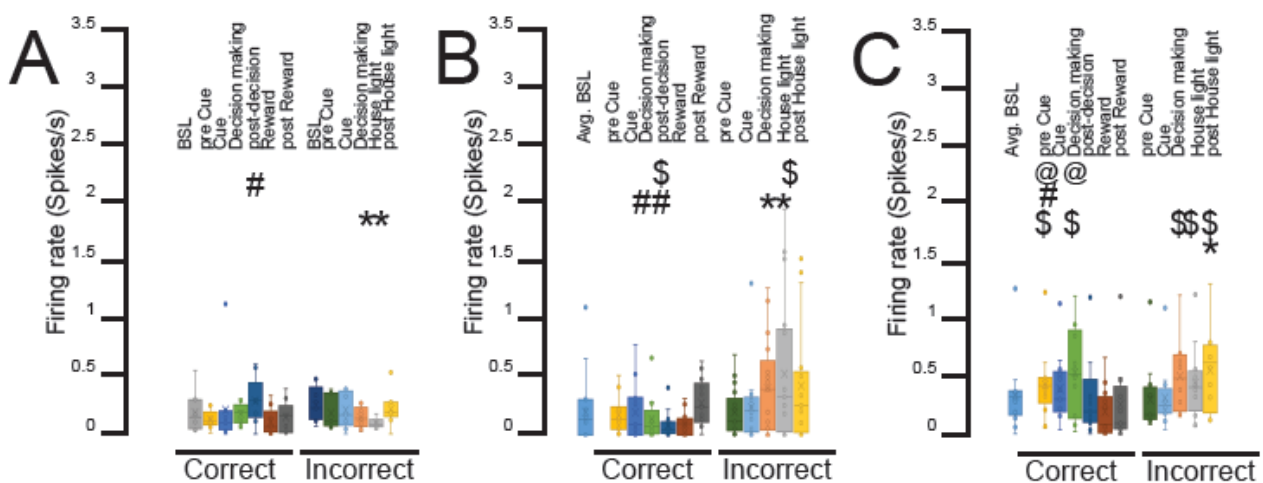


Figure 71. Firing rate of mPFC cells, recorded in WT, *dys*<sup>+/-</sup>, and *dys*<sup>+/-</sup>*D2L*<sup>+/-</sup> mice, during EDS stage. The firing rate is averaged for different periods around correct and incorrect choices. EDS: Extra Dimensional Shift. A) WT mice. B) *dys*<sup>+/-</sup> mice. C) *dys*<sup>+/-</sup>*D2L*<sup>+/-</sup> mice. Statistics: \* AVG BSL vs all periods; # correct vs incorrect; \$ WT vs *dys*<sup>+/-</sup>; @ *dys*<sup>+/-</sup> vs *dys*<sup>+/-</sup>*D2L*<sup>+/-</sup>; \* $p<0.05$ , WT, *dys*<sup>+/-</sup>: AVB BSL vs decision-making incorrect, house light; *dys*<sup>+/-</sup>*D2L*<sup>+/-</sup>: AVB BSL vs post-house light. #  $p<0.05$ , *dys*<sup>+/-</sup>: decision-making correct vs decision-making incorrect, post-decision correct vs post-decision incorrect (house light). \$  $p<0.05$ , WT vs *dys*<sup>+/-</sup>: post-decision correct, house light. WT vs *dys*<sup>+/-</sup>*D2L*<sup>+/-</sup>: pre-cue correct, decision-making correct, decision-making incorrect, house light, post-house light. @  $p<0.05$ , pre-cue correct *dys*<sup>+/-</sup> VS pre-cue correct *dys*<sup>+/-</sup>*D2L*<sup>+/-</sup>, decision-making correct *dys*<sup>+/-</sup> vs decision-making correct *dys*<sup>+/-</sup>*D2L*<sup>+/-</sup>. Data are expressed as Mean $\pm$ SEM. N WT=7 mice. N *dys*<sup>+/-</sup>=4 mice. N *dys*<sup>+/-</sup>*D2L*<sup>+/-</sup>=4 mice.

I compared the results with those of WT and *dys*<sup>+/-</sup> mice, to see which are the differences in the mPFC activity that lead to the restoration of the performance in EDS.

Looking at the firing rate of mPFC, I found that *dys*<sup>+/-</sup>*D2L*<sup>+/-</sup> mice increased the firing activity during the pre-cue period related to a correct choice (paired t-test,  $p=0.006$ ), decision-making period of both correct (paired t-test,  $p=0.012$ ) and incorrect (paired t-test,  $p=0.003$ ) choices, house light period (paired t-test,  $p=0.004$ ), and post-house light (paired t-test,  $p=0.014$ ), compared to WT mice (Figure 71A,C).

Comparing with *dys*<sup>+/-</sup> mice, I found that *dys*<sup>+/-</sup>*D2L*<sup>+/-</sup> increased the firing during the pre-cue period (paired t-test,  $p=0.011$ ), and decision making period (paired t-test,  $p=0.012$ ) of a correct choice (Figure 71B,C).

What I found, comparing the IFRs of mPFC cells, for *dys*<sup>+/-</sup>-D2L<sup>+/-</sup> is that the mPFC continued to increase the firing rate through the three periods of an incorrect choice like *dys*<sup>+/-</sup>, but with a stronger frequency. The important thing is that, although the mPFC in *dys*<sup>+/-</sup>-D2L<sup>+/-</sup> mice presented an increase in the decision-making period of a correct choice like *dys*<sup>+/-</sup>, its activity increased also in the post-decision period, like the mPFC activity of WT mice, and it didn't increase during the reward period, present in *dys*<sup>+/-</sup> (Figure 72).

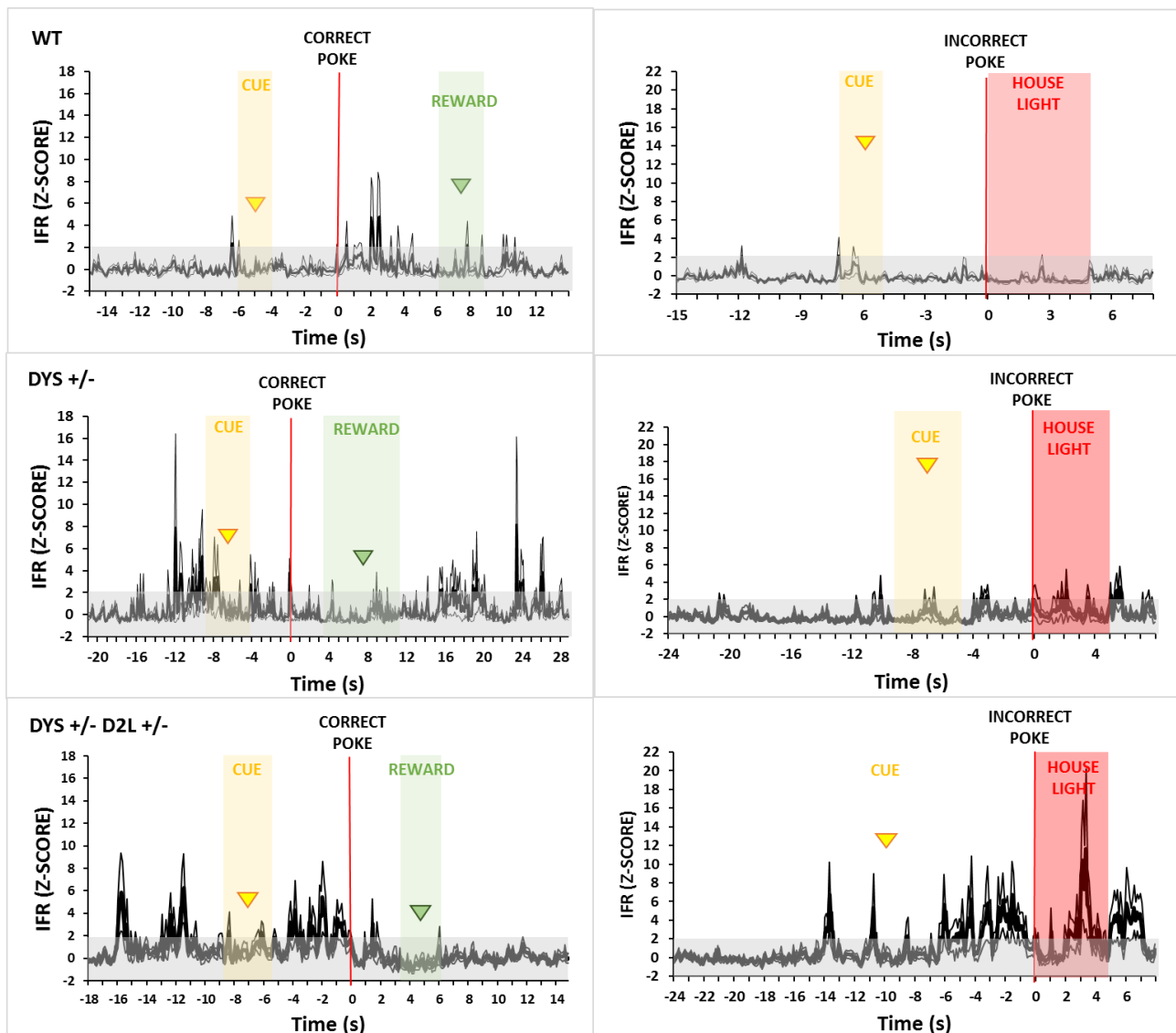


Figure 72. Instantaneous Firing Rate (IFR) of mPFC cells, recorded in WT, *dys*<sup>+/-</sup>, and *dys*<sup>+/-</sup>-D2L<sup>+/-</sup> mice, for the correct and incorrect choices of EDS stage. It represents the variation of the mPFC activity around a correct (left) or incorrect (right) poke. Top: WT mice. Middle: *dys*<sup>+/-</sup> mice. Bottom: *dys*<sup>+/-</sup>-D2L<sup>+/-</sup> mice. X-axis: time, expressed in seconds. EDS: Extra-Dimensional Shift The axis is centered in the instant of the correct poke. Y-axis: z-score of the IFR. Gray square: represents the interval in which the firing is not significantly different from the baseline of 3 seconds in the beginning. Yellow arrow: it represents the average time of the cue delivery. Yellow square: represent the  $\pm$ SEM of the average time of cue delivery. Red line: the instant of correct/incorrect poke. Green arrow: it represents the average time of the first entry in the food magazine. Green square: represent the  $\pm$ SEM of the average time of first entry in the food magazine. Red square: represent the duration of the house-light on. Data are expressed as Mean $\pm$ SEM. N WT=7 mice. N *dys*<sup>+/-</sup> =4 mice. N *dys*<sup>+/-</sup>-D2L<sup>+/-</sup> =4 mice.

Then I focalized my attention on the IDS2Re stage.

During the intertrial interval, the firing rate was  $0.38 \pm 0.16$  Hz, and no significant difference was found for correct and incorrect trials (paired t-test,  $p=0.219$ ), so I pooled together the average activity. The activity increased during the decision-making related to a correct choice ( $0.65 \pm 0.11$  Hz; paired t-test,  $p=0.017$ ), and decreased during post-reward period ( $0.27 \pm 0.09$  Hz; paired t-test,  $p=0.037$ ). But for the decision making related to an incorrect choice, no effect was found (paired t-test,  $p=0.607$ ). The activity also decreased during the cue period related to an incorrect choice ( $0.24 \pm 0.09$  Hz; paired t-test,  $p=0.032$ ), but for the same period, no effect was found during correct trials (paired t-test,  $p=0.127$ ). For all other epochs in correct and incorrect trials, no significant differences in the average firing rate were observed (paired t-test,  $p>0.05$ ). Pairwise comparison of the variation of the firing rate using paired t-test in correct and incorrect show that the firing was significantly higher during the cue period associated with correct trials compared to incorrect ( $p=0.014$ ). All other comparisons were not showing any significant differences ( $p>0.05$ ) (Figure 73C).

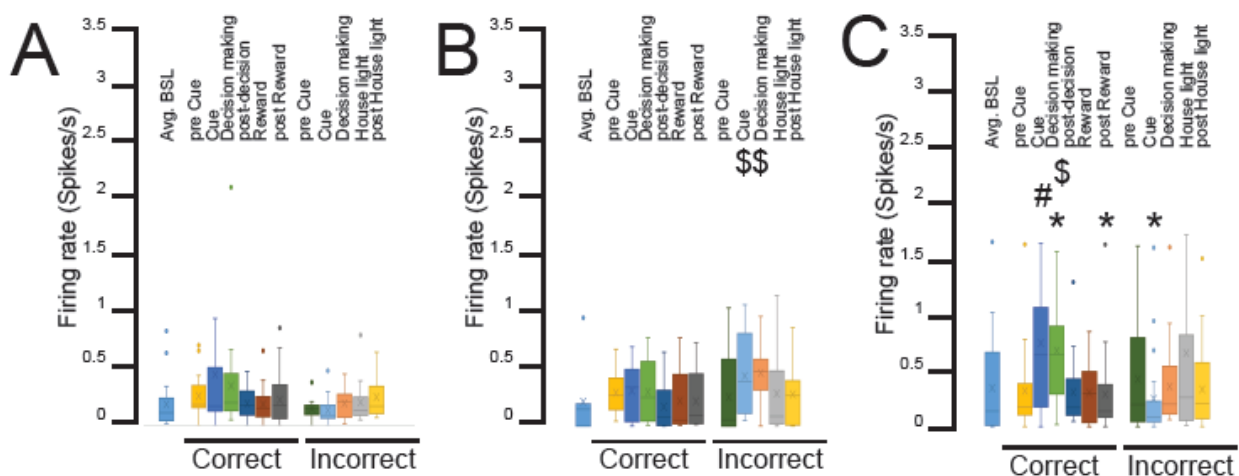


Figure 73. Firing rate of mPFC cells, recorded in WT, D2L<sup>+/-</sup>, and dys<sup>+/-</sup>D2L<sup>+/-</sup> mice, during IDS2Re stage. The firing rate is averaged for different periods around correct and incorrect choices. IDS2Re: Intra Dimensional Shift 2. A) WT mice. B) D2L<sup>+/-</sup> mice. C) dys<sup>+/-</sup>D2L<sup>+/-</sup> mice. Statistics: \* AVG BSL vs all periods; # correct vs incorrect; \$ WT vs dys<sup>+/-</sup>; \* $p<0.05$ , dys<sup>+/-</sup>D2L<sup>+/-</sup>: AVG BSL vs decision-making correct, post-reward, cue incorrect. #  $p<0.05$ , dys<sup>+/-</sup>D2L<sup>+/-</sup>: cue correct vs cue incorrect. \$  $p<0.05$ , WT vs D2L<sup>+/-</sup>: cue incorrect, decision-making incorrect; WT vs dys<sup>+/-</sup>D2L<sup>+/-</sup>: decision-making correct. Data are expressed as Mean $\pm$ SEM. N WT=7 mice. N D2L<sup>+/-</sup>=7 mice. N dys<sup>+/-</sup>D2L<sup>+/-</sup>=4 mice.

I also compared the results with those of WT and D2L<sup>+/-</sup> mice, to see which are the differences in the mPFC activity that lead to the restoration of the performance in IDS2Re.

Looking at the firing rate of mPFC, I found that dys<sup>+/-</sup>D2L<sup>+/-</sup> mice increased the firing activity during the decision-making related to a correct choice (paired t-test,  $p=0.047$ ), compared to WT mice (Figure 73A,C).

Comparing with D2L<sup>+/-</sup> mice, I found that dys<sup>+/-</sup>-D2L<sup>+/-</sup> presented no differences in the firing activity (paired-test,  $p > 0.05$ ) (Figure 73B,C).

What I found is that mPFC of dys<sup>+/-</sup>-D2L<sup>+/-</sup> mice increases the firing in the decision-making period of a correct choice, like wt. Moreover, it doesn't increase the firing in the decision-making period of incorrect choices, unlike D2L<sup>+/-</sup> (Figure 74).

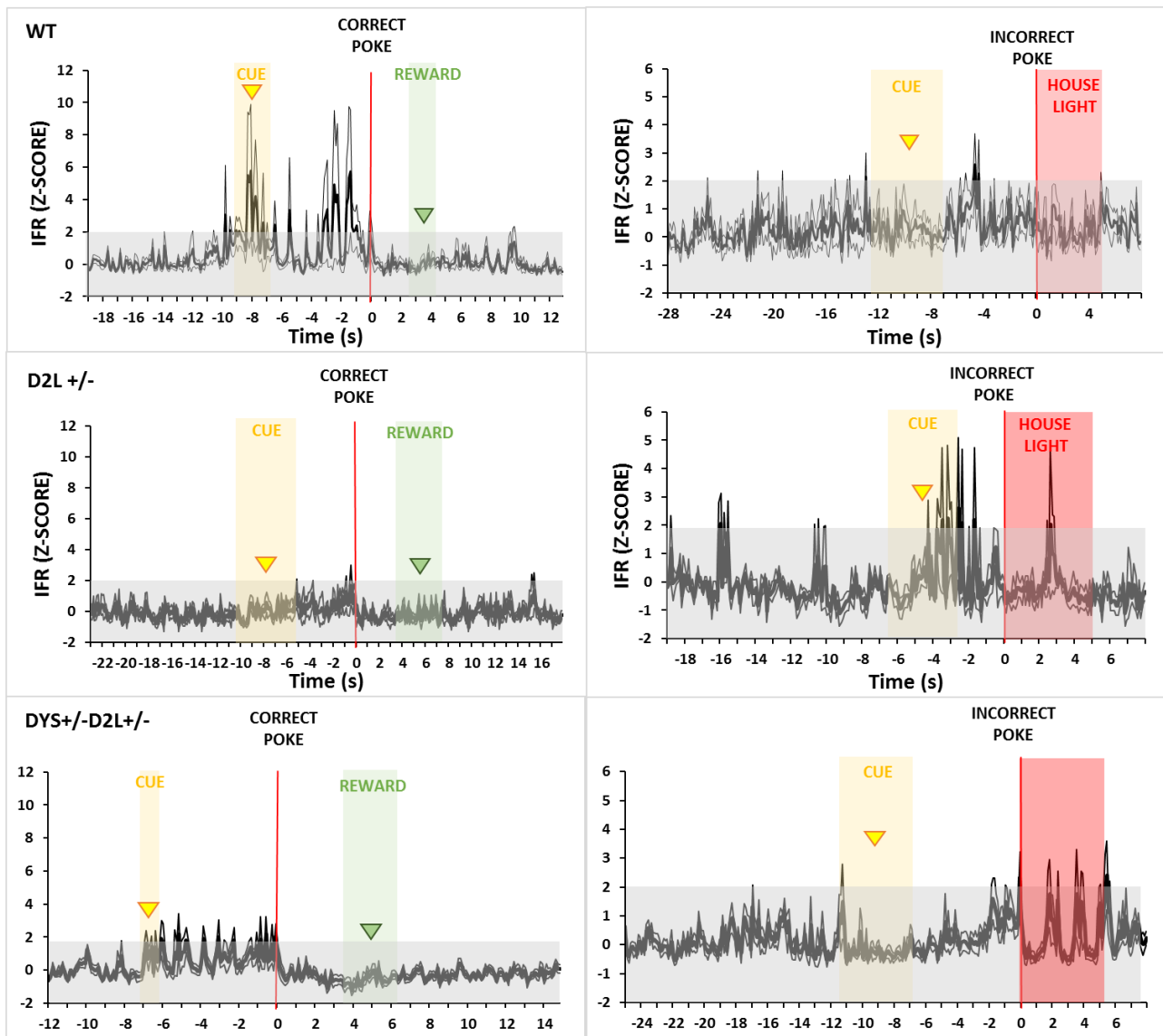


Figure 74. Instantaneous Firing Rate (IFR) of mPFC cells, recorded in WT, D2L<sup>+/-</sup>, and dys<sup>+/-</sup>-D2L<sup>+/-</sup> mice, for the correct and incorrect choices of IDS2Re stage. It represents the variation of the mPFC activity around a correct (left) or incorrect (right) poke. Top: WT. Middle: D2L<sup>+/-</sup>. Bottom: dys<sup>+/-</sup>-D2L<sup>+/-</sup>. X-axis: time, expressed in seconds. IDS2Re: Intra-Dimensional Shift 2 Reversal. The axis is centered in the instant of the correct poke. Y-axis: z-score of the IFR. Gray square: represents the interval in which the firing is not significantly different from the baseline of 3 seconds in the beginning. Yellow arrow: it represents the average time of the cue delivery. Yellow square: represent the  $\pm$ SEM of the average time of cue delivery. Red line: the instant of correct/incorrect poke. Green arrow: it represents the average time of the first entry in the food magazine. Green square: represent the  $\pm$ SEM of the average time of first entry in the food magazine. Red square: represent the duration of the house-light on. Data are expressed as Mean $\pm$ SEM. N WT=7 mice. N D2L<sup>+/-</sup> = 7 mice. N dys<sup>+/-</sup>-D2L<sup>+/-</sup> = 4 mice.

## Conclusion

The aim of my thesis was to characterize the functioning of PFC neurons in the acquisition and the maintenance of information, and the ability to adjust already-learned behavior in a different context. Because imaging data in humans suggest that the PFC is important for the switch from intra-dimensional shift to extra-dimensional shift, I used the ID/ED set-shifting task. Similarly, because reversal learning and behavioral flexibility are dependent on normal dopamine activity, I used clinically relevant genetically modified mice to study the importance of dopamine/D2 receptors in such behavior. One of the main findings of my thesis is that the PFC activity seems to vary during all the stages, and not only during the EDS stage. Moreover, I revealed that the PFC encode differently the epochs surrounding a correct or an incorrect poke.

Looking at single-cell activity and oxygen consumption during the ID/ED set-shifting task, I found that the PFC is differently activated when a mouse performs the different cognitive exercise. This PFC activity is either lost or inverted when looking at the same epochs in the D2S and Dys mutant mice. In particular, my data from clinically-relevant genetically modified mice provide an initial investigation on how common genetic variants might impact different cognitive flexibility domains and the related mPFC neuronal activity.

My thesis is the first report using in vivo electrophysiology combined with the automated ID/ED set-shifting task. Indeed, similar previous works in rodents were done using the digging version of the ID/ED set-shifting task (Cho *et al.*, 2015; Kim *et al.*, 2016). However, in the latter setting, different confounding factors could influence the activity of the mPFC including the constant human intervention and the combined presence of the food reward with the choice made.

In contrast, the recent development of an automatic version of the attentional set-shifting task, allow to avoid all these technical confounding factors and have been proved to give directly predictable results in healthy human subjects as well as patients with schizophrenia tested in the WCST test (Scheggia *et al.*, 2014, 2018). Moreover, in our mouse task as well as in the human CANTAB ID/ED task, the performance of the subjects is evaluated through different and sequential stages, which allow understanding of the abilities of the subject to perform a correct shift from a previously rewarded cue to the previously non-rewarded cue. This particular shift in the cognitive process involves the disengagement of a cognitive set to allow the acquisition of a newly generated one.

In psychology are used such tasks allow us to study the relationship between the PFC and the executive functions.

However, no study before has investigated the activity at the cellular level of this brain region while encoding for the different cognitive flexibility stages, and in particular for the extra-dimensional shift. While the cellular investigation was not possible in humans, I identified the recorded single units based on the average firing rate and the CV, finding that the great majority of them were slow-firing units, considered as putative pyramidal neurons.



Notably, in the case of the EDS stage, I found that the mPFC activity was higher during the post-decision period, but not the pre-decision making. This difference was evident when looking at the correct response trials. Interestingly, this pattern of activity during EDS greatly differed from intra-dimensional shifts (i.e. CD, IDS, IDS2 stages). Indeed, in all these other stages the mPFC was more active during the decision-making period for both the correct and incorrect responses.

Furthermore, during all different within-dimension reversal stages, the mPFC was overall silent before and after the decision-making action. This latter finding might be related to previous lesion studies indicating that the reversal stages are not altered by mPFC disruption (Dias, Robbins and Roberts, 1996; Birrell and Brown, 2000; Bissonette *et al.*, 2008). However, in the last reversal of the consecutive series of stages with the same relevant dimension (IDS2Re), I observed an increase of activity during the decision-making of a correct choice, similar to the one observed during IDS stages. This might suggest that not only acquired the attentional set but also that the strength of the set is increasing with the repetition of the stages. This also suggests an adaptation of the PFC neurons to encode differently the attentional set, and its intensity.

This highlights that initial reversal choices might follow different neuronal mechanisms compared to serial reversal learning actions. This latter hypothesis is in agreement with finding from our laboratory and from Trevor Robbins laboratory (Scheggia *et al.*, 2014). Indeed, initial and serial reversal, although they have the same rule, that is the inversion of the reinforcement contingencies of two exemplars within a perceptual dimension (i.e. previously correct is then incorrect and vice versa), have a different type of learning process. During an initial reversal, subjects have to inhibit a previously acquired learning in order to acquire new learning, never seen before. While during a serial reversal, the subjects have to apply in a new contest the information learned and acquired before. This can be assimilated into the goal-directed and habit formation. In a goal-directed acquisition, the animal will associate the action (poke) to the outcome (sugar pellet). In a habit learning, the animal will be less motivated by the outcome (reward). Several studies confirmed the involvement of the PFC in goal-directed, while the OFC trigger mostly habit acquisition (Gremel and Costa, 2013). The comparison between study, allow us to suggest that the PFC neurons encode mostly goal-directed behavior (IDS2, IDS2Re) and need to be inhibited during the shift to EDS to “build” a new attentional set. Indeed, similarly to what I found in SD, following IDS and IDSRe, it is very likely that the animals are mostly processing the behavior under a habit learning processes.

Overall, these findings are summarized in *Table 2* and might underline a different and specific involvement of the mPFC in the extra-dimensional shift abilities, suggesting that the contribution of cortical neurons after correct choices and their absence during incorrect choices is important for understanding that a new attentional set has to be developed.


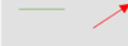

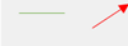



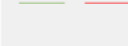


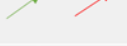
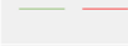
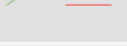
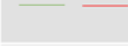
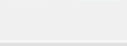
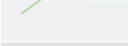
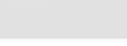
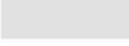
	DECISION PERIOD	POST DECISION
SD		
CD		
CDRE		
IDS		
IDSRE		
IDS2		
IDS2RE		
EDS		
EDSRE		

Table 2. mPFC activity changing of WT mice before and after responses, in the different stages of the task. Green: correct responses. Red: incorrect responses. SD: Simple Discrimination; CD: Compound Discrimination; CDRe: Compound Discrimination Reversal; IDS: Intra-Dimensional Shift; IDSRe: Intra-Dimensional Shift Reversal; IDS2: Intra-Dimensional Shift 2; IDS2Re: Intra-Dimensional Shift 2 Reversal; EDS: Extra-Dimensional Shift; EDSRe: Extra-Dimensional Shift Reversal. Periods analyzed: decision (pre response) and post-decision (post response).

After the initial analyses in WT mice, I wanted to understand how the PFC-coding of these executive functions might be modulated by genetic variants modifying the dopaminergic signaling and which might have an implication for psychiatric disorders and their treatments. I used genetically modified mice implicated in schizophrenia-cognitive alterations: *dys*<sup>+/-</sup> and *D2L*<sup>+/-</sup> mice. Unfortunately, it was not possible to reduced or abolished the D2-receptors specifically in the prefrontal cortex, and I had to use mutants with the mutation widely expressed.

I focalized my attention also in mice with concomitant alterations of both these genes, as the interaction between these two genetic variants has been shown to have a strong implication for cognitive responses to antipsychotic drugs in both mice and human patients (Scheggia *et al.*, 2018; Leggio *et al.*, 2019).

In the group of mice with the mutation of *Dys* (*dys*<sup>+/-</sup>) genes, I found that they had an impairment in the EDS stage compared to WT mice, where they needed more trials and time to reach the criterion. At the level of the single-cell electrophysiology, during EDS the PFC of *dys*<sup>+/-</sup> mice seems to encode similarly correct and incorrect answers. The discrepancies observed in the EDS of WT mice between correct and incorrect are thus lost. Looking at the firing rate, differently from WT mice, the increase of the firing rate in the post-decision of a correct choice shifted in the post-decision period of an incorrect choice.

It is clear that *dys*<sup>+/-</sup> mice have an impairment in mPFC coding of the extra-dimensional shift.

Inducing the mutation  $D2L^{+/-}$  in the mice, the performance of EDS was restored, confirming our previous findings (Scheggia *et al.*, 2018). Interestingly, what I found from my study, is that at the level of mPFC, although the activity was the same as for  $dys^{+/-}$  mice, the encoding after a correct choice was restored (Table 3). Moreover, the mPFC of double mutant mice increased the firing rate in the decision-making period of both choices, compared to WT mice. This suggests that when patients with reduced expression of gene *dys* are treated with D2-specific antipsychotics, the PFC activity is not fully restored, but it is introduced a new coding, the one after correct decisions, and is induced an increase of the firing rate in case of decision making, important for the restoring of the performance. This observation is important in healthy subjects, as D2L is important for the development of a new attentional set. In



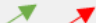
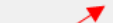
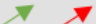
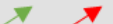
	DECISION PERIOD	POST DECISION
WT		
DYS		
DYS-D2L		

Table 3. mPFC activity changing of WT (top),  $dys^{+/-}$  (middle), and  $dys^{+/-}D2L^{+/-}$  (bottom) mice before and after responses, in EDS. Green: correct responses. Red: incorrect responses. EDS: Extra-Dimensional Shift. Periods analyzed: decision (pre response) and post-decision (post response).

Considering now the  $D2L^{+/-}$ -mice, what I found is that they had an impairment in serial reversal learning, in particular in the IDS2Re stage, compared to WT mice, where they needed more trials and time to reach the criterion.

Considering the firing rate of the mPFC cells, what I found is that  $D2L^{+/-}$  mice increased the firing in the pre-decision period of an incorrect choice compared to WT mice.  $D2L^{+/-}$  seemed no to be able to distinguish a correct choice from an incorrect one, activating the cells in the same way in both cases. This is not like WT, where they seemed to have an increasing trend in the pre-decision period of a correct choice, which returned to the baseline in case of incorrect choice.

Investigating the mPFC activity, what was possible to see is that, unlike WT mice where there was an increase of activity in the decision-making period of correct choices, the cortical neurons increased the firing in the decision-making and post-decision of incorrect choices. It is clear that  $D2L^{+/-}$  mice have an impairment in mPFC coding of serial reversal learning.

Introducing the mutation  $dys^{+/-}$  in these mice, the performance of IDS2Re was restored.

Interestingly, what I found from my study is that at the level of mPFC, the increase in the decision of incorrect choices was suppressed, and the coding before correct choices was restored, with an increased of the firing rate in the decision making period of a correct choice (*Table 4*).

This indicates that with an unbalanced ratio of the two isoforms of the receptor D2 and when the expression of the gene dys is reduced, the PFC activity is restored to the normality in case of correct choices, that in healthy subject is important for the correct consolidation of the attentional set and the correct performance of serial reversal learning.


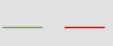




	DECISION PERIOD	POST DECISION
WT		
D2L		
DYS-D2L		

Table 4. mPFC activity changing of WT (top), D2L<sup>+/-</sup> (middle), and dys<sup>+/-</sup>-D2L<sup>+/-</sup> (bottom) mice before and after responses, in IDS2Re. Green: correct responses. Red: incorrect responses. IDS2Re: Intra-Dimensional Shift 2 Reversal. Periods analyzed: decision (pre response) and post-decision (post response).

Considering IDS2Re and EDS in case of dys<sup>+/-</sup>-D2L<sup>+/-</sup>, I found a similar activation of mPFC comparing it with WT mice: an increase of the firing in the decision-making period of a correct choice. This suggests that double mutant mice are able to restore the performance of the stages thanks to this great involvement of the mPFC in the coding of a correct choice.

Taken together, this finding illustrates how the neuronal coding of executive functions within the mPFC might be altered in the context of different genetic backgrounds leading to different cognitive performances in different cognitive domains. However, the presence of D2 receptors in multiple structures, including the dorsal striatum might affect the firing of PFC neurons throughout multiple synapses circuits. Repeating these experiments in other structures will be interesting and necessary.

## Future perspective

My study provides a detailed analysis of mPFC coding of different aspects of cognitive functions related to executive functions and flexible choices. This provides a solid base for future more mechanistic investigations trying to determine which type of neurons might be responsible for the signals I was able to record. In particular, our future perspective is to characterize the selective involvement of different types of neurons (e.g. principal neurons, SOM+ and PV+ interneurons) within the mPFC in cognitive flexibility, always through the use of the automatized OPERON ID/ED task. Based on the data gathered so far, for example, we might target each type of these subpopulations of neurons in specific epochs (e.g. before or after the decision in the operant task) with the optogenetic, which enables verification of physiology-based classification of neurons recorded in vivo (Kvitsiani *et al.*, 2013; Roux *et al.*, 2014). So, we can combine chronic in vivo recording with optical tagging, in order to follow the activity of each group of neurons.

Moreover, my study is purely correlative and does not yet provide any direct causal link between the different patterns of neuronal activity and the different cognitive performances in different cognitive domains. However, it provides specific indications on what could be the critical time points in every single cognitive domain investigated that could be manipulated to provide this more direct causal link. For example, through optogenetic manipulations, we can design experiments to inhibit or excite the mPFC in the decision-making period of correct and incorrect choices to provide a causal link with behavioral performance, and with the development of an attentional set. In the case of EDS, it could be interesting to understand if manipulating the mPFC activity in the post correct responses, this stage becomes impossible to be solved or becomes “simple” like the immediately before stages, used to develop the attentional set. Moreover, this optogenetic manipulation can be further applied to understand the different types of neurons of the mPFC involved and try to understand the contribution of each one in cognitive flexibility.

Here I focused on the PFC. However, the PFC works within a more complex network related to high-level cognitive performance. In particular, it is known that the dlPFC and Postero Parietal Cortex (PPC) are two parts of a broader brain network involved in the control of cognitive functions such as working memory, spatial attention, and decision-making (Katsuki and Constantinidis, 2012). These are two major hubs of the so-called default mode network. Moreover, the PPC receives direct prefrontal input (Crowe *et al.*, 2013). Thus it would be interesting to directly manipulate the PFC-PPC circuit to investigate its involvement in executive functions.

# Bibliography

- Abi-Dargham, A. *et al.* (2000) 'Increased baseline occupancy of D2 receptors by dopamine in schizophrenia', *Proceedings of the National Academy of Sciences*, 97(14), pp. 8104–8109. doi: 10.1073/pnas.97.14.8104.
- Addington, J. and Addington, D. (1999) 'Neurocognitive and Social Functioning in Schizophrenia', *Schizophrenia Bulletin*, 25(1), pp. 173–182. doi: 10.1093/oxfordjournals.schbul.a033363.
- Albus, M. *et al.* (2002) 'A prospective 2-year follow-up study of neurocognitive functioning in patients with first-episode schizophrenia', *European Archives of Psychiatry and Clinical Neuroscience*, 252(6), pp. 262–267. doi: 10.1007/s00406-002-0391-4.
- Allen, N. C. *et al.* (2008) 'Systematic meta-analyses and field synopsis of genetic association studies in schizophrenia: the SzGene database', *Nature Genetics*, 40(7), pp. 827–834. doi: 10.1038/ng.171.
- Amato, D., Vernon, A. C. and Papaleo, F. (2018) 'Dopamine, the antipsychotic molecule: A perspective on mechanisms underlying antipsychotic response variability', *Neuroscience & Biobehavioral Reviews*, 85, pp. 146–159. doi: 10.1016/j.neubiorev.2017.09.027.
- Amminger, G. P. *et al.* (1997) 'Premorbid adjustment and remission of positive symptoms in first-episode psychosis', *European Child and Adolescent Psychiatry*. D. Steinkopff-Verlag, 6(4), pp. 212–218. doi: 10.1007/BF00539928.
- Anderson, S. W. *et al.* (1999) 'Impairment of social and moral behavior related to early damage in human prefrontal cortex', *Nature Neuroscience*, 2(11), pp. 1032–1037. doi: 10.1038/14833.
- Arain, M. *et al.* (2013) 'Maturation of the adolescent brain', *Neuropsychiatric Disease and Treatment*, pp. 449–461. doi: 10.2147/NDT.S39776.
- Badcock, J. C., Michie, P. T. and Rock, D. (2005) 'Spatial Working Memory and Planning Ability: Contrasts between Schizophrenia and Bipolar Disorder', *Cortex*, 41(6), pp. 753–763. doi: 10.1016/S0010-9452(08)70294-6.
- Balleine, B. W. and Dickinson, A. (1998) 'Goal-directed instrumental action: Contingency and incentive learning and their cortical substrates', in *Neuropharmacology*, pp. 407–419. doi: 10.1016/S0028-3908(98)00033-1.
- Barnett, J. H. *et al.* (2010) 'Assessing cognitive function in clinical trials of schizophrenia', *Neuroscience & Biobehavioral Reviews*, 34(8), pp. 1161–1177. doi: 10.1016/j.neubiorev.2010.01.012.
- Barrash, J., Tranel, D. and Anderson, S. W. (2000) 'Acquired Personality Disturbances Associated With Bilateral Damage to the Ventromedial Prefrontal Region', *Developmental Neuropsychology*, 18(3), pp. 355–381. doi: 10.1207/S1532694205Barrash.
- Benson, M. A. *et al.* (2001) 'Dysbindin, a Novel Coiled-coil-containing Protein That Interacts with the Dystrobrevins in Muscle and Brain', *Journal of Biological Chemistry*, 276(26), pp. 24232–24241. doi: 10.1074/jbc.M010418200.
- Berg, E. A. (1948) 'A Simple Objective Technique for Measuring Flexibility in Thinking', *The Journal of General Psychology*, 39(1), pp. 15–22. doi: 10.1080/00221309.1948.9918159.
- Bertolino, A. *et al.* (2009) 'Functional variants of the dopamine receptor D2 gene modulate prefronto-striatal phenotypes in schizophrenia.', *Brain: a journal of neurology*. Oxford University Press, 132(Pt 2), pp. 417–25. doi: 10.1093/brain/awn248.
- Best, J. R. and Miller, P. H. (2010) 'A Developmental Perspective on Executive Function', *Child Development*, pp. 1641–1660. doi: 10.1111/j.1467-8624.2010.01499.x.
- Birrell, J. M. and Brown, V. J. (2000) 'Medial frontal cortex mediates perceptual attentional set shifting in

- the rat.', *The Journal of neuroscience : the official journal of the Society for Neuroscience*, 20(11), pp. 4320–4. Available at: <http://www.ncbi.nlm.nih.gov/pubmed/10818167> (Accessed: 2 December 2019).
- Bissonette, G. B. *et al.* (2008) 'Double Dissociation of the Effects of Medial and Orbital Prefrontal Cortical Lesions on Attentional and Affective Shifts in Mice', *Journal of Neuroscience*, 28(44), pp. 11124–11130. doi: 10.1523/JNEUROSCI.2820-08.2008.
- Bissonette, G. B. and Powell, E. M. (2012) 'Reversal learning and attentional set-shifting in mice', *Neuropharmacology*, 62(3), pp. 1168–1174. doi: 10.1016/j.neuropharm.2011.03.011.
- Björklund, A. and Dunnett, S. B. (2007) 'Dopamine neuron systems in the brain: an update', *Trends in Neurosciences*, pp. 194–202. doi: 10.1016/j.tins.2007.03.006.
- Blaeser, A. S., Connors, B. W. and Nurmikko, A. V. (2017) 'Spontaneous dynamics of neural networks in deep layers of prefrontal cortex', *Journal of Neurophysiology*, 117(4), pp. 1581–1594. doi: 10.1152/jn.00295.2016.
- Blanchard, J. J. *et al.* (2011) 'Toward the Next Generation of Negative Symptom Assessments: The Collaboration to Advance Negative Symptom Assessment in Schizophrenia', *Schizophrenia Bulletin*, 37(2), pp. 291–299. doi: 10.1093/schbul/sbq104.
- Van Den Bogaert, A. *et al.* (2003) 'The DTNBP1 (dysbindin) gene contributes to schizophrenia, depending on family history of the disease.', *American journal of human genetics*. Elsevier, 73(6), pp. 1438–43. doi: 10.1086/379928.
- Boulay, D. *et al.* (2000) 'Haloperidol-induced catalepsy is absent in dopamine D2, but maintained in dopamine D3 receptor knock-out mice', *European Journal of Pharmacology*, 391(1–2), pp. 63–73. doi: 10.1016/S0014-2999(99)00916-4.
- Braver, T. S., Barch, D. M. and Cohen, J. D. (1999) 'Cognition and control in schizophrenia: a computational model of dopamine and prefrontal function.', *Biological psychiatry*, 46(3), pp. 312–28. doi: 10.1016/s0006-3223(99)00116-x.
- Brown, A. S. (2011) 'The environment and susceptibility to schizophrenia', *Progress in Neurobiology*, pp. 23–58. doi: 10.1016/j.pneurobio.2010.09.003.
- Brown, T. E., Reichel, P. C. and Quinlan, D. M. (2009) 'Executive Function Impairments in High IQ Adults With ADHD', *Journal of Attention Disorders*, 13(2), pp. 161–167. doi: 10.1177/1087054708326113.
- Brown, V. J. and Bowman, E. M. (2002) 'Rodent models of prefrontal cortical function.', *Trends in neurosciences*, 25(7), pp. 340–3. doi: 10.1016/s0166-2236(02)02164-1.
- Burdick, K. E. *et al.* (2006) 'Genetic variation in DTNBP1 influences general cognitive ability', *Human Molecular Genetics*. Narnia, 15(10), pp. 1563–1568. doi: 10.1093/hmg/ddi481.
- Burgess, P. W. and Simons, J. S. (2005) 'Theories of frontal lobe executive function: clinical applications', in *The Effectiveness of Rehabilitation for Cognitive Deficits*. Oxford University Press, pp. 211–231. doi: 10.1093/acprof:oso/9780198526544.003.0018.
- Burkett, J. P. and Young, L. J. (2012) 'The behavioral, anatomical and pharmacological parallels between social attachment, love and addiction', *Psychopharmacology*, 224(1), pp. 1–26. doi: 10.1007/s00213-012-2794-x.
- Carr, D. B. *et al.* (1999) 'Dopamine terminals in the rat prefrontal cortex synapse on pyramidal cells that project to the nucleus accumbens', *Journal of Neuroscience*, 19(24), pp. 11049–11060. doi: 10.1523/jneurosci.19-24-11049.1999.
- Castañé, A., Theobald, D. E. H. and Robbins, T. W. (2010) 'Selective lesions of the dorsomedial striatum impair serial spatial reversal learning in rats', *Behavioural Brain Research*, 210(1), pp. 74–83. doi: 10.1016/j.bbr.2010.02.017.
- Ceaser, A. E. *et al.* (2008) 'Set-shifting ability and schizophrenia: a marker of clinical illness or an

- intermediate phenotype?', *Biological psychiatry*, 64(9), pp. 782–8. doi: 10.1016/j.biopsych.2008.05.009.
- Chen, X.-W. *et al.* (2008) 'DTNBP1, a schizophrenia susceptibility gene, affects kinetics of transmitter release', *The Journal of Cell Biology*, 181(5), pp. 791–801. doi: 10.1083/jcb.200711021.
- Cho, K. K. A. *et al.* (2015) 'Gamma Rhythms Link Prefrontal Interneuron Dysfunction with Cognitive Inflexibility in Dlx5/6+/- Mice', *Neuron*, 85(6), pp. 1332–1343. doi: 10.1016/j.neuron.2015.02.019.
- Chou, I. J. *et al.* (2017) 'Familial aggregation and heritability of schizophrenia and co-aggregation of psychiatric illnesses in affected families', *Schizophrenia Bulletin*. Oxford University Press, 43(5), pp. 1070–1078. doi: 10.1093/schbul/sbw159.
- Chudasama, Y. and Robbins, T. W. (2006) 'Functions of frontostriatal systems in cognition: comparative neuropsychopharmacological studies in rats, monkeys and humans.', *Biological psychology*, 73(1), pp. 19–38. doi: 10.1016/j.biopsycho.2006.01.005.
- Clarke, H. F. *et al.* (2011) 'Dopamine, but not serotonin, regulates reversal learning in the marmoset caudate nucleus.', *The Journal of neuroscience : the official journal of the Society for Neuroscience*. Society for Neuroscience, 31(11), pp. 4290–7. doi: 10.1523/JNEUROSCI.5066-10.2011.
- Collins, A. and Koechlin, E. (2012) 'Reasoning, learning, and creativity: frontal lobe function and human decision-making.', *PLoS biology*. Edited by J. P. O'Doherty, 10(3), p. e1001293. doi: 10.1371/journal.pbio.1001293.
- Cornblatt, B. *et al.* (1997) 'Attention and clinical symptoms in schizophrenia.', *The Psychiatric quarterly*, 68(4), pp. 343–59. doi: 10.1023/a:1025495030997.
- Cornblatt, B. *et al.* (1998) 'Hillside study of risk and early detection in schizophrenia.', *The British journal of psychiatry. Supplement*, 172(33), pp. 26–32. Available at: <http://www.ncbi.nlm.nih.gov/pubmed/9764123> (Accessed: 2 December 2019).
- Cox, M. M. *et al.* (2009) 'Neurobehavioral abnormalities in the dysbindin-1 mutant, sandy, on a C57BL/6J genetic background.', *Genes, brain, and behavior*. NIH Public Access, 8(4), pp. 390–7. doi: 10.1111/j.1601-183X.2009.00477.x.
- Crowe, D. a *et al.* (2013) 'Prefrontal neurons transmit signals to parietal neurons that reflect executive control of cognition.', *Nature neuroscience*. Nature Publishing Group, 16(10), pp. 1484–91. doi: 10.1038/nn.3509.
- Cuesta, M. J., Peralta, V. and Zarzuela, A. (2001) 'Effects of olanzapine and other antipsychotics on cognitive function in chronic schizophrenia: a longitudinal study', *Schizophrenia Research*. Elsevier, 48(1), pp. 17–28. doi: 10.1016/S0920-9964(00)00112-2.
- Dautan, D. *et al.* (2016) 'Segregated cholinergic transmission modulates dopamine neurons integrated in distinct functional circuits', *Nature Neuroscience*. doi: 10.1038/nn.4335.
- Dean, K. and Murray, R. M. (2005) 'Environmental risk factors for psychosis.', *Dialogues in clinical neuroscience*, 7(1), pp. 69–80. Available at: <http://www.ncbi.nlm.nih.gov/pubmed/16060597> (Accessed: 2 December 2019).
- Dias, R., Robbins, T. W. and Roberts, A. C. (1996) 'Dissociation in prefrontal cortex of affective and attentional shifts', *Nature*, 380(6569), pp. 69–72. doi: 10.1038/380069a0.
- Dickerson, F. *et al.* (1999) 'Social functioning and neurocognitive deficits in outpatients with schizophrenia: a 2-year follow-up.', *Schizophrenia research*, 37(1), pp. 13–20. doi: 10.1016/s0920-9964(98)00134-0.
- Dickman, D. K. and Davis, G. W. (2009) 'The Schizophrenia Susceptibility Gene dysbindin Controls Synaptic Homeostasis', *Science*, 326(5956), pp. 1127–1130. doi: 10.1126/science.1179685.
- Eilam, D., Golani, I. and Szechtman, H. (1989) 'D2-agonist quinpirole induces perseveration of routes and hyperactivity but no perseveration of movements', *Brain Research*, 490(2), pp. 255–267. doi: 10.1016/0006-8993(89)90243-6.



- Eling, P., Derckx, K. and Maes, R. (2008) 'On the historical and conceptual background of the Wisconsin Card Sorting Test', *Brain and Cognition*, 67(3), pp. 247–253. doi: 10.1016/j.bandc.2008.01.006.
- Elliott, R. *et al.* (1995) 'Neuropsychological evidence for frontostriatal dysfunction in schizophrenia.', *Psychological medicine*, 25(3), pp. 619–30.
- Elston, G. N. (2003) 'Cortex, Cognition and the Cell: New Insights into the Pyramidal Neuron and Prefrontal Function', *Cerebral Cortex*, 13(11), pp. 1124–1138. doi: 10.1093/cercor/bhg093.
- Erlenmeyer-Kimling, L. (2000) 'Neurobehavioral deficits in offspring of schizophrenic parents: liability indicators and predictors of illness.', *American journal of medical genetics*, 97(1), pp. 65–71. doi: 10.1002/(sici)1096-8628(200021)97:1<65::aid-ajmg9>3.0.co;2-v.
- Espy, K. A. *et al.* (2004) 'The Contribution of Executive Functions to Emergent Mathematic Skills in Preschool Children', *Developmental Neuropsychology*, 26(1), pp. 465–486. doi: 10.1207/s15326942dn2601\_6.
- Etkin, A., Gyurak, A. and O'Hara, R. (2013) 'A neurobiological approach to the cognitive deficits of psychiatric disorders', *Dialogues in Clinical Neuroscience*, 15(4), pp. 419–429.
- Everett, J. *et al.* (2001) 'Performance of patients with schizophrenia on the Wisconsin Card Sorting Test (WCST).', *Journal of psychiatry & neuroscience : JPN*. Canadian Medical Association, 26(2), pp. 123–30. Available at: <http://www.ncbi.nlm.nih.gov/pubmed/11291529> (Accessed: 2 December 2019).
- Fallgatter, A. J. *et al.* (2006) 'DTNBP1 (Dysbindin) Gene Variants Modulate Prefrontal Brain Function in Healthy Individuals', *Neuropsychopharmacology*. Nature Publishing Group, 31(9), pp. 2002–2010. doi: 10.1038/sj.npp.1301003.
- Fett, A.-K. J. *et al.* (2011) 'The relationship between neurocognition and social cognition with functional outcomes in schizophrenia: A meta-analysis', *Neuroscience & Biobehavioral Reviews*. Pergamon, 35(3), pp. 573–588. doi: 10.1016/J.NEUBIOREV.2010.07.001.
- Floresco, S. B. and Magyar, O. (2006) 'Mesocortical dopamine modulation of executive functions: beyond working memory', *Psychopharmacology*, 188(4), pp. 567–585. doi: 10.1007/s00213-006-0404-5.
- Fox, M. T., Barense, M. D. and Baxter, M. G. (2003) 'Perceptual attentional set-shifting is impaired in rats with neurotoxic lesions of posterior parietal cortex.', *The Journal of neuroscience : the official journal of the Society for Neuroscience*, 23(2), pp. 676–81.
- Gabbott, P. L. A. *et al.* (2005) 'Prefrontal cortex in the rat: Projections to subcortical autonomic, motor, and limbic centers', *The Journal of Comparative Neurology*, 492(2), pp. 145–177. doi: 10.1002/cne.20738.
- Gaspar, P., Bloch, B. and Moine, C. (1995) 'D1 and D2 Receptor Gene Expression in the Rat Frontal Cortex: Cellular Localization in Different Classes of Efferent Neurons', *European Journal of Neuroscience*, 7(5), pp. 1050–1063. doi: 10.1111/j.1460-9568.1995.tb01092.x.
- Gejman, P. V., Sanders, A. R. and Duan, J. (2010) 'The Role of Genetics in the Etiology of Schizophrenia', *Psychiatric Clinics of North America*, 33(1), pp. 35–66. doi: 10.1016/j.psc.2009.12.003.
- Ghiani, C. A. *et al.* (2010) 'The dysbindin-containing complex (BLOC-1) in brain: developmental regulation, interaction with SNARE proteins and role in neurite outgrowth.', *Molecular psychiatry*. NIH Public Access, 15(2), pp. 115, 204–15. doi: 10.1038/mp.2009.58.
- Giguère, N., Nanni, S. B. and Trudeau, L. E. (2018) 'On cell loss and selective vulnerability of neuronal populations in Parkinson's disease', *Frontiers in Neurology*. Frontiers Media S.A. doi: 10.3389/fneur.2018.00455.
- Girault, J.-A. and Greengard, P. (2004) 'The Neurobiology of Dopamine Signaling', *Archives of Neurology*, 61(5), p. 641. doi: 10.1001/archneur.61.5.641.
- Glickstein, S. B., Hof, P. R. and Schmauss, C. (2002) 'Mice lacking dopamine D2 and D3 receptors have spatial working memory deficits.', *The Journal of neuroscience : the official journal of the Society for*

*Neuroscience*, 22(13), pp. 5619–29. doi: 20026543.

Goldman-rakic, P. S. (1998) ‘The prefrontal landscape: implications of functional architecture for understanding human mentation and the central executive’, in *The Prefrontal Cortex Executive and Cognitive Functions*. Oxford University Press, pp. 87–102. doi: 10.1093/acprof:oso/9780198524410.003.0007.

González-Blanch, C. *et al.* (2010) ‘Prognostic value of cognitive functioning for global functional recovery in first-episode schizophrenia’, *Psychological Medicine*, 40(6), pp. 935–944. doi: 10.1017/S0033291709991267.

Goto, Y. and Grace, A. A. (2005) ‘Dopaminergic modulation of limbic and cortical drive of nucleus accumbens in goal-directed behavior’, *Nature Neuroscience*, 8(6), pp. 805–812. doi: 10.1038/nn1471.

Goyal, N. *et al.* (2008) ‘Neuropsychology of prefrontal cortex’, *Indian Journal of Psychiatry*, 50(3), p. 202. doi: 10.4103/0019-5545.43634.

Granseth, B., Andersson, F. K. and Lindström, S. H. (2015) ‘The initial stage of reversal learning is impaired in mice hemizygous for the vesicular glutamate transporter (VGluT1)’, *Genes, Brain and Behavior*, 14(6), pp. 477–485. doi: 10.1111/gbb.12230.

Green, M. F., Lee, J. and Ochsner, K. N. (2013) ‘Adapting Social Neuroscience Measures for Schizophrenia Clinical Trials, Part 1: Ferrying Paradigms Across Perilous Waters’, *Schizophrenia Bulletin*, 39(6), pp. 1192–1200. doi: 10.1093/schbul/sbt131.

Gremel, C. M. and Costa, R. M. (2013) ‘Orbitofrontal and striatal circuits dynamically encode the shift between goal-directed and habitual actions.’, *Nature communications*, 4, p. 2264. doi: 10.1038/ncomms3264.

Gruber, O., Santucci, A. C. and Aach, H. (2014) ‘Magnetic resonance imaging in studying schizophrenia, negative symptoms, and the glutamate system’, *Frontiers in Psychiatry*. Frontiers Media SA. doi: 10.3389/fpsy.2014.00032.

Hampshire, A. and Owen, A. M. (2006) ‘Fractionating attentional control using event-related fMRI.’, *Cerebral cortex (New York, N.Y. : 1991)*, 16(12), pp. 1679–89. doi: 10.1093/cercor/bhj116.

Harvey, P. D. and Keefe, R. S. (2001) ‘Studies of cognitive change in patients with schizophrenia following novel antipsychotic treatment.’, *The American journal of psychiatry*, 158(2), pp. 176–84. doi: 10.1176/appi.ajp.158.2.176.

Hasbi, A., O’Dowd, B. F. and George, S. R. (2011) ‘Dopamine D1-D2 receptor heteromer signaling pathway in the brain: emerging physiological relevance’, *Molecular Brain*, 4(1), p. 26. doi: 10.1186/1756-6606-4-26.

Hashimoto, R., Noguchi, H., Hori, H., Nakabayashi, T., *et al.* (2009) ‘A genetic variation in the dysbindin gene (DTNBP1) is associated with memory performance in healthy controls’, *World Journal of Biological Psychiatry*, 11(2 Pt 2), pp. 1–8. doi: 10.1080/15622970902736503.

Hashimoto, R., Noguchi, H., Hori, H., Ohi, K., *et al.* (2009) ‘Association between the dysbindin gene (DTNBP1) and cognitive functions in Japanese subjects’, *Psychiatry and Clinical Neurosciences*, 63(4), pp. 550–556. doi: 10.1111/j.1440-1819.2009.01985.x.

Heisler, J. M. *et al.* (2015) ‘The attentional set shifting task: A measure of cognitive flexibility in mice’, *Journal of Visualized Experiments*. Journal of Visualized Experiments, (96). doi: 10.3791/51944.

Henriksen, M. G., Nordgaard, J. and Jansson, L. B. (2017) ‘Genetics of schizophrenia: Overview of methods, findings and limitations’, *Frontiers in Human Neuroscience*. Frontiers Media S. A. doi: 10.3389/fnhum.2017.00322.

Hill, E. L. (2004) ‘Executive dysfunction in autism☆’, *Trends in Cognitive Sciences*, 8(1), pp. 26–32. doi: 10.1016/j.tics.2003.11.003.

Hultman, C. M. *et al.* (1999) ‘Prenatal and perinatal risk factors for schizophrenia, affective psychosis, and reactive psychosis of early onset: case-control study Prenatal and perinatal risk factors for early onset schizophrenia, affective psychosis, and reactive psychosis’, *BMJ*, 318(7181), pp. 421–426. doi:

10.1136/bmj.318.7181.421.

Iizuka, Y. *et al.* (2007) 'Evidence That the BLOC-1 Protein Dysbindin Modulates Dopamine D2 Receptor Internalization and Signaling But Not D1 Internalization', *Journal of Neuroscience*, 27(45), pp. 12390–12395. doi: 10.1523/JNEUROSCI.1689-07.2007.

Ingvar, D. and Franzén, G. (1974) 'DISTRIBUTION OF CEREBRAL ACTIVITY IN CHRONIC SCHIZOPHRENIA', *The Lancet*. Elsevier, 304(7895), pp. 1484–1486. doi: 10.1016/S0140-6736(74)90221-9.

Jablensky, A. (2010) 'The diagnostic concept of schizophrenia: its history, evolution, and future prospects.', *Dialogues in clinical neuroscience*, 12(3), pp. 271–87. Available at: <http://www.ncbi.nlm.nih.gov/pubmed/20954425> (Accessed: 24 January 2020).

Jazbec, S. *et al.* (2007) 'Intra-dimensional/extra-dimensional set-shifting performance in schizophrenia: Impact of distractors', *Schizophrenia Research*, 89(1–3), pp. 339–349. doi: 10.1016/j.schres.2006.08.014.

Jenni, N. L., Larkin, J. D. and Floresco, S. B. (2017) 'Prefrontal dopamine D1 and D2 receptors regulate dissociable aspects of decision making via distinct ventral striatal and amygdalar circuits', *Journal of Neuroscience*. Society for Neuroscience, 37(26), pp. 6200–6213. doi: 10.1523/JNEUROSCI.0030-17.2017.

Ji, Y. *et al.* (2009) 'Role of dysbindin in dopamine receptor trafficking and cortical GABA function', *Proceedings of the National Academy of Sciences*, 106(46), pp. 19593–19598. doi: 10.1073/pnas.0904289106.

Kaalund, S. S. *et al.* (2014) 'Contrasting changes in DRD1 and DRD2 splice variant expression in schizophrenia and affective disorders, and associations with SNPs in postmortem brain', *Molecular Psychiatry*, 19(12), pp. 1258–1266. doi: 10.1038/mp.2013.165.

Karlsgodt, K. H. *et al.* (2009) 'White Matter Integrity and Prediction of Social and Role Functioning in Subjects at Ultra-High Risk for Psychosis', *Biological Psychiatry*, 66(6), pp. 562–569. doi: 10.1016/j.biopsych.2009.03.013.

Karlsgodt, K. H. *et al.* (2011) 'Reduced Dysbindin Expression Mediates N-Methyl-D-Aspartate Receptor Hypofunction and Impaired Working Memory Performance', *Biological Psychiatry*, 69(1), pp. 28–34. doi: 10.1016/j.biopsych.2010.09.012.

Katsuki, F. and Constantinidis, C. (2012) 'Early involvement of prefrontal cortex in visual bottom-up attention', *Nature Neuroscience*, 15(8), pp. 1160–1166. doi: 10.1038/nn.3164.

Keefe, R. S. E. *et al.* (2011) 'Characteristics of the MATRICS Consensus Cognitive Battery in a 29-site antipsychotic schizophrenia clinical trial', *Schizophrenia Research*. Elsevier, 125(2–3), pp. 161–168. doi: 10.1016/J.SCHRES.2010.09.015.

Keeler, J. F. and Robbins, T. W. (2011) 'Translating cognition from animals to humans', *Biochemical Pharmacology*, 81(12), pp. 1356–1366. doi: 10.1016/j.bcp.2010.12.028.

Kim, H. *et al.* (2016) 'Prefrontal Parvalbumin Neurons in Control of Attention', *Cell*, 164(1–2), pp. 208–218. doi: 10.1016/j.cell.2015.11.038.

Kirov, G. *et al.* (2004) 'Strong evidence for association between the dystrobrevin binding protein 1 gene (DTNBP1) and schizophrenia in 488 parent-offspring trios from Bulgaria', *Biological Psychiatry*, 55(10), pp. 971–975. doi: 10.1016/j.biopsych.2004.01.025.

Kleinmans, N. M. *et al.* (2011) 'fMRI evidence of neural abnormalities in the subcortical face processing system in ASD.', *NeuroImage*. NIH Public Access, 54(1), pp. 697–704. doi: 10.1016/j.neuroimage.2010.07.037.

Kopald, B. E. *et al.* (2012) 'Magnitude of Impact of Executive Functioning and IQ on Episodic Memory in Schizophrenia', *Biological Psychiatry*, 71(6), pp. 545–551. doi: 10.1016/j.biopsych.2011.11.021.

Kramer, J. H. *et al.* (2007) 'Magnetic resonance imaging correlates of set shifting', *Journal of the*

- International Neuropsychological Society*, 13(3), pp. 386–392. doi: 10.1017/S1355617707070567.
- Kuperberg, G. and Heckers, S. (2000) ‘Schizophrenia and cognitive function.’, *Current opinion in neurobiology*, 10(2), pp. 205–10. doi: 10.1016/s0959-4388(00)00068-4.
- Kvitsiani, D. *et al.* (2013) ‘Distinct behavioural and network correlates of two interneuron types in prefrontal cortex’, *Nature*, 498(7454), pp. 363–366. doi: 10.1038/nature12176.
- Lee, E. *et al.* (2016) ‘Enhanced Neuronal Activity in the Medial Prefrontal Cortex during Social Approach Behavior’, *Journal of Neuroscience*, 36(26), pp. 6926–6936. doi: 10.1523/JNEUROSCI.0307-16.2016.
- Leggio, G. M. *et al.* (2019) ‘The epistatic interaction between the dopamine D3 receptor and dysbindin-1 modulates higher-order cognitive functions in mice and humans.’, *Molecular psychiatry*. doi: 10.1038/s41380-019-0511-4.
- Lehto, J. E. and Elorinne, E. (2003) ‘Gambling as an executive function task.’, *Applied neuropsychology*, 10(4), pp. 234–8. doi: 10.1207/s15324826an1004\_5.
- Lewicki, M. S. (1998) ‘A review of methods for spike sorting: the detection and classification of neural action potentials.’, *Network (Bristol, England)*, 9(4), pp. R53-78. Available at: <http://www.ncbi.nlm.nih.gov/pubmed/10221571> (Accessed: 3 December 2019).
- Li, P., L. Snyder, G. and E. Vanover, K. (2016) ‘Dopamine Targeting Drugs for the Treatment of Schizophrenia: Past, Present and Future’, *Current Topics in Medicinal Chemistry*. Bentham Science Publishers Ltd., 16(29), pp. 3385–3403. doi: 10.2174/1568026616666160608084834.
- Li, W. *et al.* (2003) ‘Hermansky-Pudlak syndrome type 7 (HPS-7) results from mutant dysbindin, a member of the biogenesis of lysosome-related organelles complex 1 (BLOC-1)’, *Nature Genetics*, 35(1), pp. 84–89. doi: 10.1038/ng1229.
- Locke, H. S. and Braver, T. S. (2008) ‘Motivational influences on cognitive control: Behavior, brain activation, and individual differences’, *Cognitive, Affective and Behavioral Neuroscience*, 8(1), pp. 99–112. doi: 10.3758/CABN.8.1.99.
- Luciano, M. *et al.* (2009) ‘Variation in the dysbindin gene and normal cognitive function in three independent population samples’, *Genes, Brain and Behavior*, 8(2), pp. 218–227. doi: 10.1111/j.1601-183X.2008.00462.x.
- Lunt, L. *et al.* (2012) ‘Prefrontal cortex dysfunction and “Jumping to Conclusions”: Bias or deficit?’, *Journal of Neuropsychology*, 6(1), pp. 65–78. doi: 10.1111/j.1748-6653.2011.02005.x.
- MacKenzie, N. E. *et al.* (2018) ‘Antipsychotics, Metabolic Adverse Effects, and Cognitive Function in Schizophrenia’, *Frontiers in Psychiatry*, 9, p. 622. doi: 10.3389/fpsy.2018.00622.
- Mamelak, M. (2018) ‘Parkinson’s Disease, the Dopaminergic Neuron and Gammahydroxybutyrate’, *Neurology and Therapy*. Springer Healthcare, pp. 5–11. doi: 10.1007/s40120-018-0091-2.
- Markov, V. *et al.* (2009) ‘Genetic variation in schizophrenia-risk-gene dysbindin 1 modulates brain activation in anterior cingulate cortex and right temporal gyrus during language production in healthy individuals’, *NeuroImage*, 47(4), pp. 2016–2022. doi: 10.1016/j.neuroimage.2009.05.067.
- McAlonan, K. and Brown, V. J. (2003) ‘Orbital prefrontal cortex mediates reversal learning and not attentional set shifting in the rat’, *Behavioural Brain Research*, 146(1–2), pp. 97–103. doi: 10.1016/j.bbr.2003.09.019.
- McDonald, C. and Murphy, K. C. (2003) ‘The new genetics of schizophrenia’, *Psychiatric Clinics of North America*, 26(1), pp. 41–63. doi: 10.1016/S0193-953X(02)00030-8.
- De Mei, C. *et al.* (2009) ‘Getting specialized: presynaptic and postsynaptic dopamine D2 receptors’, *Current Opinion in Pharmacology*, 9(1), pp. 53–58. doi: 10.1016/j.coph.2008.12.002.
- Miller, E. K. (2000) ‘The prefrontal cortex and cognitive control’, *Nature Reviews Neuroscience*, 1(1), pp. 59–65. doi: 10.1038/35036228.

- Miller, E. K. and Cohen, J. D. (2001) 'An Integrative Theory of Prefrontal Cortex Function', *Annual Review of Neuroscience*, 24(1), pp. 167–202. doi: 10.1146/annurev.neuro.24.1.167.
- Milner, B. (1963) 'Effects of Different Brain Lesions on Card Sorting', *Arch Neurol*, 9, pp. 100–110.
- Milner, B. (1982) 'Some Cognitive Effects of Frontal-Lobe Lesions in Man', *Philosophical Transactions of the Royal Society B: Biological Sciences*, 298(1089), pp. 211–226. doi: 10.1098/rstb.1982.0083.
- Miyake, A. *et al.* (2000) 'The Unity and Diversity of Executive Functions and Their Contributions to Complex "Frontal Lobe" Tasks: A Latent Variable Analysis', *Cognitive Psychology*, 41(1), pp. 49–100. doi: 10.1006/cogp.1999.0734.
- Morice, R. and Delahunty, A. (1996) 'Frontal/Executive Impairments in Schizophrenia', *Schizophrenia Bulletin*, 22(1), pp. 125–137. doi: 10.1093/schbul/22.1.125.
- Moritz, S. *et al.* (2002) 'Executive functioning in obsessive-compulsive disorder, unipolar depression, and schizophrenia.', *Archives of clinical neuropsychology: the official journal of the National Academy of Neuropsychologists*, 17(5), pp. 477–83. Available at: <http://www.ncbi.nlm.nih.gov/pubmed/14592001> (Accessed: 2 December 2019).
- Nagahama, Y. *et al.* (2001) 'Dissociable Mechanisms of Attentional Control within the Human Prefrontal Cortex', *Cerebral Cortex*, 11(1), pp. 85–92. doi: 10.1093/cercor/11.1.85.
- Nagahama, Y. (2005) 'The cerebral correlates of different types of perseveration in the Wisconsin Card Sorting Test', *Journal of Neurology, Neurosurgery & Psychiatry*, 76(2), pp. 169–175. doi: 10.1136/jnnp.2004.039818.
- National Institute of Health and Clinical Excellence (2014) 'Psychosis and schizophrenia in adults', *The NICE guidelines on treatment and management*, (February), pp. 74–80. doi: 10.1002/14651858.CD010823.pub2.Copyright.
- Nęcka, E. and Orzechowski, J. (2004) 'Higher-order cognition and intelligence', in *Cognition and Intelligence: Identifying the Mechanisms of the Mind*. Cambridge University Press, pp. 122–141. doi: 10.1017/CBO9780511607073.008.
- Numakawa, T. *et al.* (2004) 'Evidence of novel neuronal functions of dysbindin, a susceptibility gene for schizophrenia', *Human Molecular Genetics*, 13(21), pp. 2699–2708. doi: 10.1093/hmg/ddh280.
- Nyhus, E. and Barceló, F. (2009) 'The Wisconsin Card Sorting Test and the cognitive assessment of prefrontal executive functions: A critical update', *Brain and Cognition*. Academic Press, 71(3), pp. 437–451. doi: 10.1016/J.BANDC.2009.03.005.
- Ongur, D. and Price, J. L. (2000) 'The Organization of Networks within the Orbital and Medial Prefrontal Cortex of Rats, Monkeys and Humans', *Cerebral Cortex*, 10(3), pp. 206–219. doi: 10.1093/cercor/10.3.206.
- Orellana, G. and Slachevsky, A. (2013) 'Executive functioning in schizophrenia', *Frontiers in Psychiatry*. Frontiers Research Foundation. doi: 10.3389/fpsy.2013.00035.
- Ortiz-Prado, E. *et al.* (2010) 'A method for measuring brain partial pressure of oxygen in unanesthetized unrestrained subjects: the effect of acute and chronic hypoxia on brain tissue PO<sub>2</sub>', *Journal of neuroscience methods*. NIH Public Access, 193(2), pp. 217–25. doi: 10.1016/j.jneumeth.2010.08.019.
- Otis, J. M. *et al.* (2017) 'Prefrontal cortex output circuits guide reward seeking through divergent cue encoding', *Nature*, 543(7643), pp. 103–107. doi: 10.1038/nature21376.
- Owen, A. M. *et al.* (1991) 'Extra-dimensional versus intra-dimensional set shifting performance following frontal lobe excisions, temporal lobe excisions or amygdalo-hippocampectomy in man.', *Neuropsychologia*, 29(10), pp. 993–1006.
- Owen, A. M. *et al.* (1993) 'Contrasting mechanisms of impaired attentional set-shifting in patients with frontal lobe damage or Parkinson's disease', *Brain*, 116(5), pp. 1159–1175. doi: 10.1093/brain/116.5.1159.
- Pantelis, C. *et al.* (1999) 'Comparison of set-shifting ability in patients with chronic schizophrenia and

frontal lobe damage.’, *Schizophrenia research*, 37(3), pp. 251–70.

Papaleo, F. *et al.* (2012) ‘Dysbindin-1 modulates prefrontal cortical activity and schizophrenia-like behaviors via dopamine/D2 pathways’, *Molecular Psychiatry*, 17(1), pp. 85–98. doi: 10.1038/mp.2010.106.

Papaleo, F. and Weinberger, D. R. (2011) ‘Dysbindin and Schizophrenia: It’s Dopamine and Glutamate All Over Again’, *Biological Psychiatry*, 69(1), pp. 2–4. doi: 10.1016/j.biopsych.2010.10.028.

Patel, K. R. *et al.* (2014) ‘Schizophrenia: Overview and treatment options’, *P and T. Medi Media USA Inc*, pp. 638–645.

Protais, P., Dubuc, I. and Costentin, J. (1983) ‘Pharmacological characteristics of dopamine receptors involved in the dual effect of dopamine agonists on yawning behaviour in rats’, *European Journal of Pharmacology*, 94(3–4), pp. 271–280. doi: 10.1016/0014-2999(83)90416-8.

Puig, M. V., Antzoulatos, E. G. and Miller, E. K. (2014) ‘Prefrontal dopamine in associative learning and memory’, *Neuroscience*, 282, pp. 217–229. doi: 10.1016/j.neuroscience.2014.09.026.

Puri, B. K. and Steiner, R. (1998) ‘Sustained remission of positive and negative symptoms of schizophrenia following treatment with eicosapentaenoic acid (multiple letters)’, *Archives of General Psychiatry*, pp. 188–189. doi: 10.1001/archpsyc.55.2.188.

Ragozzino, M. E. (2002) ‘The effects of dopamine D1 receptor blockade in the prelimbic-infralimbic areas on behavioral flexibility’, *Learning and Memory*, 9(1), pp. 18–28. doi: 10.1101/lm.45802.

Rahman, S. *et al.* (1999) ‘Specific cognitive deficits in mild frontal variant frontotemporal dementia’, *Brain*, 122(8), pp. 1469–1493. doi: 10.1093/brain/122.8.1469.

Rangel-Barajas, C., Coronel, I. and Florán, B. (2015) ‘Dopamine receptors and neurodegeneration’, *Aging and Disease*. International Society on Aging and Disease, pp. 349–368. doi: 10.14336/AD.2015.0330.

Rey, H. G., Pedreira, C. and Quiñero, R. (2015) ‘Past, present and future of spike sorting techniques’, *Brain Research Bulletin*, 119, pp. 106–117. doi: 10.1016/j.brainresbull.2015.04.007.

Rich, E. L. and Shapiro, M. (2009) ‘Rat Prefrontal Cortical Neurons Selectively Code Strategy Switches’, *Journal of Neuroscience*, 29(22), pp. 7208–7219. doi: 10.1523/JNEUROSCI.6068-08.2009.

Robbins, T. W. (2007) ‘Shifting and stopping: fronto-striatal substrates, neurochemical modulation and clinical implications’, *Philosophical Transactions of the Royal Society B: Biological Sciences*, 362(1481), pp. 917–932. doi: 10.1098/rstb.2007.2097.

Roberts, A. C., Robbins, T. W. and Everitt, B. J. (1988) ‘The effects of intradimensional and extradimensional shifts on visual discrimination learning in humans and non-human primates.’, *The Quarterly journal of experimental psychology. B, Comparative and physiological psychology*, 40(4), pp. 321–41. Available at: <http://www.ncbi.nlm.nih.gov/pubmed/3145534> (Accessed: 2 December 2019).

Robinson, J. E. and Gradinaru, V. (2018) ‘Dopaminergic dysfunction in neurodevelopmental disorders: recent advances and synergistic technologies to aid basic research’, *Current Opinion in Neurobiology*. Elsevier Ltd, pp. 17–29. doi: 10.1016/j.conb.2017.08.003.

Roux, L. *et al.* (2014) ‘In vivo optogenetic identification and manipulation of GABAergic interneuron subtypes’, *Current Opinion in Neurobiology*, 26, pp. 88–95. doi: 10.1016/j.conb.2013.12.013.

Santana, N., Mengod, G. and Artigas, F. (2009) ‘Quantitative Analysis of the Expression of Dopamine D1 and D2 Receptors in Pyramidal and GABAergic Neurons of the Rat Prefrontal Cortex’, *Cerebral Cortex*, 19(4), pp. 849–860. doi: 10.1093/cercor/bhn134.

Scheggia, D. *et al.* (2014) ‘The Ultimate Intra-/Extra-Dimensional Attentional Set-Shifting Task for Mice’, *Biological Psychiatry*, 75(8), pp. 660–670. doi: 10.1016/j.biopsych.2013.05.021.

Scheggia, D. *et al.* (2018) ‘Variations in Dysbindin-1 are associated with cognitive response to antipsychotic drug treatment’, *Nature Communications*, 9(1), p. 2265. doi: 10.1038/s41467-018-04711-w.

- Scheggia, D. *et al.* (2020) 'Somatostatin interneurons in the prefrontal cortex control affective state discrimination in mice', *Nature Neuroscience*, 23(1), pp. 47–60. doi: 10.1038/s41593-019-0551-8.
- Schwab, S. G. *et al.* (2003) 'Support for Association of Schizophrenia with Genetic Variation in the 6p22.3 Gene, Dysbindin, in Sib-Pair Families with Linkage and in an Additional Sample of Triad Families', *The American Journal of Human Genetics*, 72(1), pp. 185–190. doi: 10.1086/345463.
- Seeman, P. (2010) 'Dopamine D2 receptors as treatment targets in schizophrenia', *Clinical Schizophrenia and Related Psychoses*, pp. 56–73. doi: 10.3371/CSRP.4.1.5.
- Seeman, P. (2013) 'Schizophrenia and dopamine receptors', *European Neuropsychopharmacology*, pp. 999–1009. doi: 10.1016/j.euroneuro.2013.06.005.
- Snitz, B. E. *et al.* (2005) 'Lateral and Medial Hypofrontality in First-Episode Schizophrenia: Functional Activity in a Medication-Naive State and Effects of Short-Term Atypical Antipsychotic Treatment', *American Journal of Psychiatry*, 162(12), pp. 2322–2329. doi: 10.1176/appi.ajp.162.12.2322.
- Spencer, R. C., Devilbiss, D. M. and Berridge, C. W. (2015) 'The Cognition-Enhancing Effects of Psychostimulants Involve Direct Action in the Prefrontal Cortex', *Biological Psychiatry*, 77(11), pp. 940–950. doi: 10.1016/j.biopsych.2014.09.013.
- Stark, E. *et al.* (2013) 'Inhibition-Induced Theta Resonance in Cortical Circuits', *Neuron*, 80(5), pp. 1263–1276. doi: 10.1016/j.neuron.2013.09.033.
- Starke, K., Gothert, M. and Kilbinger, H. (1989) 'Modulation of neurotransmitter release by presynaptic autoreceptors', *Physiological Reviews*, 69(3), pp. 864–989. doi: 10.1152/physrev.1989.69.3.864.
- Straub, R. E. *et al.* (2002) 'Genetic Variation in the 6p22.3 Gene DTNBP1, the Human Ortholog of the Mouse Dysbindin Gene, Is Associated with Schizophrenia', *The American Journal of Human Genetics*, 71(2), pp. 337–348. doi: 10.1086/341750.
- Tait, D., Chase, E. and Brown, V. (2014) 'Attentional Set-Shifting in Rodents: A Review of Behavioural Methods and Pharmacological Results', *Current Pharmaceutical Design*, 20(31), pp. 5046–5059. doi: 10.2174/1381612819666131216115802.
- Takahashi, H., Yamada, M. and Suhara, T. (2012) 'Functional Significance of Central D1 Receptors in Cognition: Beyond Working Memory', *Journal of Cerebral Blood Flow & Metabolism*, 32(7), pp. 1248–1258. doi: 10.1038/jcbfm.2011.194.
- Talbot, K. *et al.* (2004) 'Dysbindin-1 is reduced in intrinsic, glutamatergic terminals of the hippocampal formation in schizophrenia', *Journal of Clinical Investigation*, 113(9), pp. 1353–1363. doi: 10.1172/JCI20425.
- Tang, J. *et al.* (2009) 'Dysbindin-1 in dorsolateral prefrontal cortex of schizophrenia cases is reduced in an isoform-specific manner unrelated to dysbindin-1 mRNA expression', *Human Molecular Genetics*, 18(20), pp. 3851–3863. doi: 10.1093/hmg/ddp329.
- Thimm, M. *et al.* (2010) 'The effects of a DTNBP1 gene variant on attention networks: an fMRI study.', *Behavioral and brain functions : BBF*. BioMed Central, 6, p. 54. doi: 10.1186/1744-9081-6-54.
- Tolias, A. S. *et al.* (2007) 'Recording Chronically From the Same Neurons in Awake, Behaving Primates', *Journal of Neurophysiology*, 98(6), pp. 3780–3790. doi: 10.1152/jn.00260.2007.
- Totah, N. K. B. *et al.* (2009) 'Anterior cingulate neurons represent errors and preparatory attention within the same behavioral sequence.', *The Journal of neuroscience : the official journal of the Society for Neuroscience*. Society for Neuroscience, 29(20), pp. 6418–26. doi: 10.1523/JNEUROSCI.1142-09.2009.
- Trivedi, J. (2006) 'Cognitive deficits in psychiatric disorders: Current status', *Indian Journal of Psychiatry*. Medknow, 48(1), p. 10. doi: 10.4103/0019-5545.31613.
- Trobalon, J. B. *et al.* (2003) 'Intradimensional and extradimensional shifts in spatial learning.', *Journal of Experimental Psychology: Animal Behavior Processes*, 29(2), pp. 143–152. doi: 10.1037/0097-

7403.29.2.143.

Turner, D. C. *et al.* (2004) 'Modafinil improves cognition and attentional set shifting in patients with chronic schizophrenia.', *Neuropsychopharmacology: official publication of the American College of Neuropsychopharmacology*, 29(7), pp. 1363–73. doi: 10.1038/sj.npp.1300457.

Tyrer, P. J. *et al.* (2010) 'Behavioral Flexibility: Attentional Shifting, Rule Switching and Response Reversal', in *Encyclopedia of Psychopharmacology*. Springer Berlin Heidelberg, pp. 209–213. doi: 10.1007/978-3-540-68706-1\_340.

Usiello, A. *et al.* (2000) 'Distinct functions of the two isoforms of dopamine D2 receptors', *Nature*, 408(6809), pp. 199–203. doi: 10.1038/35041572.

Vallone, D., Picetti, R. and Borrelli, E. (2000) 'Structure and function of dopamine receptors.', *Neuroscience and biobehavioral reviews*, 24(1), pp. 125–32. doi: 10.1016/s0149-7634(99)00063-9.

Vertes, R. P. (2004) 'Differential projections of the infralimbic and prelimbic cortex in the rat', *Synapse*, 51(1), pp. 32–58. doi: 10.1002/syn.10279.

Vijayraghavan, S. *et al.* (2007) 'Inverted-U dopamine D1 receptor actions on prefrontal neurons engaged in working memory', *Nature Neuroscience*, 10(3), pp. 376–384. doi: 10.1038/nn1846.

Vilella, E. *et al.* (2008) 'Association of schizophrenia with DTNBP1 but not with DAO, DAOA, NRG1 and RGS4 nor their genetic interaction', *Journal of Psychiatric Research*, 42(4), pp. 278–288. doi: 10.1016/j.jpsychires.2007.02.005.

Volkow, N. D. *et al.* (2007) 'Dopamine in drug abuse and addiction: Results of imaging studies and treatment implications', *Archives of Neurology*, pp. 1575–1579. doi: 10.1001/archneur.64.11.1575.

Vyazovskiy, V. V. *et al.* (2009) 'Cortical Firing and Sleep Homeostasis', *Neuron*, 63(6), pp. 865–878. doi: 10.1016/j.neuron.2009.08.024.

Walder, D. J. *et al.* (2014) 'Genetic liability, prenatal health, stress and family environment: risk factors in the Harvard Adolescent Family High Risk for schizophrenia study.', *Schizophrenia research*, 157(1–3), pp. 142–8. doi: 10.1016/j.schres.2014.04.015.

Wanat, M. J. *et al.* (2009) 'Phasic dopamine release in appetitive behaviors and drug addiction', *Current Drug Abuse Reviews*, pp. 195–213. doi: 10.2174/1874473710902020195.

Wang, M., Vijayraghavan, S. and Goldman-Rakic, P. S. (2004) 'Selective D2 Receptor Actions on the Functional Circuitry of Working Memory', *Science*, 303(5659), pp. 853–856. doi: 10.1126/science.1091162.

Weickert, C. S. *et al.* (2004) 'Human Dysbindin (DTNBP1) Gene Expression in Normal Brain and in Schizophrenic Prefrontal Cortex and Midbrain', *Archives of General Psychiatry*, 61(6), p. 544. doi: 10.1001/archpsyc.61.6.544.

Weickert, C. S. *et al.* (2008) 'Reduced DTNBP1 (dysbindin-1) mRNA in the hippocampal formation of schizophrenia patients', *Schizophrenia Research*, 98(1–3), pp. 105–110. doi: 10.1016/j.schres.2007.05.041.

Weinberger, D. R. and Berman, K. F. (1996) 'Prefrontal function in schizophrenia: confounds and controversies', *Philosophical Transactions of the Royal Society of London. Series B: Biological Sciences*, 351(1346), pp. 1495–1503. doi: 10.1098/rstb.1996.0135.

Weinberger, D. R., Berman, K. F. and Zec, R. F. (1986) 'Physiologic dysfunction of dorsolateral prefrontal cortex in schizophrenia. I. Regional cerebral blood flow evidence.', *Archives of general psychiatry*, 43(2), pp. 114–24.

Williams, N. M. *et al.* (2004) 'Identification in 2 Independent Samples of a Novel Schizophrenia Risk Haplotype of the Dystrobrevin Binding Protein Gene (DTNBP1)', *Archives of General Psychiatry*, 61(4), p. 336. doi: 10.1001/archpsyc.61.4.336.

Wolf, C. *et al.* (2011) 'Dysbindin-1 genotype effects on emotional working memory.', *Molecular psychiatry*. Europe PMC Funders, 16(2), pp. 145–55. doi: 10.1038/mp.2009.129.



Yoon, J. H. *et al.* (2008) 'Association of dorsolateral prefrontal cortex dysfunction with disrupted coordinated brain activity in schizophrenia: Relationship with impaired cognition, behavioral disorganization, and global function', *American Journal of Psychiatry*, 165(8), pp. 1006–1014. doi: 10.1176/appi.ajp.2008.07060945.

Zhang, J.-P., Lencz, T. and Malhotra, A. K. (2010) 'D<sub>2</sub> Receptor Genetic Variation and Clinical Response to Antipsychotic Drug Treatment: A Meta-Analysis', *American Journal of Psychiatry*, 167(7), pp. 763–772. doi: 10.1176/appi.ajp.2009.09040598.

Zhang, Z. *et al.* (2015) 'Role of Prelimbic GABAergic Circuits in Sensory and Emotional Aspects of Neuropathic Pain', *Cell Reports*, 12(5), pp. 752–759. doi: 10.1016/j.celrep.2015.07.001.

# Acknowledgment

I would like to express my sincere gratitude to my supervisor Dr. Francesco Papaleo for the opportunity to do the PhD in his laboratory and for his support during these three years, for his motivation, enthusiasm, knowledge.

I would like to thank:

- Simone Guadagna, Daniel Dautan, Diego Scheggia, Patrick Latuske, and Marco Nigro for helping me, for their support, their knowledge, and their great participation in this project;
- Federica Maltese, Gabriella Trigilio, Gabriella Contarini, Giulia Castellani, and Alessandra Bonavia, the PhD girls and fellow with whom I spent most of my time in IIT and with whom I also made a splendid friendship;
- Francesca Managò, Valentina Ferretti, Celine Devroye, and Weronika Bracik, the Post Doc of my group, who support me every time;
- Giacomo Pruzzo, Alessandro Parodi, Claudia Chiabrera, and all the member of the Animal Facility for their excellent technical support;
- Aldo Genovesio (associate professor of University “La Sapienza” of Rome), and Marco Dal Maschio (assistant professor of University of Padua) for taking the time to review my thesis, for their excellent advice and comments.
- All the people of IIT, and, in particular, all the guys of the NBT.